R. & M. No. 3285

MINISTRY OF AVIATION

AERONAUTICAL RESEARCH COUNCIL
REPORTS AND MEMORANDA

Seaplane Impact—A Review of Theoretical and Experimental Results

By T. Arlotte, P. Ward Brown, B.Sc., and P. R. Crewe, M.A.
Edited by A. G. Smith

LONDON: HER MAJESTY'S STATIONERY OFFICE
1962
PRICE £1 12s. 6d. NET

Seaplane Impact—A Review of Theoretical and Experimental Results

By T. ARLOTTE,* P. WARD BROWN, B.Sc.,† and P. R. CREWE, M.A.*

Edited by A. G. SMITH‡

Reports and Memoranda No. 3285§

December, 1958

FOREWORD

By SIR HARRY GARNER,

CHAIRMAN OF THE SEAPLANE COMMITTEE OF THE AERONAUTICAL RESEARCH COUNCIL

Discussions have taken place over a number of years in which all the available information on the impact of seaplanes with the water has been reviewed. Much theoretical work has been done, but there is a dearth of experimental information, both model and full scale. The model work has been done in the United States and the full scale, in the main, in this country.

The work has been reviewed in this report. Because of the low priority given to seaplane work in this country it has not been possible for the authors to give as much time to the subject as was desirable. Furthermore, much more experimental work is needed before a solid assessment of the impact loads on a complicated shape such as a modern seaplane hull can be determined. Nevertheless the review is thought to be of great value and to contain all the information available to us at present on the subject of impact. It will provide a useful starting point for further work on the subject.

The curve of acceleration against time, perhaps the most useful criterion for the seaplane designer, obtained in the model experiments was found to agree very well with the theoretical curve. Agreement on draught and vertical velocity however was found to be poor. These quantities are much more difficult to measure than acceleration and time, and it would seem that most of the discrepancy can be attributed to experimental errors.

The disagreement between full-scale results and theory is more serious. The curve of acceleration against time for the *Sunderland* flying boat is much flatter than the theoretical curve, the acceleration reaching the same maximum value in a time which is two thirds longer than the theoretical. This discrepancy has been studied at great length. The review suggests that although the errors of measurement are about twice as great full scale as on the model, these do not explain the elongation of the acceleration curve. This may be caused by such factors as the pointed step, large step fairing, chine immersion, suction caused by the presence of the afterbody, scale effect and the airframe elasticity. The full-scale rates of variation of load with time are thus considerably less than would be suggested by theoretical work and model tests on simple shapes, indicating that the complications in shape introduced by the seaplane designer have had considerable structural advantages.

Some more recent American work on the Martin Model 270 would confirm that better correlation is obtained if full account can be taken of these factors, particularly those of hull-bottom shape.

* Of Saunders-Roe Limited, Osborne, Isle of Wight.

† Formerly of Short Brothers and Harland Limited, Belfast.

‡ Formerly of Marine Aircraft Experimental Establishment, Felixstowe.

§ Previously issued as A.R.C. 20,617 (a revision of A.R.C. 18,843).

Summary. Full-scale impact tests made on a *Sunderland* at the Marine Aircraft Experimental Establishment were in disagreement both with basic model tests and existing theories. The existing information on theoretical, model and full-scale work has therefore been examined to clarify as far as possible the position at the time of writing.

Detailed considerations have had to be limited to a few selected numerical examples of impact but the treatment has been kept as general as possible.

None of the general theoretical solutions convincingly fit both model and full-scale experimental evidence. Fair agreement is obtained between model data and theoretical prediction but not between the *Sunderland* full-scale data and theory as so far taken. There is generally a much longer time to peak accelerations full scale, although the peak-acceleration values are of the right order. Somewhat better agreement is obtained with some few American results but the basic theoretical errors are still in the same sense. Use of a more empirical theory does, however, give good agreement in one case—the Martin Model 270.

These theories are all based on an assumption of transfer of momentum to an associated mass of water and the selection of the value of this is open to a whole range of interpretations.

Assuming this approach to be valid, the value depends very much on the geometry of the wetted hull surface and how this varies with time. There is evidence that the consequent errors in time could be very large for small aspect ratios, which are normally much less than 1 in seaplane impacts. This error is also much increased in the same sense by the effects of rotation, flexibility, possible flow sticking to the afterbody and above the chines. It is also likely that a quasi-static assumption of the values of speed draught and incidence is not permissible when deducing associated mass values.

The report shows that the total impact force can be calculated from an equivalent planing force defined by the forward speed draught and incidence multiplied by a factor to allow for vertical velocity. The value of the planing force is then normally deducible from quasi-static conditions of planing-force measurements but extrapolation still depends on associated mass assumptions. When reasonable assumptions can be made of the appropriate pressure distributions for individual hull forms one example shows quite good agreement. It may therefore be that it will be necessary for some time to determine the three-dimensional planing forces and pressures experimentally on models of individual hull forms in order to deduce full-scale impacts. Even then, care will be required in correcting for dynamic effects such as rotation and flow suctions.

---

1. *Introduction.* Serious theoretical and experimental attention has been given to the seaplane impact problem since 1929, when von Kármán made a simple but fundamental contribution[1] using the concept of transfer of momentum to an associated mass of water. This treatment was considerably developed by Wagner in the early '30's, to include transverse pressure-distribution prediction and the effect of rise of water above the undisturbed level. These early theoretical treatments were strictly applicable to the relatively uncomplicated conditions occurring in vertical drops at zero incidence, where the associated mass remains in contact with the wedge. A brief outline of such treatments is contained in Appendix I. An extensive experimental programme was carried out at the Marine Aircraft Experimental Establishment (under the direction of Sir Harry Garner) to verify these theories, with particular reference to the study of impact pressures, Ref. 2 being a useful British report produced in the period up to 1939.

Detailed investigations of impact in which the aircraft has an appreciable forward speed and incidence began in the mid-'40's[3, 4, 5, 6, 7, 8] and were carried on more or less independently in the United States and Great Britain. In due course several fundamentally equivalent theories were developed, all of which appeared to agree satisfactorily with model experiments. The discussion of

the theories given in the main body of this report is limited to those dealing with the effect of downwash imparted to the wake in the presence of forward speeds.

The conditions represented were necessarily somewhat simplified compared with those found in an actual full-scale impact, and in 1948 full-scale measurements made by the Royal Aircraft Establishment indicated discrepancies from the available theories[9, 10] basically in the time from impact to peak acceleration. The Marine Aircraft Experimental Establishment, Felixstowe, therefore undertook a series of full-scale tests on a *Sunderland V* flying boat, the results of which were issued in Refs. 31 to 36. At the same time, a review and extension of the theory was made jointly by representatives of the Royal Aircraft Establishment and the Saunders-Roe Co.[11, 12].

The full-scale evidence so obtained was, however, still in disagreement both with model tests and theoretical results and the discrepancies unresolved. The state of knowledge existing at the conclusion of this work has been reviewed in this report.

The report has been confined largely to investigations of the total forces occurring in impacts. A considerable amount of work has been done on pressure distributions and is contained in some of the references given herein, but an adequate theoretical treatment for pressure distribution has yet to be published.

Systematic investigations of rotation in pitch and rough-water effects are further outstanding requirements (1958).

2. *Experimental Evidence.* 2.1. *Model Tests.* A comprehensive report giving the results of model impact experiments is Ref. 13, which tabulates measurements and gives a detailed list of references of tests made in the N.A.C.A., Langley Field, impact basin. The models represented the forebodies only of flying boats or floats, complete with bows and having substantial lengths of rear forebody with constant dead rise. (Fig. 1a.)

The attitude and forward speed were kept constant throughout the impact in all these tests.

The description of an impact is in general restricted to behaviour at the moments of maximum acceleration, maximum penetration and water exit, the geometrical parameters investigated being at first impact:

Dead rise	Attitude
β deg	τ deg
$22\frac{1}{2}$	3, 6, 9, 12
30	6, 15
40	3, 6, 9, 12

Full time descriptions are given in 4 cases:

β deg	τ deg
$22\frac{1}{2}$	3 and 12
30	6 and 15

Other N.A.C.A. reports[14, 15] gives results for

β deg	τ deg
10	20 and 30
$22\frac{1}{2}$	-3 and 0

In all the above cases, peak acceleration generally occurred before the chines submerged (chines wet) although they may have been wetted by the water upwash and spray. The beam, and hence maximum draught, was therefore low and representative of orthodox hull design.

Some experimental data on chines-wet cases are given in Refs. 16 to 19. In these cases the beam loading is high, giving large draught at full immersion and these cases have become important with the use of long narrow hulls and hydroskis.

The effect of allowing attitude to vary during impact is investigated in Ref. 20.

The effect of structural elasticity is estimated for a flying-boat configuration in Ref. 21 and for hydroskis mounted on shock absorbers in Ref. 22.

The effect of the presence of an afterbody is investigated in Ref. 23.

The theoretical treatments of impact depend in some cases on the estimation of forces in analogous planing conditions. Of the many reports on planing experiments, the most useful N.A.C.A. reports are Refs. 24 and 25 which also contain detailed lists of references.

	β deg	τ deg
Ref. 24	20 40	2, 4, 6, 12, 18, 24, 30 4, 6, 12, 18, 24, 30
Ref. 25	0	2, 4, 6, 9, 12, 18, 24, 30

In all these cases the chines are immersed but a limited N.A.C.A. study of chines-dry conditions has recently been made in Ref. 26 (which also refers to Shoemaker's 1934 tests[27], but not to the early British and German work). An analysis of some planing test results in models is given in Ref. 69 and some 25 deg wedge data in Ref. 70.

A comparison between experimental pressure distributions obtained in impact conditions with chine immersion and in analogous planing conditions is made in Refs. 28 and 29, which refer to 30 deg dead rise and flat-plate conditions respectively.

The effect of rough water on the impact of a flying-boat forebody of 30 deg dead rise is given in Ref. 30.

2.2. *Full-Scale Tests.* The main full-scale evidence is the British work described in the following Refs.:

Ref. No.	Subject Matter
9	Dynamic landing loads on a *Sunderland* with primary reference to induced wing inertia loads.
10	Preliminary comparison of results of main-step impacts and theory.
31	Description of test instrumentation for seaplane impact measurements.
32	Main-step impacts on a *Sunderland.*
33	Preliminary pressure measurements on rough-water impact of a *Sunderland.*
34	More detailed evidence on some of the main-step-impact results described in Ref. 32.
35	Afterbody impacts on a *Sunderland.*
36	Rough-water impacts on a *Sunderland.*

All the measurements were made on *Sunderland V* aircraft, and this type of hull has a pointed and faired main step which differs from the idealised wedge shapes of model test and theory. The results are also somewhat limited in that afterbody and step-fairing pressures were not measured in main-step impacts, and at least some angular motion in pitch was usually present.

American results have been obtained on a *Vought Sikorsky* S-43 amphibian, Ref. 37, and the Martin Model 270, Ref. 38. The former reference is very limited in evidence and is concerned with a hull having a transverse step with no fairing and conventional fineness ratio. The latter reference contains a general discussion of empirical theory and full-scale measurements on the *Martin* 270 aircraft, which aircraft has a rather-pointed highly-faired main step and high fineness ratio. These results have not been analysed in detail because they were not available until late.

3. *Theoretical Evidence.* 3.1. *General Discussion.* Before outlining the various special theories advanced since 1929 up to the present, a brief description is given of the general theory of the motion of a solid body in a liquid far from a boundary (Section 3.2). From this it is shown that the general classical theory would give an analogous form for seaplane impact if

$$F(1+\mu) = F_{pe}\left[k_3 + k_1\left(\frac{V_v}{V_H \tan\tau}\right) + k_2\left(\frac{V_v}{V_H \tan\tau}\right)^2\right]$$

where

μ	Ratio of associated mass to total mass of solid
F	Total force
$F_{pe} = F_{p0}$	Planing force at draught and incidence at time considered
V_v	Velocity normal to surface
V_H	Velocity parallel to surface
τ	Angle of incidence.

It is then shown that all the theories considered in the report are special cases of this general form. For the later theories $k_3 = 1$, $k_1 = 2$ and $k_2 = 1$. F_{p0} is as given by planing experiments or potential theory.

3.2. *General Theory.* A general theory for the motion of a solid body located far from a boundary, in a liquid, is discussed in Lamb's Hydrodynamics[39].

The discussion is not immediately relevant to the present problem but may be of some use in judging the treatment used by the various impact theories. Consider, for example, the motion of a cylinder in two dimensions, given in pages 184 *et seq.* of Ref. 39. Using the notation of Fig. 16, it may be shown that the force on the cylinder F is

$$F = \frac{d}{dt}(AV_n + BV_T + G_q) - q(BV_n + CV_T + H_q) + \kappa\rho V_T - \rho\alpha q$$

where κ is the cyclic constant of the circulatory motion associated with lift in steady motion. The constants A to H can be regarded as virtual or associated masses and moments of inertia of the disturbed water, which are not in general simply related to one another and are independent of α and κ. The last are functions of velocity as well as geometry.

When rotation is absent, $q = 0$, and the expression becomes

$$F = \frac{d}{dt}(AV_n) + \frac{d}{dt}(BV_T) + \kappa\rho V_T .$$

If it be assumed that the impact of a simple V-wedge with a water surface be analogous, the resultant water force on the body, disregarding friction, acting normal to the keel, will correspond to F, and V_T will be constant.

The important difference between simple impact and planing is algebraically that in the former the velocity tangential to the keel is zero and in the latter the velocity V_v normal to the surface is zero. In seaplane landings neither V_T nor V_v is zero and there is a mixture of the two cases.

In impact theories either V_T or V_H is usually considered to remain constant throughout immersion but there is little difference in result, and the V_T constant assumption will be used in this report.

When V_T is constant, the formula above can conveniently be written

$$F = F_i + F_p + V_v V_T \frac{dB}{dh},$$

where

$$F_i = \frac{AdV_n}{dt} + \left(\frac{V_H \tan\tau}{V_v} + 1\right) F_v$$

and

$$F_v = V_v^2 \cos\tau \frac{dA}{dh}.$$

Then

$$F_i = \frac{AdV_n}{dt} + F_v \text{ when } V_H \text{ is zero}$$

and

$$F = F_i \text{ when } V_T \text{ is zero.}$$

$$F_p = \frac{\kappa}{\kappa_p}\left(1 - \frac{V_v \tan\tau}{V_H}\right) F_{p0}$$

where

$$F_{p0} = \kappa_p \rho V_H \cos\tau,$$

and κ_p is a cyclic constant appropriate to conditions $V_v = 0$.

Also

$$F_p = F_{p0} \text{ when } V_v = 0$$

and

$$F = F_{p0} \text{ when } V_H \text{ is constant and } V_v \text{ is zero.}$$

Therefore in terms of the associated mass analogy with simple impact and planing phenomena F_i and F_{p0} are analogous to the total water forces occurring in (a) simple impact with V_T zero and (b) steady planing respectively with V_v zero, while F_v corresponds to an important associated mass force occurring in vertical drops. These are illustrated in Fig. 2.

If F is the only external force acting on the body, its linear acceleration is given by

$$F = -\frac{W}{g}\frac{dVn}{dt}$$

$$F = \frac{AdVn}{dt} = F\left(1 + \frac{Ag}{W}\right).$$

κ will not in general equal κ_p due to differences in the Kutta trailing-edge condition, an intuitive value for κ/κ_p analogous to impact motion, possibly being

$$\left(1+\frac{V_v}{V_H\tau}\right)\sqrt{\left\{1+\left(\frac{V_v}{V_H}\right)^2\right\}}\ \text{(Fig. 2b)}.$$

With these assumptions,

$$F\left(1+\frac{Ag}{W}\right) = (V_H\sin\tau)^2\left[\left(1+\frac{V_v}{V_H\tan\tau}\right)\frac{V_v}{V_H\sin\tau}\left(\frac{dA}{dh}\right)+\right.$$
$$+\left(1+\frac{V_v}{V_H\tau}\right)\left(1-\frac{V_v\tan\tau}{V_H}\right)\frac{F_{p0}}{(V_H\sin\tau)^2}\sqrt{\left\{1+\left(\frac{V_v}{V_H}\right)^2\right\}}+$$
$$\left.+\frac{V_v}{V_H\tan\tau}\left(1-\frac{V_v\tan\tau}{V_H}\right)\frac{dB/dh}{\sin\tau}\right].$$

Steady planing experiments show that the water force analogous to F_{p0} is proportional to V_H^2, while the associated mass terms A, (dA/dh) and (dB/dh) are functions of geometry only.

In impact cases of practical interest, V_v/V_H and τ are usually both much less than unity in magnitude.

With these assumptions,

$$F\left(1+\frac{Ag}{W}\right) \doteqdot F_{p0}\left[1+k_1\frac{V_v}{V_H\tan\tau}+k_2\left(\frac{V_v}{V_H\tan\tau}\right)^2\right]$$

where k_1 and k_2 depend on geometry only.

In impact theory the associated mass analogous to A is often written $(w/g)\mu$, and usually μ is much less in magnitude than unity (Fig. 1c). Thus an impact formula analogous to the above would be

$$F(1+\mu) \doteqdot F_{p0}\left[1+k_1\left(\frac{V_v}{V_H\tan\tau}\right)+k_2\left(\frac{V_v}{V_H\tan\tau}\right)^2\right],$$

or without the approximations,

$$F(1+\mu) = \left(\frac{V_H\tan\tau}{V_v}+1\right)F_v+F_p+V_vV_T\frac{dB}{dh}$$

which can also be written $F = F_i + F_p + V_vV_T dB/dh$. If B were constant the expressions would become

$$F(1+\mu) \doteqdot F_{p0}\left[\left(1+\frac{V_v}{V_H\tan\tau}\right)\left(1+k_2\frac{V_v}{V_H\tan\tau}\right)\right]$$

and

$$F(1+\mu) = \left(\frac{V_H\tan\tau}{V_v}+1\right)F_v+F_p \text{ respectively.}$$

It may be noted that

$$\left(1+\frac{V_v}{V_H\tan\tau}\right) = \frac{V_n}{V_H\sin\tau},\quad \text{(Fig. 1b)}$$

and expressions can be formulated in the latter form instead, if desired, but the explicit presentation of V_v is considered the more useful when making comparisons with experiment.

3.3. *Current Theories for Impact Force.* Current theoretical treatments for estimating impact time histories of simple V-wedges when the chines do not submerge, no rotation is present, but the craft may have appreciable forward speed, are described in Refs. 12, 13 and 40. These three theories were developed almost independently but are fundamentally equivalent, although the various writers use somewhat different numerical values for the parameters. A number of earlier reports, containing preliminary statements of the ideas, are listed in the above references. There is also a discussion on the assumptions made on associated mass in these theories in Ref. 16.

In all three cases the total water force on the body can be expressed in the form

$$F(1+\mu) = \left(\frac{V_H \tan\tau}{V_v} + 1\right) F_v + \left(1 + \frac{V_v}{V_H \tan\tau}\right)\left(1 - \frac{V_v \tan\tau}{V_H}\right) F_{p0}$$

which is equivalent to the analogue equation above if

(a) the associated mass B is assumed to be constant or zero,

(b) the ratio of circulation constants κ/κ_p is taken as $(1+V_v/V_H \tan\tau)$.

This approximates to the previous intuitive assumption, for V_v/V_H reasonably small, and means that F_p is taken as $(V_n V_T/V_H{}^2 \sin\tau\cos\tau)F_{p0}$, $V_H{}^2 \sin\tau\cos\tau$ being the value $V_n V_T$ takes when V_v is zero (Fig. 2c).

On the basis of model tests, and in order to obtain a simplified differential equation Refs. 12, 13 and 40 all assume that the associated mass $(W/g)\mu$ is a function of h^3, and is related to F_{p0} by

$$\frac{d}{dh}\frac{W}{g}\mu = \frac{F_{p0}}{V_H{}^2 \sin^2\tau\cos\tau}.$$

This gives

$$\frac{d}{dh}\left(\frac{W}{g}\mu\right) = \frac{3W\mu}{gh} \text{ and } F_v = \left(\frac{V_v}{V_H \sin\tau}\right)^2 F_{p0}.$$

Substituting this relationship gives

$$F(1+\mu) = F_{p0}\left(1 + \frac{V_v}{V_H \tan\tau}\right)^2$$

corresponding to the equation on line 5, page 4 of Ref. 41. k_1 and k_2 of the general form thus take the simple values 2 and 1 respectively.

None of the Refs. 12, 13 and 40 refers to the classical analogue discussed above, but instead rely largely on intuitive justifications for the detailed form of the equation of motion.

Monaghan and Crewe Theory. In Ref. 12 it is assumed that the total force is made up of a 'pure impact' term F_i, independent of V_T and an 'impact planing' term

$$F_p \equiv \frac{V_n V_T F_{p0}}{V_H{}^2 \sin\tau\cos\tau}.$$

The associated velocity terms are illustrated in Fig. 3. Numerical calculations were based on evaluation of $(W/g)\mu$ by an empirical generalisation of the rigorous mathematical solution for elliptic plates

$$\frac{W}{g}\mu = \frac{\rho 8}{3\pi}\frac{(\text{area})^2}{\text{perimeter}}\left(1 - \frac{\beta}{\pi}\right)$$

where area and perimeter refer to the projected hull-bottom area sustaining pressure (Fig. 3b and Appendix II of Ref. 12).

Experience showed that in practical cases the 'impact planing' term was more important than the 'pure impact' term, and therefore in later uncirculated Saunders-Roe reports F_{p0} was obtained from planing experiments and $(W/g)\mu$ calculated in terms of it, using the previously mentioned relationship

$$F_v = \left(\frac{V_v}{V_H \sin\tau}\right)^2 F_{p0}.$$

This preserved the simple form of the general differential equation with $k_2 = 1$.

Milwitsky Theory. In Ref. 13 a 'strip theory' treatment based on momentum concepts is employed. Two-dimensional considerations are applied to each transverse flow plane, fixed in space. Integration over all the flow planes gives the total force, and the same relationships as above are found to exist between the geometrical coefficients of the various terms, but the absolute magnitudes used in numerical calculation are rather different. The treatment of each flow plane in isolation from the rest is clearly an approximation, which is particularly suspect when the aspect ratio of the wetted area is small, as it often is when the chines are dry. The presentation of the theory is necessarily rather complex but centres of pressure and pitching moments can also be deduced.

Ward Brown Theory. In Ref. 40, F is taken to be equal to a total rate of change of momentum of a virtual mass of fluid, the latter being made up of the rate of change under the body, and the rate of shedding of momentum of virtual mass to the wake, corresponding to F_i and F_p respectively. The two terms obtained are identical in form with the 'pure impact' and 'impact planing' forces of Ref. 12. This approach was also considered generally in Refs. 11 and 12 before an arbitrary assumption of separate terms was made. An effective virtual mass is specifically deduced from the planing force. The values of planing force appropriate to any attitude and draught differ somewhat from those of other writers, and are derived in Ref. 42.

Earlier impact force theories. Before discussing various theoretical criticisms of the above theory, some different theoretical approaches that have been published by other authors will be briefly considered.

In Ref. 43, April, 1945, an approximate theory is developed for vertical impact which can be expressed as

$$F(1+\mu) = V_H^2 \sin^2\tau \frac{d}{dh}\left(\frac{W}{g}\mu\right)\left(1 + \frac{V_v}{V_H \tan\tau}\right)\left[\frac{V_v}{V_H \tan\tau} + 1 - \sqrt{\left\{1 + \left(\frac{V_v}{V_H}\right)^2\right\}}\right].$$

When V_v/V_H and τ are small this approximates to $F = F_i$ and can be written

$$F(1+\mu) = V_H^2 \sin^2\tau \frac{d}{dh}\left(\frac{W}{g}\mu\right)\left\{\frac{V_v}{V_H \tan\tau} + \left(\frac{V_v}{V_H \tan\tau}\right)^2\right\}.$$

Thus, unlike the theories just discussed, the F_p term is virtually omitted and the solution thus tends to zero, instead of to a steady planing force, when V_v tends to zero.

In Ref. 5, August, 1945, a theory was proposed based on simple planing forces. This can be expressed as

$$F = \left(1 + \frac{V_v}{V_H \tau}\right) F_{p0},$$

i.e., to $F = F_p$ if the circulation-constant ratio is taken as

$$\left(1 + \frac{V_v}{V_H \tan\tau}\right),$$

the value appropriate to the Refs. 12, 13 and 40 theories.

In this case in the general equation the F_i term has been ignored, $k_1 = 1$, and $k_2 = 0$, instead of 2 and 1 respectively, as assumed by Refs. 12, 13 and 40.

From this discussion it is clear that, for practical purposes all the theories are covered by a slight modification of the suggested classical analogue formula where except in the Ref. 43 case $k_3 = 1{\cdot}0$ and $F_{pe} = F_{p0}$, the steady planing force at the same draught and attitude.

3.4. *Some Defects of Current Theories. Possible interaction of effects of associated mass and Kutta trailing-edge condition.* Some criticisms will be considered which have been made of the values of F_{pe} and k's used in the theories of Refs. 12, 13 and 40.

Professor H. B. Squire has pointed out that in aerodynamic experiments associated mass effects have been found to be reduced considerably in the presence of a Kutta condition of flow tangency at the trailing edge. If the associated mass is assumed to be reduced by a factor k in the F_i term only, the equation for F will become

$$F(1+\mu) = F_{p0}\left[1 + (1+k)\left(\frac{V_v}{V_H \tan\tau}\right) + k\left(\frac{V_v}{V_H \tan\tau}\right)^2\right],$$

i.e., the effects of variation of vertical velocity are reduced.

In pursuance of this possibility it is suggested in Ref. 44 that only the vertical velocity, V_v, part of the F_i term might occur in practice, when V_H is not zero, the whole effect of the latter being covered by the F_p term. (Compare Fig. 4a with Fig. 3a.) The equation then becomes:

$$\begin{aligned} F(1+\mu) &= F_v + F_p \\ &= F_{p0}\left[1 + \frac{V_v}{V_H \tan\tau} + \left(\frac{V_v}{V_H \tan\tau}\right)^2\right], \end{aligned}$$

i.e.,

$$k_1 = k_2 = 1{\cdot}0.$$

Possible scale effect on water pile-up. Mr. P. Crewe has suggested that the water surface might not rise against the bottom in quite the same way under model and full-scale conditions. A reduced pile-up would reduce the value of F_{p0} at a given attitude and draught and therefore either reduce the general level of F or perhaps only affect the F_p term giving

$$F(1+\mu) = F_{p0}\left[k + (1+k)\left(\frac{V_v}{V_H \tan\tau}\right) + \left(\frac{V_v}{V_H \tan\tau}\right)^2\right]$$

where k is less than $1{\cdot}0$.

Effect of wing lift. Dr. Williams has noted that the theories had taken no account of the fact that as an aircraft descends at a steady angle, part of the weight is being accounted for by the incidence of the flight path. On contacting the water that part of the lift due to downward velocity is then effectively lost. This loss was, however, shown to be negligible in Ref. 45 since the weight was balanced out just at touchdown.

Earlier American calculations on a vertical drop[46] differed in assuming a constant out-of-balance condition in which the wing lift was $\frac{2}{3}$ of the weight throughout. In the latter case the time from touchdown to peak acceleration was increased by 15 per cent, but the time from a zero-acceleration condition to peak acceleration was virtually unaffected (Fig. 4b). This suggests that care is required in defining the effective initiation of impact.

The possibility of serious effects from ground cushioning have been suggested by Mr. Knowler but model test data under controlled conditions are not available.

The effect of chine immersion. The impact-force theories so far discussed have been concerned mainly with cases in which the chines remain dry. The pressure-distribution theories have, however, applied to chines wet and dry.

An American theory for chine-immersed impact forces has been published in Ref. 17. It is again a 'strip theory' like that of Ref. 13, but its formulation is more complex. A chines-wet theory, based on the approach of Ref. 12 has been developed by Crewe and Arlotte, and also based on Ref. 40 by Ward Brown, but neither has been published.

It may be remarked that a theory could well be satisfactory when the wetted length is large, and yet be insufficiently accurate at small wetted length, chines-dry conditions, where water pile-up is relatively much more important.

The effect of rotation in pitch. An American strip theory to assess the effect of rotation in pitch is given in Ref. 20. The formulae are complicated and solutions are obtained by iteration.

No attempt is made here to discuss an analogue of the classical equations given at the beginning of Section 3 of this report, but in order to obtain a possible indication of the maximum likely order of magnitude given by this form, an argument in terms of effective horizontal planing velocity is presented below.

Consider Fig. 6. In the case without rotation the effective planing velocity is the velocity in space of the intersection of the centreline of the V-wedge with the unpiled-up water surface. If the same relationship applied when rotation is present, the effective velocity will in the cases of τ and V_v/V_H reasonably small be nearly enough

$$V_H + V_v \cot \tau - [(h - x_s \tau_0) \operatorname{cosec}^2 \tau - z_s] \frac{d\tau}{dt}$$

where τ_0 is the touchdown value of τ.

This assumes that the quantities V_v, V_H, h and acceleration refer to the aircraft centre of gravity, not the step heel.

If they refer to the step heel the expression becomes exactly

$$V_H + V_v \cot \tau - h \operatorname{cosec}^2 \tau \frac{d\tau}{dt}.$$

In order to adjust experimental results in which rotation is present to an equivalent fixed-attitude condition it is necessary to make theoretical assumptions with regard to the relationship between force and draught, attitude and velocity. Since the main theoretical assumption under criticism is that

$$F = \frac{F_{p\,0}}{(1+\mu)} (1 + V_v/V_H \tan \tau)^2$$

where τ remains constant, the correction for attitude change will be based on this. Furthermore, to allow the greatest possibility for rotational effect, the force under rotating conditions will be taken as

$$F = \frac{F_{p\,0}}{(1+\mu)} \left\{ 1 + \frac{V_v}{V_H \tan \tau} - \frac{h \operatorname{cosec}^2 \tau}{V_H} \frac{d\tau}{dt} \right\}.$$

The results could be corrected to an average τ, or to the initial τ. Denote the attitude to which they are corrected by τ_0.

Given $F(\tau, h)$ at a certain h, V_v, and varying attitude τ, the corrected force at this draught is nearly enough

$$\frac{F(\tau, h)(y)^2}{\left(1 + \frac{V_v}{V_H \tan\tau} - \frac{h \operatorname{cosec}^2\tau \frac{d\tau}{dt}}{V_H}\right)^2} \frac{\tau_0}{\tau} \frac{1+\mu(\tau, h)}{1+\mu(\tau_0, h)}$$

where

$$\log\left\{\frac{y}{1 + \frac{V_{v0}}{V_T \sin\tau_0}}\right\} + 2\left[\frac{1}{y^3} - \frac{1}{\left(1 + \frac{V_{v0}}{V_T \sin\tau_0}\right)^3}\right]$$

$$= \frac{g}{W V_H^2 \cos\tau_0 \sin^2\tau_0} \int_0^h \frac{F(\tau, h)(\tau_0/\tau)}{\left(1 + \frac{V_v}{V_H \tan\tau} - \frac{h \operatorname{cosec}^2\tau \frac{d\tau}{dt}}{V_H}\right)^2} \times \left\{\frac{1+\mu(\tau, h)}{1+\mu(\tau_0, h)}\right\} dh.$$

This assumes that at a given draught, F_{p0} varies linearly with τ. Fig. 7 shows that this is a reasonable assumption for trim changes of the order being considered, but curves similar to that in the figure can be employed to make a more sophisticated correction if required, τ/τ_0 being replaced by $F_{p0}(\tau_0, h)/F_{p0}(\tau, h)$.

If the finally corrected results are given non-dimensionally as for example by $u'' \sim u^2/(1+u^3)$, the coefficients must be based on the value of the parameter Λ appropriate to τ_0. Note that $\mu(\tau, h) = \Lambda(\tau)h^3$.

3.5. *Planing Theories. Pressure distributions in planing.* Criticisms of impact-force theories might be based on a comparison of pressure distributions occurring in impact and in steady planing. Refs. 47 and 48 contain recent theoretical work on pressures, and also refer to the important earlier work, especially that of Wagner.

In Ref. 48 it is stated that at a given attitude and draught, the planing and impact pressures on a simple V-wedge or flat plate are in general related in the ratio of V_H^2 to $(V_H + V_v \cot\tau)^2$. Thus impact is like planing but at an effective forward velocity $V_H + V_v \cot\tau$ (Fig. 5a). An Appendix to the report discusses possible deviations from this simple relationship due to (*a*) forward pile-up of water, which will only be significant when the dead rise and draught are small (this effect should increase the impact pressures) and (*b*) deceleration normal to the keel (which should reduce the pressures, especially when the wetted area is large).

As already stated the impact-force theories of Refs. 12, 13 and 40 can be expressed in the form

$$F(1+\mu) = F_{p0}\left(1 + \frac{V_v}{V_H \tan\tau}\right)^2.$$

In the usual case when μ has a magnitude much less than unity

$$F \doteqdot F_{p0}\left(1 + \frac{V_v}{V_H \tan\tau}\right)^2,$$

and is thus also of the form of a steady planing force arising from an effective forward velocity $V_H + V_v \cot\tau$ assumed in Ref. 48.

The $(1+\mu)$ term provides a correction which is related to the pressure adjustment under (*b*) above.

In Ref. 44 it is argued that such a relationship between impact and planing is theoretically unjustified since in the pure planing analogue the velocity of flow at the step trailing edge would be

$V_H + V_v \cot \tau$, whereas in fact, from Bernouilli's equation it must be of order $\sqrt{(V_H^2 + V_v^2)}$ in general a much smaller quantity. (Fig. 5b.) This, however, may not always be so.

Recent published work on planing theories relevant to impact theory is given in Refs. 26, 25 and 42. These refer to chines-dry V-wedges, flat plates and both plates and wedges respectively. Extensive lists of references to earlier work are provided.

All the above references depend on associated mass concepts and require the empirical choice of constants to obtain agreement with experiment.

The theories will not be discussed in detail since once a relationship between impact and planing has been established, it is, in principle, unimportant whether the impact forces are estimated from planing theory or directly from curves of results of planing experiments.

It should be noted, however, that in the case of immediate interest, a chines-dry V-wedge, both Refs. 26 and 42 assume that the planing lift at a given attitude depends upon the square of the draught. Unfortunately both experimental and theoretical evidence for determining the attitude and aspect-ratio effects is limited, and different writers use rather different values of normal-force coefficient. This is illustrated by Fig. 7 which refers to a dead rise appropriate to the *Sunderland V* tests.

However, the assumptions made on associated mass may reflect seriously on the final impact answer, especially if the suggestions of Ref. 66 be valid, that quasi-static conditions cannot be assumed. In such cases the water flow will sort itself out to suit the variation of geometry with time.

A recent study of planing ratio by Squire[6,7], considers the slope of surface produced in two-dimensional motion of a single wedge and thence calculates the pressure distributions and total force on the wedge. Methods of thin-aerofoil theory were used for this purpose so avoiding the difficulties inherent in the associated mass technique.

4. *Methods of Presentation of Results.* The choice of a satisfactory method of presenting impact results, both experimental and theoretical, presents a considerable problem in itself. Different writers use widely different notations, and a variety of non-dimensional plots have been published.

In writing the present paper some further thought has been given to determining the most useful methods of presentation and choosing suitable and existing symbols that will be reasonably easy to understand and remember.

In experimental work acceleration, time and craft location are measured directly. The accuracy of time measurements is generally high (say 0·1 per cent), and acceleration should be reasonable (say better than $\pm$ 10 per cent at average values). Attitude is fixed or measured directly to an accuracy better than $\pm$ 10 per cent. Draught measurements are in general less accurate, and are themselves often used as a basis for computing vertical velocity. If vertical velocity at touchdown is known, integration of the acceleration/time curves will give the time history of velocity variation, from which draught can be obtained by a further integration.

Plots of acceleration against time, therefore, provide the most direct experimental description of an impact, should in general have a relatively high accuracy, and are concerned with the physical quantities of greatest design importance. It has been found that in general they indicate the effects of varying the theory quite clearly.

An acceleration/draught 'loop' presentation better illustrates the relationship that exists between impact and planing forces. At a given draught, attitude and forward speed, the planing force is known, and varies linearly with draught squared when the chines are dry.

In the general formula for impact force

$$F(1+\mu) = F_{p\,0}\left[1 + k_1\left(\frac{V_v}{V_H \tan\tau}\right) + k_2\left(\frac{V_v}{V_H \tan\tau}\right)^2\right],$$

$F_{p\,0}$ varies at h^2, and $F = F_{p\,0}/(1+\mu)$ when $V_v = 0$, *i.e.*, at maximum draught.

Deviation of the total force F from the straight line giving the planing force in terms of draught^2 therefore illustrates the effect of the vertical velocity term V_v, Fig. 9. It also checks the general shape of the experimental points.

It is useful to call the line of planing force against draught as the scaffolding for the force variation. If the peak acceleration be early in the impact, well before maximum draught, then the loop has maximum volume.

This form of plotting is first given in Ref. 13 but using draught instead of draught^2. Planing-force scaffold lines were absent.

It is sometimes convenient to plot acceleration against draught, since integration under the curve gives the variation of V_v^2 with draught.

Since the vertical velocity must be fully destroyed at maximum draught, integration of acceleration up to the maximum draught condition must give the initial velocity. This provides an important means of checking the validity of the stated magnitude of the latter quantity and of proposals affecting the change of impact parameters with draught. (Fig. 13.)

Illustration of acceleration vs. *draught plots.* The results of Ref. 13 have been analysed and plotted in Figs. 10, 11 and 12 using the symbols of the original report. The relationship between these symbols and those used in this report is given in Appendix III.

Fig. 10 shows an analogous plot of acceleration against draught squared as found for the planing theory, impact theory and model impact experiment for a particular approach case.

Fig. 11 gives a similar result for a series of impacts for the same wedge.

Statistical considerations. The nature of the experimental evidence, and the inevitable inaccuracies introduced into theoretical estimates of magnitudes of quantities, due to their dependence upon measured quantities of doubtful accuracy, such as draught and vertical velocity, suggest that statistical evaluation is advisable. As a result some brief statistical investigations based on an unpublished paper written by Ward Brown, have been included in the present report. Normal distributions of quantities have been assumed, and standard deviations and probabilities of error estimated. Only peak accelerations and times to peak acceleration have been investigated. Fig. 14 gives general curves of magnitude of error against standard deviation with probability of occurrence as parameter; they are referred to again in Section 6.4.

5. *Comparisons Between Experiment and Theory.* 5.1. *Model Impact Data.* Although statistical methods of analysis are advisable they have not been used in previous published discussions of the evidence, so that non-statistical comparisons between experiment and theory will be considered first, with the proviso that the comments made might need some modification as the result of detailed statistical treatment of the data.

Examination of the comparisons between N.A.C.A. constant-trim model tests and theory[12, 13, 14] indicates

(*a*) maximum impact loads agree well,

(*b*) theoretical times to peak acceleration are definitely of the right order.

It might be possible to justify an increase of time of about 10 per cent for dead-rise angles of $22\frac{1}{2}$ deg, 30 deg and 40 deg. In the 10 deg dead rise this might become an average increase of 25 to 30 per cent, but the number of test results is low.

(*c*) Maximum draught and exit times are in fair agreement with theory.

In the lower dead-rise cases chine immersion is affecting the motion.

(*d*) Some comparisons of impact pitching moment in Ref. 13 in constant-attitude landings show reasonable agreement between experiment and theory.

However, the experimental moments have a small-amplitude high frequency imposed upon them, which was attributed to structural vibrations induced in the equipment.

5.1.1. *Loop plot analysis.* There are, however, discrepancies in detail with theory. Possible implications of these discrepancies are not easily seen from the methods of presentation used in Ref. 13 and these are replotted in Figs. 11, 15, 16 and 17 in terms of acceleration and draught^2 parameters.

Although the peak accelerations, and draughts at peak acceleration and maximum draught agree quite well, the accelerations prior to the maximum tend to be rather low, and subsequent to maximum are rather scattered compared with the calculated figures.

When $K = V_T \sin\tau/V_{v0} = 10{\cdot}27$, a large value, which corresponds to a low impact angle, the discrepancies are greatest. In Ref. 13 it is stated that evidence subsequent to maximum acceleration becomes increasingly unreliable, but the difference during the build-up of the impact experimental and theoretical forces requires explanation.

The results have therefore been replotted for $K = 0{\cdot}48$ and $2{\cdot}0$ cases as acceleration, vertical velocity and draught against time in Figs. 18 to 25, and compared with calculated values.

Fig. 18 shows the measured acceleration/time curve for the $\beta = 22\frac{1}{2}$ deg, $\tau = 3$ deg, $K = 0{\cdot}48$ case, compared with the theoretical curve for the quoted initial conditions.

Fig. 19 shows the measured vertical-velocity variation compared with theory.

Fig. 20 gives the measured draught/time curve, together with curves obtained by integration from the acceleration and vertical-velocity measurements.

The dashed lines above and below the measured curves represent the quoted error limits in the maximum measurement of each quantity.

It will be seen from the scatter of the estimated draught curves of Fig. 20 that the experimental errors must be quite large.

Integration under the measured acceleration/draught curve indicates an initial vertical velocity of $4{\cdot}5$ ft/sec compared with the quoted values of $4{\cdot}91$ ft/sec. Evaluation of the theory with $V_{v0} = 4{\cdot}5$ ft/sec yields the acceleration, velocity and draught histories superimposed as dotted curves on Figs. 18 to 20. It will be seen that this assumption improves the draught/time correlation, but requires a constant shift of about $0{\cdot}5$ ft/sec in the velocity measurement. The difference in initial force build-up is largely accounted for by this change in initial conditions, but the measured peak force is closer to that given by the theory using the quoted initial conditions.

A similar analysis for the $\beta = 30$ deg, $\tau = 6$ deg, $K = 2{\cdot}0$ case (Figs. 21 to 23) indicates less scatter, the discrepancies being generally within quoted accuracy limits.

These two model cases have been further analysed to show the effect of removing the V_v (vertical velocity) component (Figs. 24 and 25) using the general relationship,

$$F(1+\mu) = F_{p\,0}\left[1 + k_1\left(\frac{V_v}{V_H \tan\tau}\right) + k_2\left(\frac{V_v}{V_H \tan\tau}\right)^2\right].$$

The dotted curves have been obtained by factoring the measured acceleration curves by

$$1/\{1 + (V_v/V_H \tan\tau)\}^2$$

using the measured V_v variation to obtain a quantity formally equivalent to pure planing force, $F_{p\,0}$, appropriate to the instantaneously occurring acceleration and measured velocity.

The chain-dotted curves have been obtained by using the Ref. 13 assumptions to calculate the effective $F_{p\,0}$ from the measured draughts, and then multiplying by 1·0 and by $\{1 + (V_v/V_H \tan\tau)\}^2$, where V_v also takes the measured values. This gives the effective planing force and the total impact force at each moment appropriate to the instantaneously occurring measured draught and velocity.

In the $K = 0{\cdot}48$ case (Fig. 24) there is a discrepancy between the measured total impact force and the value calculated from draught and velocity which at the peak amounts to 16 per cent and increases with time. The discrepancy is considerably greater than that between the measured force and the values estimated by the theory of Ref. 13 using the initial conditions but not measured velocities or draughts occurring at subsequent times.

The calculated simple planing force is considerably less than the total impact calculated and measured.

It is also interesting to note that the maximum single planing force obtained from the measured critical impact conditions is only half the value based on measured velocity and draught. As shown by Fig. 7, the use of a different pure planing theory would not substantially alter this discrepancy.

The $K = 2{\cdot}0$ case, Fig. 25, which is nearer to a planing condition, shows qualitatively similar effects but the magnitude of the discrepancies is much less.

It is concluded that the impact theory is predicting the effect of vertical velocity as well as longitudinal velocity on impact conditions satisfactorily; or that the impact force is a function of the simple planing force and the vertical and longitudinal velocities.

It is also clear that experimental values of draught and velocity during impact are rather inaccurate.

5.1.2. *Error analysis.* Extensive experimental values of peak acceleration and time to peak are tabulated in Ref. 13. Figs. 26 and 27 present the ratios of results of experiment to theory for the test results at dead-rise angles of $22\frac{1}{2}$ deg and 30 deg for a range of approach conditions. While the scatter is quite large the arithmetic mean values are seen to be close to 1·0.

Figs. 28 and 29 are histograms for the results of Figs. 26 and 27.

Results correspond roughly to normal distributions of error, with standard deviations $\sigma_R = 0{\cdot}1229$ and 0·1673 for acceleration and time respectively. These deviations assume Sheppard's grouping correction.

Errors in time to peak acceleration. In the notation of Ref. 12, the maximum acceleration and the time at which it occurs is related to the initial conditions by formulae

$$\frac{dV_n}{dt} = -A_0 K^{1/3} V_{n\,0}^2/(W/\rho g)^{1/3}$$

$$t = (B_0/V_{v\,0})(\cos\tau/K)^{1/3}(W/\rho g)^{1/3}$$

where A_0 and B_0 are functions of $1/y_0$ and when τ is small

$$y_0 = 1 + (V_{v0}/V_{H0}\tan\tau).$$

Consider the impact case given in Fig. 25 where the impact conditions resemble those occurring in full-scale landings for initial conditions of

$$\beta = 30 \text{ deg}, \quad \tau = 6 \text{ deg}, \quad V_{H0} = 88{\cdot}9 \text{ ft/sec}, \quad V_{v0} = 4{\cdot}6 \text{ ft/sec}.$$

Then $1/y_0 = 2/3$, and it can easily be shown that

$$\text{Error in } A_0/\text{error in } (V_{v0}/V_{H0}\tan\tau) = 0{\cdot}63$$

$$\text{Error in } B_0/\text{error in } (V_{v0}/V_{H0}\tan\tau) = 0{\cdot}30.$$

At this value of β and τ

$$\text{Error in } K^{1/3}/\text{error in } \tau = 0{\cdot}47$$

$$\text{Error in } (\cos\tau)^{1/3}/\text{error in } \tau = 0{\cdot}10, \text{ and since } V_{n0} = (V_{H0}\sin\tau)\,(1 + V_{v0}/V_{H0}\tan\tau)$$

$$\text{Error in } (1 + V_{v0}/V_{H0}\tan\tau)/\text{error in } (V_{v0}/V_{H0}\tan\tau) \doteqdot 0{\cdot}33.$$

In these model tests τ is fixed so that its error will be very small. Quoted accuracies for the maximum values of other quantities, attained during an impact, and the corresponding percentage errors assumed are

$$V_{v0} = \pm 0{\cdot}2 \text{ ft/sec or } \pm 4{\cdot}3 \text{ per cent},$$

$$V_{H0} = \pm 0{\cdot}5 \text{ ft/sec or } \pm 0{\cdot}6 \text{ per cent},$$

$$\text{draught } h = \pm 0{\cdot}02 \text{ ft or } \pm 4{\cdot}8 \text{ per cent},$$

$$\text{vertical acceleration} = +5 \text{ to } -10 \text{ per cent or } \pm 7{\cdot}5 \text{ per cent}.$$

Assuming $E = AB^2/CD^2$ the standard deviations are related by

$$\sigma_E^2 = \sigma_A^2 + 4\sigma_B^2 + \sigma_C^2 + 4\sigma_D^2.$$

Since at a given probability of error, the error is proportional to the standard deviation (Fig. 14), it follows that if all the quoted accuracies are equally probable, the quoted errors imply the following resultant errors

$$\frac{V_{v0}}{V_{H0}\tan\tau} \pm 4{\cdot}4 \text{ per cent}$$

$$\frac{\text{measured peak acceleration}}{\text{theoretical peak acceleration}} \pm 8{\cdot}6 \text{ per cent}$$

$$\frac{\text{measured time to peak}}{\text{theoretical time to peak}} \pm 4{\cdot}5 \text{ per cent}.$$

At the quoted dispersions of $0{\cdot}123$ and $0{\cdot}167$ the corresponding probabilities of the stated errors being exceeded are 48 and 61 per cent respectively. The time value is perhaps higher because no allowance for error in measured time has been made.

The high probabilities of the quoted errors being exceeded arise in part from using percentage errors expressed in terms of a characteristic case. The actual errors quoted are usually not percentages, *e.g.*, for V_{v0}, $\pm 0{\cdot}2$ ft/sec.

Taking a more vertical impact in which

$$\tau = 60 \text{ deg}, \; V_{H0} = 35{\cdot}4 \text{ ft/sec}, \; V_{v0} = 1{\cdot}59,$$

the percentage errors become

$$V_{v0} \pm 12{\cdot}5 \text{ per cent}$$

$$V_{H0} \pm 1{\cdot}4 \text{ per cent}$$

and

$$\frac{\text{measured peak acceleration}}{\text{theoretical peak acceleration}} \pm 14{\cdot}2 \text{ per cent.}$$

At a standard deviation of 0·123, the probability of the error being exceeded is less than 25 per cent.

Thus the standard deviations of the histograms would seem to imply probabilities of error being exceeded lying in the range 25 to 48 per cent. Perhaps a value of about 33 per cent, which is often used in quoting errors, is therefore appropriate to the model tests.

Errors in acceleration at given attitude, draught and velocity. Another interesting error comparison is between measured acceleration at any moment, and acceleration calculated from instantaneously measured values of attitude, draught and velocity. Assume

$$F = \{F_{p0}/(1+\mu)\}[1 + V_v/V_H \tan\tau]^2$$

where

$$F_{p0} \propto V_H{}^2 h^2 \sin\tau .$$

Taking the moment of peak acceleration, in the characteristic case again, the velocity is at 40 per cent of the initial value, and the draught is about 90 per cent of maximum value.

Errors are therefore at least as much as follows:

$$V_v = \pm 10{\cdot}8 \text{ per cent}$$

$$V_H = \pm 0{\cdot}6 \text{ per cent}$$

$$h = \pm 5{\cdot}3 \text{ per cent}$$

$$\text{acceleration} = \pm 7{\cdot}5 \text{ per cent}$$

$$V_v/V_H \tan\tau = \pm 10{\cdot}8 \text{ per cent}$$

$$1 + V_v/V_H \tan\tau = \pm 1{\cdot}8 \text{ per cent}$$

$$\frac{\text{measured acceleration}}{\text{(acceleration estimated from instantaneous conditions)}} \pm 13{\cdot}5 \text{ per cent,}$$

with a probability of being exceeded at least of order 33 per cent.

The estimated error iso ptimistic, because, as stated in Ref. 13, 'measurements of instantaneous values which require the use of more than one record trace, such as the acceleration at the instant of maximum draught, involve additional errors due to instrument response (primarily lag) and time-correlation difficulties.'

Referring to Fig. 25, the errors estimated as above compare with the actual errors in the particular case as follows, assuming that the theory is correct.

	Actual (per cent)	Estimated (per cent)
$\frac{\text{measured peak acceleration}}{\text{theoretical acceleration}}$	+ 4·1	± 8·6
$\frac{\text{measured time to max. acceleration}}{\text{theoretical time}}$	+ 2·8	± 4·5
$\frac{\text{measured peak acceleration}}{\text{acceleration estimated from instantaneous conditions}}$	− 1·8	± 13·5

Thus the actual errors in this case lie well within the estimated values that have about a 33 per cent probability of being exceeded.

In the Fig. 24 case,

	Actual (per cent)	Estimated (per cent)
$\frac{\text{measured peak acceleration}}{\text{acceleration based on instantaneous conditions}}$	16	17

Thus the discrepancies shown are within the limits of experimental error, at least in the neighbourhood of maximum acceleration.

5.1.3. *Planing and impact data.* It is of interest to compare the pressure distributions found in impact and simple planing cases from the point of view of the analogy postulated between the two in this paper.

Fig. 30 shows some experimental pressure measurements, presented in the form of coefficients, pressure/$\frac{1}{2}\rho(V_H + V_v \cot \tau)^2$.

Fig. 30a compares results obtained on the centreline of a flat plate in planing and impact conditions respectively[29]. They clearly support the view that pressure depends upon an effective forward velocity $V_H + V_v \cot \tau$, impact being analogous to planing at the same attitude with such a velocity.

At 6 deg attitude the scatter of the results, near the trailing edge, disguises the implications, but at 15 deg there is a more definite indication of local trailing-edge differences between planing and impact, as already discussed theoretically in Section 3. However, four other cases given in Ref. 29 are indeterminate in this respect. The peak pressures may be seen to approach a value of unity. Extensive evidence supports this view, but shows the necessity of introducing a correction to the effective velocity to allow for forward pile-up of water (*see* Section 3). This correction is believed to be unimportant when the dead rise is appreciable.

Fig. 30b compares experimental centreline pressure variations for flat plates and 30 deg dead-rise wedges at the same attitudes. The results are taken from Ref. 48. Agreement is moderately good

especially at high attitude, but the stagnation pressures are not achieved, and at low attitude the trailing-edge discrepancy is also considerable. The stagnation pressure on a V-wedge only occurs at the centreline, and along the peak-pressure line there is a rapid fall away to a nearly constant pressure which is sustained across most of the wedge width, *see* Fig. 30c. For this reason the peak centreline value is never obtained experimentally using pressure instruments of finite area.

It will be appreciated from these results that there is good circumstantial evidence for the simple planing-impact analogy but that there are detailed discrepancies which may be particularly serious in the chines out cases, for which little systematic evidence is available.

5.2. *Full-Scale Data.* 5.2.1. *Vought-Sikorsky S*-43. Some full-scale results obtained on the *Vought-Sikorsky S*-43 are given in Figs. 31 and 32[37]. The hull geometry of this aircraft is illustrated in Fig. 31. An analysis of the results in the form experiment/theory for maximum acceleration and time to maximum acceleration is given in Figs. 32 and 33. These are plotted in terms of the ratio of experimental to theoretical values of maximum acceleration and time against an approach angle parameter.

In the case of acceleration the experiment and theory agree within the order of accuracy but there is a very large order of scatter, so long as the chine is not immersed.

In the case of the time to maximum acceleration there are only two measurements but these show the experimental time to be about 1·35 the theoretical time.

5.2.2. *Sunderland.* Analysis of the '*Sunderland*' results, as stated in Ref. 32, shows that

(1) good agreement is achieved between measured maximum impact forces and those predicted by (Refs. 12 and 13) theories,

(2) the shapes of the measured and theoretical force/time curves do not agree. In particular, the measured times to maximum force are up to twice those given by these theories.

Analyses in Ref. 41 indicate that the force developed in the '*Sunderland*' tests is less than the planing force which would be developed in steady planing at the same trim, draught and forward speed.

Analyses in Ref. 44 show that while the scatter is considerable, the results lie roughly about a predicted planing-force value. The apparent discrepancy in these two analyses is probably partly due to the different planing-force assumptions, the former using an empirical planing-lift expression which is about 25 per cent higher than the planing assumption of the latter.

The M.A.E.E. impact cases included the effects of change of incidence. The effect of correcting for this is shown in Fig. 34 using the method of Section 3 of this report.

It will be seen that the trim correction has an increasingly large effect as the impact proceeds but that the corrected loop is anti-clockwise. The corresponding effective planing-force variation with draught, deduced by the assumption, made in applying trim correction, that total force

$$F = \frac{F_{p0}}{(1+\mu)}\left\{1 + \frac{V_v}{V_H \tan\tau} - \frac{h\,\mathrm{cosec}^2\tau}{V_H}\frac{d\tau}{dt}\right\}^2$$

is shown in Fig. 35, and is also anti-clockwise.

If the expected vertical velocity effects were occurring in the M.A.E.E. results, the effective planing force should be the same at a given draught, on both 'arms of the loop'. Suppose, for example, that the part of the curve in Fig. 35, subsequent to maximum draught, where experimental error is known to be large, is in error, and that the effective force both increases and decreases along the lower part of the curve. The loop curve of u'' against $u^2/(1+u^3)$ corrected to initial attitude, given in Fig. 36, is then obtained, and is correctly clockwise, but the local peaking near maximum draught is obviously unrealistic.

These points provide a further illustration to that given in, for example, Figs. 40 and 41, that the expected vertical velocity effects do not appear to be occurring in the M.A.E.E. results.

The following points are also made in Ref. 41:

(1) The maximum experimental impact coincides with the maximum experimental draught, whereas theoretically maximum impact precedes maximum draught.

(2) Despite wide variations in the shape of the experimental and theoretical acceleration/time curves, the two draught/time curves in the first tenth of a second or so are very similar. The measurements of draught generally confirm the experimentally determined values of vertical velocity at touchdown, bearing in mind the possible effects of rotation in pitch. A mildly systematic discrepancy between the draughts determined photographically and by double integration of the acceleration curve and those determined from the pressure pick-ups is shown.

(3) No simple rational correction to the experimental data, such as scaling the elapsed time, will improve the theoretical-experimental correlation. Such scaling to bring the times to peak into agreement makes the peak-acceleration values very different.

Integration under the acceleration/time curves presented in Ref. 34, in conjunction with the quoted initial vertical velocities shows that the associated velocity curves are always consistent, as are the draught curves plotted except for runs 14 and 17 where the draught from the camera record is shown to be different from that obtained by integration.

A comparison of the theoretical total impulses with the experimental values for the complete impacts indicates fairly good agreement, although the experimental values are always somewhat larger (*see* Fig. 37).

A comparison of the experimental and fixed-trim theoretical acceleration, velocity and draught time histories for run 12 is given in Figs. 38 and 39. A theoretical treatment in which the 'pure impact' term F_i is ignored is also shown. It will be seen that the theoretical velocity and draught variations differ appreciably from the measured values, and that neglecting the 'pure impact' term does tend to improve the correlation.

Since the measured vertical velocity and draught variations differ considerably from those predicted by theory using the initial conditions, it is of interest to evaluate the forces which might be expected theoretically at the measured draught and velocity values at each instant.

5.2.3. *Loop-plot analysis.* In Figs. 40 and 41 the run 12 case has been analysed in a manner similar to that discussed in Section 5.1. In Fig. 40 the dashed curve has been obtained by using the Ref. 13 assumptions to calculate the effective F_{p0} from measured draughts and trims, and then multiplying by $\{1 + (V_v/V_H \tan\tau)\}^2$ to obtain F, using the measured V_v values. This gives a predicted

total impact force at each moment appropriate to the instantaneously occurring measured draught and velocity. In these tests rotation in pitch is present. The effect of such rotation is discussed in Section 3, where it is shown that its maximum effect is approximately given by reducing the effective planing velocity by $h \operatorname{cosec}^2 \tau (d\tau/dt)$. The dotted curve on Fig. 40 has been derived in this way. In Fig. 41 the effect of removing the V_v component is illustrated, the dashed curve representing the effective planing force F_{p0} appropriate to the measured draughts and trims while the dotted curve represents the F_{p0} value when corrected for trim rotation as discussed above.

It may be observed from these figures that during the force build-up the measured force is considerably less than the theoretically-predicted total force using the measured draughts and velocities and that the theoretical peak still occurs before the measured peak force (Fig. 40). When the vertical velocity effect is removed (Fig. 41), the predicted force build-up and peak time agree much better with the measured curve. The predicted maximum effect of pitch rotation is seen to reduce the forces appreciably, while not affecting the times to peak, and the best agreement between experiment and theory for this run is obtained when the V_v effect is removed and the rotation effect is included in the theory. It may be noted that in the similar analysis of model results given in Figs. 24 and 25, removal of the V_v effect in the theoretical prediction reduced the agreement between theory and experiment.

A similar analysis to that discussed above is repeated in Figs. 42 to 45 for the run 17 case. It will be seen from Figs. 44 and 45 that the measured force in this case is again considerably less than theoretically-predicted values using the measured velocities and draughts. It may be noted that two draught curves are presented in Ref. 34 for this run, and for run 14, one curve having been derived by integration and the other obtained from the camera record. In the analyses given here the former curve, which indicates the smaller instantaneous draughts, has been used in the prediction of theoretical force values. While the theoretical treatment ignoring V_v gives fairly good force agreement at the beginning of the impact, thereafter it is considerably higher than measurement and reaches a peak value after a somewhat greater time (Fig. 45).

Figs. 46 to 49 repeat the analysis for run 14. In this case the predicted total-force curves are fairly similar in form to the measured curve, although somewhat higher (Fig. 48). A treatment ignoring V_v effects gives very good agreement in force build-up but predicts a somewhat higher time to peak and higher forces thereafter (Fig. 49).

In Figs. 50 and 51 a comparison of the Ref. 34 experiment with theory for maximum acceleration and time to maximum acceleration is given. It will be seen that, while the acceleration results are scattered, in general they tend to support the theory. The marked increase in time to peak is evident from Fig. 51. Unlike other results examined, the experimental time is never less than the theoretical value.

5.2.4. *Error analysis.* Histograms for the '*Sunderland*' results are given in Fig. 52. If these results are represented by normal distributions of error, the standard deviations are $\sigma_R = 0{\cdot}275$ and $0{\cdot}254$ for acceleration and time respectively.

It will be appreciated that the number of experimental cases available is far too small to make a reliable statistical assessment, hence the very approximate agreement between the histograms and the corresponding normal curves.

The methods of analysis described under the model-experiment comparison have been applied to the full-scale runs 17 and 14 shown in Figs. 42 to 45 and 46 to 49 respectively.

The conditions of the runs, the accuracies quoted in Ref. 34, and the corresponding percentage errors are as follows:

		Run 14		Run 17	
Quantity	Accuracy	Measured Quantity	Error (per cent)	Measured Quantity	Error (per cent)
Initial conditions and peak acceleration					
Attitude, τ_0	$\pm 0{\cdot}5°$	$4{\cdot}3°$	± 17	$3{\cdot}2°$	$\pm 15{\cdot}6$
$V_{v\,0}$	$\pm 1{\cdot}0$ ft/sec	5 ft/sec	± 20	$5{\cdot}8$ ft/sec	$\pm 17{\cdot}2$
$V_{H\,0}$	$\pm 2{\cdot}0$ ft/sec	128 ft/sec	$\pm\ 1{\cdot}6$	159 ft/sec	$\pm\ 1{\cdot}3$
Time, t	$\pm 0{\cdot}1\%$	—	$\pm\ 0{\cdot}1$	—	$\pm\ 0{\cdot}1$
Acceleration	$\pm 0{\cdot}1g$	$0{\cdot}7g$	$\pm 14{\cdot}3$	$0{\cdot}78g$	$\pm 12{\cdot}8$
Instantaneous conditions at time when theoretical peak occurs					
τ	$\pm 0{\cdot}5°$	$4{\cdot}6°$	$\pm 10{\cdot}8$	$3{\cdot}6°$	$\pm 13{\cdot}9$
draught, h	$\pm 0{\cdot}2$ ft	$1{\cdot}09$ ft	$\pm 18{\cdot}4$	$1{\cdot}12$ ft	$\pm 17{\cdot}8$
V_v	± 1 ft/sec	$2{\cdot}9$ ft/sec	$\pm 34{\cdot}4$	$4{\cdot}8$ ft/sec	$\pm 20{\cdot}8$
V_H	± 2 ft/sec	128 ft/sec	$\pm\ 1{\cdot}6$	159 ft/sec	$\pm\ 1{\cdot}3$
acceleration	$\pm 0{\cdot}1g$	$0{\cdot}62g$	$\pm 16{\cdot}1$	$0{\cdot}5g$	$\pm 20{\cdot}0$

The results obtained are:

	Run 14		Run 17	
	Estimated (per cent)	Discrepancy actually occurring (per cent)	Estimated (per cent)	Discrepancy actually occurring (per cent)
$\frac{\text{measured peak acceleration}}{\text{theoretical acceleration}}$	± 29	$+\ 2$	± 26	-13
$\frac{\text{measured time to peak acceleration}}{\text{theoretical time}}$	± 23	$+25$	± 19	$+68$
$\frac{\text{measured peak acceleration}}{\text{acceleration estimated from instantaneous conditions}}$	± 45	-61	± 46	-66

Consideration of these results with the histograms of Fig. 52 indicates that the probabilities for the given limits to be exceeded are as follows:

	Mean estimated error for runs 14 and 17	Standard deviation of histogram	Probability (per cent)
$\frac{\text{measured peak acceleration}}{\text{theoretical acceleration}}$	$\pm 27{\cdot}5$	$0{\cdot}275$	$32{\cdot}0$
$\frac{\text{measured time to peak acceleration}}{\text{theoretical time}}$	$\pm 21{\cdot}0$	$0{\cdot}254$	$41{\cdot}0$

5.2.5. *Martin Model* 270. The shape of this hull is given in Fig. 62. The results of the two impacts given in Ref. 38 are reproduced in Figs. 63. There is considerable scatter, of the same order as for the *Sunderland*, as would be expected of full-scale measurements. The effect of change of trim has not been calculated but it is not thought this would reduce this scatter.

A comparison of these experimental times, Fig. 63, to peak acceleration with the calculated values using the method of Ref. 12, gives ratios of $1{\cdot}37$ and $1{\cdot}30$.

In Ref. 38 an empirical pressure-distribution theory is used to predict planing forces on arbitrary bottom shapes. Predictions by this method for simple V-wedges with chine flare appear to give good agreement with the experimental results of Refs. 24 and 65. The force in impact then appears to be obtainable by multiplying the planing force by

$$\left(1 + \frac{V_v}{V_H \tan \tau}\right)^2.$$

The basic theory is therefore seen to be similar to the current impact theories discussed in this report except that it does introduce empirical terms to allow for the effect of a complex bottom shape on the forces.

The curve of peak acceleration obtained by the Ref. 38 treatment for a rigid aircraft is seen to be considerably lower than the Ref. 13 theory (Fig. 63). It may be concluded that, unless too many approximations have been introduced in Ref. 38, the reason for the difference is due to the complex bottom shape of the *M* 270. A direct comparison of a time-history solution by the Ref. 38 treatment and by the Ref. 13 theory is shown in Fig. 64. It may be noted that the Ref. 38 treatment does give the same curve shape and peak times as that actually measured full-scale, so that it would appear likely that the various factors introduced to represent the complex bottom shape can cause a considerable shift in peak time from simple wedge treatments.

The Ref. 38 treatment is of particular interest in that it combines the hydrodynamic and structural flexibility effects for a complex system into one set of equations, including chine immersion and trim freedom. However, even with simplifications, this makes analogue-computer solution desirable.

5.3. *Conclusions.* In the comparison of theoretical results given in Section 2 with experimental data it may be concluded that

(*a*) In both the model and full-scale cases, the quoted limits of accuracy have a probability of being exceeded of about 33 per cent.

(*b*) The full-scale cases have much the higher experimental errors, *e.g.*,

Item	Model (per cent)	Full scale [average of runs 14 and 17 cases above] (per cent)
	negligible	±12·4
V_v estimated (measured acceleration)	±10·8	±27·6
error in (acceleration based on instantaneous conditions)	±13·5	±45·5

(*c*) The full-scale experimental values for peak acceleration agree very well with theory within the limits of accuracy existing.

(*d*) The full-scale experimental times to peak acceleration are, to the accuracies of measurement existing, consistent with the argument that the theoretical values are exceeded in a constant ratio of 1·75 (Fig. 47).

(*e*) The estimated total-impact forces, and even the simple planing forces, calculated from instantaneous velocities, attitudes and draughts, in general exceed the measured values by appreciably more than 33 per cent probable error would predict.

(*f*) The impact forces calculated from pressure distribution adjusted for detail hull shape give reasonable agreement with measured full-scale impacts on the cases of the *Martin*. The basic theory is similar to that reviewed in this note but arbitrarily adjusted for detail hull geometry, *e.g.*, including the effect of vertical velocity.

The comparison with Ref. 13 theory does, however, point to a 35 per cent greater time full scale than theory, which result indicates the possible importance of the departure of hull geometry from that of the simple wedge.

6. *Possible Sources of Discrepancy between Experiment and Theory.* 6.1. *Hull-Bottom Geometry; Including Chine Immersion and Afterbody Suction Effects. Sunderland.* The main geometrical differences between the *Sunderland V* aircraft employed in the full-scale tests at Felixstowe, and the models used in the systematic N.A.C.A. tests, are illustrated in Figs. 1a and 53 and are tabulated below:

	Model	Full Scale
Step planform	straight transverse	*V*
Step fairing	none	faired
Afterbody	absent	present
Lateral cross-section of bottom	straight	curved

In both cases the hulls were made of riveted aluminium alloy, and the keel and chine lines had some longitudinal curvature towards the bow.

Care was exercised during the design and construction of the models to obtain a reasonably smooth finish (Ref. 3).

The bottom of the full-scale hull was in general flush riveted, but it was rather rough and distorted compared with the models. (Ref. 31.)

Effect of V planform step. It is suggested in Ref. 12 that the effect of a faired planform step could be approximated to by assuming a straight transverse step of the same draught. This has been done in the theoretical estimates of *Sunderland V* behaviour given in the present report.

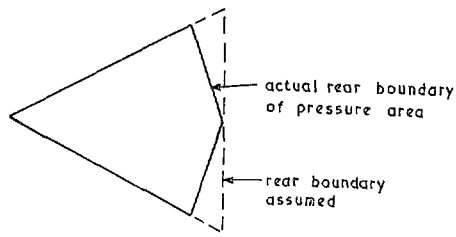

A more accurate approach, also suggested in Ref. 12, might be to use the value of (area)^2/perimeter appropriate to the actual quadrilateral projected pressure area, in calculating the associated mass coefficient μ (*see* the Section 3 discussion of Ref. 12 theory). In the case of a straight V-step, such as that of the *Sunderland*, the associated mass obtained varies as (draught)^3, and the Ref. 12 method of evaluating impact can be applied directly, only the numerical value of the associated mass parameter K being altered. The effect of this as compared with a straight transverse step of the same draught was considered in Ref. 32 for a typical full-scale case. The associated mass of the V-step was found to be 86 per cent of that of the straight transverse step, leading to a 5 per cent reduction of theoretical peak acceleration and 5 per cent increase of time to peak acceleration respectively.

Unpublished Saunders-Roe calculations used a different approach. The pressure areas were approximated to by areas appropriate to chines-wet conditions of V-wedges with straight transverse steps, *viz.*,

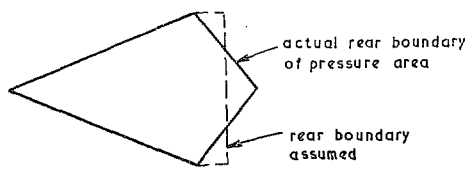

An effective associated mass was used related to the planing force appropriate to the corresponding chines in V-wedge by

$$F_v = \left(\frac{V_v}{V_H \sin \tau}\right)^2 F_{p\,0} \text{ (\textit{see} Section 3).}$$

Since the quantity obtained did not vary simply as (draught)^3 it was necessary to perform the calculation by iteration. The effect on peak-acceleration conditions was again small, acceleration being reduced by 4 per cent, and time increased by 4 per cent.

A considerably more pointed step can of course have a big effect, at least in small dead-rise cases. This has been considered for hydro-skis in Refs. 54 and 55. Fig. 54 from the former report indicates

a large increase in time to peak acceleration, as the step pointing increases, coupled with a minor decrease in the acceleration itself. For example, in the case shown a 60 deg included angle step gives a 9 per cent reduction in acceleration and a 70 per cent increase in time. This type of behaviour has been confirmed by model tests.

Is it possible that the fairing of the *Sunderland* step produces a sharp-pointed-step effect?

Effect of afterbody and step fairing. Model tests on a float with an afterbody, described in Ref. 23, appeared to show little effect due to afterbody in main-step impacts. However, it should be noted that the float bottom was scalloped in cross-section and the step was unfaired, of straight transverse planform. The scalloping complicates the application of the theory, and the degree of agreement obtained may have been to some extent fortuitous.

It was stated in Ref. 32 that ". . . afterbody interference may occur in main-step landings which outwardly satisfy the theoretical conditions. In such impacts a suction force of considerable magnitude may be present on the afterbody, particularly with faired steps. With extreme fairings such forces cause violent instability at touch-down (Refs. 56 and 57). Although there is little evidence of such instability on the 'Sunderland', there may be suction forces present which are sufficiently great to modify the acceleration-time build-up. In the absence of any full-scale data on the magnitude of these afterbody forces no attempt has been made to calculate their possible effect. At some later stage in the complete full-scale impact investigation afterbody forces will be measured."

The subsequent published measurements of afterbody pressure are contained in Refs. 35 and 36. The first gives detailed results for landings at high attitudes around 8 deg or more. At attitudes greater than 9 deg the rear step touches first, while around 8 deg the afterbody still has an important effect of a type differing from any that it might exert in normal main-step impacts. Ref. 36 is concerned mainly with landings in rough water, the one calm-water case given being at an attitude greater than 9 deg. Thus, unless there are unpublished results, adequate measurements of afterbody suctions occurring in normal main-step impacts have not yet been obtained.

Ref. 50 gave a preliminary discussion of the effects of modifications to the Ref. 12 theoretical impact force, by omission of component terms. This concept has been extended in unpublished Saunders-Roe studies to determine the effects of arbitrary suction components. Results are shown in Figs. 55, 56 and 57. It should be noted that in these figures A and B equal $F_i(g/W)$ and $F_p(g/W)$ respectively, where F_i and F_p are as in Section 3 of the present report, with Ref. 12 specific values.

In Fig. 56 a suction force of form $-2F_i$ is assumed so that the total force acting is of form

$$F_p + F_i - 2F_i = F_p - F_i.$$

It should be noted that the resulting 'B' acceleration component is not equal and opposite in magnitude to that of the normal case shown in Fig. 55, because the instantaneous values of velocity and draught on which it depends, differ in the two cases, at any given moment. The peak acceleration and time to peak acceleration are increased by 90 and 70 per cent respectively.

In Fig. 57 a suction force of form $-3F_i/2$ is taken. The peak acceleration and time to peak acceleration are increased by 28 and 51 per cent respectively. The corresponding k values (of Section 3) are nearly enough as follows:

Fig. 56, $$F(1+\mu) = F_{p0}\left[1 - \left(\frac{V_v}{V_H \tan\tau}\right)^2\right], k_1 = 0,\ k_2 = 1$$

Fig. 57, $$F(1+\mu) = F_{p0}\left[1 + \tfrac{1}{2}\left(\frac{V_v}{V_H \tan\tau}\right) - \tfrac{1}{2}\left(\frac{V_v}{V_H \tan\tau}\right)^2\right], k_1 = \tfrac{1}{2},\ k_2 = -\tfrac{1}{2}.$$

It will be seen that a reduced rate of build-up of acceleration and an increased time to peak acceleration can be obtained if suction is present. The maximum accelerations obtained are much higher than the measured values, but this might be overcome by a more sophisticated method of allowing for suction. For example, as the craft begins to rebound the water is likely to break free from the afterbody and the suction disappear.

In Ref. 35 maximum suctions approaching -10 p.s.i. were recorded about 0·2 seconds from first contact over areas of some 35 square feet immediately behind the step; the attitudes being 8 deg or more. The corresponding acceleration component would be of order $1 \cdot 0g$.

It is concluded that suction is likely to have an appreciable effect in reducing the rate of build-up of impact acceleration even at lower attitudes, but almost certainly does not provide a complete explanation of the discrepancy.

More full-scale measurements of afterbody impact pressures during main-step landings would seem to be required.

Effect of chine immersion. Very little information comparing impact behaviour chines immersed with that which would have occurred in the absence of chine immersion appears to have been published. A discussion of the effect on peak acceleration is given in Ref. 13, a relief being obtained. Ref. 14 suggests that at least for 10 deg dead rise, the chines immerse at a smaller draught than predicted in Ref. 13, and the effect is to increase the time to peak acceleration. Increases in time above the chines-out theoretical value of up to about 35 per cent were obtained. The evidence is however inconclusive since draught discrepancies with theory were found in all cases, whether the chines were immersed or not.

Ref. 32 states with regard to the M.A.E.E. tests that 'The presence of chine immersion appears to have no consistent effect on either maximum acceleration or time results. When it does occur the chine immersion is small and takes place well after the theoretical time of maximum acceleration'.

Of the full-scale main-step impacts considered in Figs. 50 and 51 of the present report, only run 18 is known to have sustained chine immersion prior to peak acceleration, and this occurred about midway between the theoretical and experimental times to peak acceleration[32]. This has been confirmed by the unusual trend of the accelerations in this case, when compared with values estimated from instantaneous draught and velocity, using chines-out assumptions.

In Ref. 41, estimates of draught variations with time were made from evidence on time of arrival of pressure peaks at various hull-bottom pressure pick-ups, given in Refs. 32 and 34. The estimates depended on assuming a water pile-up based on theory and model experiment. The values of draught obtained were in general about 14 per cent less than those given by photographic records or double integration of the acceleration curves. If unexpectedly large pile-up of water occurred, leading to chine immersion at low draught, the draught values estimated from pressure records would be discrepantly large. *See* also Section 6.6.

A large pile-up would also be expected to cause a high value of force in terms of draught below still water, whereas low values are in fact obtained (*see e.g.*, the Fig. 41 comparison between $F_{p\,0}/W$ curves and the experimental accelerations).

It is concluded that chine immersion cannot explain the discrepancy.

Lateral bottom curvature. The *Sunderland* dead rise varies from 30 deg at the keel to 19 deg at the chine. In Ref. 32 a theoretical computation was made at a constant angle of 30 deg as well as the 26 deg usually assumed. The acceleration curve at the higher angle showed slightly better agreement with theory than the other (Fig. 58), the peak acceleration being reduced by 12 per cent and the time increased by 9 per cent.

It is concluded that a small part of the discrepancy arises from a simplified dead-rise assumption.

Longitudinal curvature towards the bow. Ref. 32 states that the effect of this may immediately be discounted since the curved portion is rarely immersed before the instant of maximum acceleration.

Martin Model 270. This hull has got extreme values of pointed step, fairing in side elevation, high chine immersion during impact with deep draught. The effects of these are accounted for with apparent success by basing the simple-planing forces on arbitrary pressure distributions factored for these parameters. This force is then factored to allow for vertical velocity in the same way basically as in the Ref. 13 theory and successfully gives the measured values at the right time. The theoretical time of Ref. 13 is brought forward 30 per cent by this treatment.

6.2. *Airframe Elasticity.* The effects of elasticity of the wing in bending could increase the time to peak acceleration up to twice the static-wing value, depending on the assumptions made for the distribution of mass in the system and the natural frequency.

Using a mass ratio of 1·0 between the wings and hull bottom, and frequency of 2·5 c/s, Collar has shown that the time could be doubled (Ref. 51).

Using a similar mass ratio of 0·2 and a frequency of 3·5 c/s, Dr. Williams has shown the effect is only about 7 per cent (Ref. 50).

Investigations of the present authors suggest that the assumptions for mass ratio and natural frequency used by Dr. Williams are, in fact, about correct for the *Sunderland.*

Using these the effect of wing bending in the *Sunderland* is shown in Fig. 59. The peak acceleration is increased by 3 per cent and the time to peak by 7 per cent.

It has been argued that vibration in the wing harmonics might be a possible cause of discrepancy. However, solutions for frequencies of 3·5 and 7·0 in Ref. 50 indicate that a superposition of fundamental and 1st harmonic vibration could not produce the experimental curves.

The idea of a more complicated three-mass system has also been considered but depends upon the presence of hull flexing, which does not appear valid for the *Sunderland.*

The introduction of damping in the wing-body connection should have negligible effect since the elastic system investigations show little difference between rigid body (full damped) and two-mass undamped systems.

It has been suggested that the hull-bottom plating might part locally, with reasonably low frequency, due to association of water mass in the phenomenon, but Dr. Williams considered that it would be a secondary effect.

The M.A.E.E. accelerometers were all along the wing main spar, whereas in American full-scale tests the instruments were mounted low in the hull so as to give the bottom motion directly. However, in the British tests of Ref. 9, an accelerometer was mounted on the keelson, and agreed in readings with the wing-mounted instruments.

The results on the *Martin* 270 showed a reduction of 7 per cent in the peak acceleration for the effect of flexibility.

It is concluded that airframe elasticity accounts for only a small part of the discrepancy between theory and measurement.

6.3. *Aerodynamic Lift.* Some theoretical aspects of aerodynamic lift effect have been discussed in Section 3.

A calculation of the effect of loss of vertical velocity on wing lift is shown for the M.A.E.E. run 17

case in Fig. 60. The peak acceleration is reduced by 11 per cent and the time to peak reduced by 5 per cent. A similar analysis for run 12 gave 8 and 3 per cent respectively.

In Ref. 45 a similar, but independent, analysis has been made for run 18. The acceleration and time reductions are 6 and 1 per cent respectively.

The reduction in wing lift during the impact was only 10 per cent in the last case, and similar values would also be true of the others.

A more realistic loss of lift would be one third and this is shown in Fig. 46 to lead to a 9 per cent reduction in acceleration and a 15 per cent increase in time.

Ground cushioning effects are considered unlikely to be important.

Wing flexibility in torsion may have an effect on wing lift, but the effect is likely to be small.

It is concluded that aerodynamic-lift variation might account for a small part of the discrepancy between theory and measurement.

6.4. *Accuracy of Experimental Measurements.* The statistical analyses of Section 5 indicate that:

(*a*) in both the model and full-scale experiments the quoted errors of measurement have a probability of being exceeded of about 33 per cent,

(*b*) the full-scale experimental scatter is nearly twice as great as in the model case.

Additional errors are introduced by inaccuracy of trim measurement full scale (the model is fixed in trim).

Discrepancies between the model experiments and theory can in general be explained by inaccuracies of measurement. Differences between apparent theoretical acceleration and experiment prior to peak may arise from basing the theory on a slightly erroneous value of initial vertical velocity.

The agreement between full-scale and theoretical peak accelerations is within the limits of experimental error. The times to peak acceleration exceed the theoretical values by a constant ratio of 1·75, within the limits of experimental error. This is a discrepancy of the order 0·15 seconds.

The possibility of an experimental time-base shift of this order was felt to be unlikely. The possible error in the initial point of contact due to using the pressure signal from a pick-up not located directly at the step was considered. It was decided that this could cause an error of up to 0·1 sec —but that this effect would be to make the experimental time peak occur even later.

On the other hand, the comparisons of total impulse show the experimental values to be about 12 per cent too high. This discrepancy could be removed by a 12 per cent effective shrinkage of the time base, assuming that the accelerations remained virtually unaltered. The corresponding reduction in time to peak acceleration might be of order 0·05 seconds, but the suggestion is very tentative.

The accelerations calculated from instantaneous velocities, attitudes and draughts, in general differ from full-scale measured values by appreciably more than can be explained by experimental error. However, about two-thirds of the discrepancy could be accounted for by systematic errors in velocity and draught, within the experimental accuracies claimed.

Fig. 61 gives results of interest in this connection. Any given velocity variation with time can be reduced by a constant velocity increment without altering the slope, and thus the acceleration. The corresponding draught does however reduce, and there is an accumulative reduction in the corresponding impact force calculated from the simultaneously occurring velocity and draught conditions.

The 1·5 ft/sec reduction in velocity assumed in Fig. 61 is half as much again as the 33 per cent probability experimental error, and causes a reduction in draught of some 33 per cent. The estimated

peak impact force is reduced almost to the experimental value, from having been almost $2\frac{1}{3}$ times too large, Fig. 44.

The experimental draughts estimated from pressure recorder evidence[41] are on the average about 14 per cent less than those published in the reports presenting the experimental evidence. Such a draught discrepancy would correspond to a vertical velocity increment of about 11 per cent of the initial value. This lies well within the 33 per cent probability error in velocity of $\pm$ 20 per cent. Fig. 20 shows how an 8 per cent reduction in initial vertical velocity can cause a 12 per cent reduction in theoretical peak acceleration, and a 9 per cent increase in time.

It is tentatively concluded that systematic errors in velocity and draught measurements are occurring and are causing the theoretical estimates of peak acceleration and time to be about 17 per cent high and 12 per cent low respectively.

6.5. *Rotation in Pitch.* Some remarks on theoretical effects of rotation in pitch are given in Section 3.

The elaborate theory of Ref. 20 shows little effect, but this is not surprising since the trim variations assumed were negligible. The model experimental results presented in the same reference are inconclusive and scattered. Unlike the *Sunderland* tests, the rotations occurring were initially nose down.

The simplified theory of Section 3 is applied to the evaluation of accelerations corresponding to the instantaneous values of draught, trim and velocities in Figs. 42, 44 and 48. These indicate that the theoretical peak acceleration at a given geometrical condition might be reduced by not more than 15 per cent in an extreme case. This reduces the discrepancy with experiment. Unfortunately it has not yet been possible to make a calculation, using the simplified theory, to determine the effect of rotation on a time history, assuming only initial conditions, but on the basis that nose-up rotation reduces the general level of acceleration, whereas the impulse under the curve, up to maximum draught point, must remain constant, it is reasonable to assume an increase in time to peak acceleration of about 9 per cent in the case of the *Sunderland.*

6.6. *Hydrodynamic Scale Effects.* Hydrodynamic 'scale effects' might possibly arise due to lack of steadiness in the full-scale tests as compared with the model. It is well known that the glassy spray blisters seen in the tank are replaced by a billowing mist and broken water in the case of an actual aircraft.

Possible differences are:

(*a*) Pile-up of the water adjacent to the hull bottom.

(*b*) Failure to establish the correct theoretical flow conditions in the initial stages of the impact.

The former point has already been mentioned in Section 6.1. In the Ref. 41 estimates, the relationship between draught and pressure indications at recorders away from the centreline of the craft was obtained by assuming a theoretical pile-up, of about $\pi/2$ (Ref. 59). This assumption is supported by planing experiments. The degree of agreement between the draughts so obtained and values from the photographic records and from double integration of the acceleration curves is sufficient to conclude that model and full-scale water pile-up is similar and that both are consistent with theory.

With regard to failure to establish flow conditions, if the 'pure impact' effects, represented by F_i of Section 3, took time to become established, and could be neglected, the theoretical estimate

would approach closer to experiment. This is illustrated by conditions appropriate to case 12 shown in Fig. 38. The peak acceleration and time to peak are increased by 7 and 30 per cent respectively.

A total elimination of vertical velocity effects might give a better agreement between theory and full-scale experiment. This is illustrated by Figs. 41, 45 and 49, which show theoretical forces estimated from instantaneously occurring draughts and attitudes, but ignoring vertical velocity.

The estimated times to peak acceleration exceed the experimental values, often by quite appreciable amounts. A partial but considerable loss of vertical velocity would therefore give better agreement still.

It must be remembered however that the model experiments do not justify any such departures from the theories of Refs. 12, 13 and 40.

6.7. *Other Effects.* In the Marine Aircraft Experimental Establishment test runs were made in calm water, with 6 in. wavelets at the most. Such waves would cause a time error of the order 0·1 sec, but would be expected to give random scatter rather than a constant time-base shift.

7. *Concluding Remarks. Discrepancy between theory and full-scale tests.* Detailed analysis of acceleration against time plots, and a statistical assessment of the effects of experimental error, indicate that :

(*a*) The model experiment and theory are consistent within the accuracy with which the tests were made. This accuracy needs to be improved however, if the theory is to receive final confirmation during the rebound phase.

(*b*) No one possible source of discrepancy between the simple V-wedge theory and the *Sunderland* full-scale experiments is capable of providing a complete explanation on its own.

(*c*) A difference of 30 per cent in time to peak acceleration has been accounted for in the *Martin* 410 analyses by making arbitrary changes to the simple planing force to allow for a hull form which is very different from a wedge in planform and immersed planform.

It therefore appears that a number of causes may each provide an increment towards the total discrepancy found in the *Sunderland* tests.

This is illustrated by the table on pages 33–34, which summarises the Section 6 evidence. However, it is important to note that this evidence has been obtained from the study of a few specific cases, and so is indicative only.

It is interesting to consider the total result of a reasonable combination of the effects tabulated. For example:

Cause	*Factor on acceleration*	*Factor on time*
V-step	0·95	1·05
Lateral bottom curvature	0·94	1·04
Airframe elasticity	1·03	1·07
Aerodynamic lift constant at say 5/6 weight	0·96	1·07
Rotation in pitch	0·92	1·05
Total	0·81	1·32

Reason for discrepancy	Cases Evaluated	Percentage change produced		Remarks
		Peak Acceleration	Time to Peak	
V-step planform	*Sunderland V* step *cf.* straight transverse step at $\tau = 5$ deg	− 5	+ 5	Geometrical consideration—*see* Appendix III of Ref. 32.
	Run 17	− 4	+ 4	Unpublished Saunders-Roe results obtained by iteration.
Effectively more pointed step	Flat plate, with 60 deg included-angle step	− 9	+70	*See* Fig. 54. Such an effect might be produced by the *Sunderland* step fairing, although the percentage changes would probably be much less on a V-bottom.
Suction	Run 17	+90 +28	+70 +51	*See* Figs. 51 and 52. These values are obtained using arbitrary suction components. It is felt that changes up to the order shown by Fig. 52 could well be achieved in practice.
Chine immersion	—	—	—	Negligible effect.
Lateral bottom curvature	Run 18	−12	+ 9	*See* Fig. 56. Effect of assuming 30 deg dead rise instead of the usual mean value of 26 deg (dead rise varies between 30 deg at keel and 19 deg at chine).
Longitudinal curvature towards bow	—	—	—	Negligible, this portion of bottom rarely immersed.
Airframe elasticity	Run 17	+ 3	+ 7	*See* Fig. 55, and calculations for various assumptions given in Ref. 50.
Hull-bottom flexibility	—	—	—	This appears negligible—*see* Fig. 14 of Ref. 9.

Reason for discrepancy	Cases Evaluated	Percentage change produced		Remarks
		Peak Acceleration	Time to Peak	
Aerodynamic lift	Run 17	−11	− 5	*See* Fig. 53
	Run 12	− 8	− 3	Unpublished result
	Run 18	− 6	− 1	*See* Ref. 45.
				Calculations using the lift reduction with vertical velocity reduction.
	V-wedge in vertical drop	− 9	+15	Assuming constant $W/3$ lift deficiency.
Accuracy of acceleration measurement	—	±13	± 0·1	From accuracies given in Ref. 34.
Systematic errors of measurement of velocity and draught	Model and *Sunderland* results	+17	−12	*See* Figs. 18 to 20 and 24, pressure record draughts of Ref. 41, Figs. 34 to 45 giving forces estimated at instantaneous quoted values of velocity and draught and Fig. 57 showing the effect of a constant velocity change. The quoted percentage changes are tentative values only.
Systematic time error	*Sunderland* results	—	±12	This is a very tentative value based on total impulse comparisons given in Fig. 33.
Rotation in pitch	Runs 12, 14 and 17	−15	+ 9	*See* Figs. 36, 40 and 44. These percentage changes are believed to be maximum values likely.
Hydrodynamic scale effects	Runs 12, 14 and 17	+ 7	+30	*See* Fig. 34—if 'pure impact' effects are delayed or not present. *See* also Figs. 37, 41 and 45 for estimated forces using instantaneously occurring draughts and attitude but ignoring vertical velocity.

The reduction in acceleration brings it outside the 33 per cent probable error limits, which are about ± 13 per cent. Allowance for a systematic error in initial velocity would reduce the acceleration factor to 0·67, while increasing the time factor only to say 1·36. However, a relatively small suction effect could by itself cause factor changes of 1·16 and 1·32 for acceleration and time respectively bringing the total factors to 0·97 and 1·74.

It is concluded that a combination of relatively small known effects may well explain the discrepancy occurring.

Geometry, aerodynamic lift, airframe elasticity and rotation in pitch together do not appear sufficient to explain the whole discrepancy.

There is considerable evidence indicating that systematic errors in velocity and draught measurement may be present. These make comparisons between experimental forces and estimates, based on instantaneously occurring draughts and velocities, of very little direct use. However, the systematic errors do not greatly affect time to peak acceleration.

The residual discrepancy can easily be explained if a fairly modest amount of afterbody suction is present or if the water flow is much different from that of the simple-wedge treatment. Evidence for the latter is given by the *Martin* 270 tests results and theoretical treatment and also possibly by the conclusions of Ref. 60 that the simple associated mass can be in error in that this cannot be calculated on the basis of quasi-static values of speed, draught and incidence.

LIST OF SYMBOLS

A, B, C, G, H, Q — Constants for associated masses and moments of inertia in general hydrodynamic expression of Ref. 39 (*see* Section 3 and Fig. 1b). When $V_T = q = 0$, A is an associated mass in V_n direction

A or m_s, B or m_L — Sprung masses in two-mass system, upper and lower masses respectively

A, B — Constants in Ref. 50 assumption that $F = (W/g)(A\ddot{z}^2\dot{z} + B\dot{z}^2)$

A_0, B_0 — Maximum acceleration and time to maximum acceleration factors of Ref. 12

a, b — Constants in Ref. 51 assumption that $F = (W/g)(a\ddot{z} + b\dot{z})$

b — Beam

c — Half wetted width, *see* Appendix I

F — Total hydrodynamic force $= F_i + F_p + V_v V_T \dfrac{dB}{dh}$

A general expression from impact theories is

$$F(1+\mu) = F_{pe}\left[k_3 + k_1\left(\frac{V_v}{V_H \tan\tau}\right) + k_2\left(\frac{V_v}{V_H \tan\tau}\right)^2\right]$$

where, except for Ref. 43, $k_3 = 1{\cdot}0$ and $F_{pe} = F_{p0}$ and k_1, k_2 are constants

F_i — Values of F when $V_T = 0$, *i.e.*, pure impact cases

F_{p0} — Value of F when $V_v = 0$, $V_H =$ constant, *i.e.*, pure planing

F_p — Impact-planing forces, $\dfrac{\kappa}{\kappa_p}\left(1 - \dfrac{V_v \tan\tau}{V_H}\right) F_{p0}$

$F_p = F_{p0}$ when $V_v = 0$. κ, κ_p are circulation constants

F_v — Associated mass force for vertical drops $= V_v^2 \cos\tau \dfrac{dA}{dh}$

f_n — Natural bending frequency, c/s

g — Acceleration due to gravity, $32{\cdot}2$ ft/sec^2

h — Draught normal to water surface

K — Associated mass factor of Ref. 12

K, K_1, K_2, k_0, k_1 — Spring constants, lb/ft deflection

L — Wetted length, *see* Appendix I

M — Total mass $= m_s + m_L$ (2-mass system) $= W/g$

m_1, m_3 — Sprung masses, 3-mass system

n	$m_L/m_s = 1/r$
p	Pressure
q	Angular velocity, $d\tau/dt$, $\dot{\tau}$
r	Mass ratio $= m_s/m_L$
T, V	Kinetic and potential energies of sprung system
t	Time, sec
u	Generalized displacement of Ref. 13 $= \mu^{1/3}$
u'	Generalized velocity of Ref. 13 $= V_v/V_{v0}$
u''	Generalized acceleration of Ref. 13 $= \dfrac{dV_v}{dt}\Big/ V_{v0}{}^2\Lambda$
V_n, V_T	Component velocities, normal and parallel to keel respectively. Suffix 0 denotes initial values of V_n
V_v, V_H	Component velocities, normal and parallel to water surface respectively. Suffix 0 denotes initial values
W	Weight
x, x_0	Displacement of m_s, m_1, A
x_s	Distance from step heel to c.g., measured parallel to keel, Fig. 6
y_0	Approach parameter of Ref. 12 $\doteq \left(1 + \dfrac{V_{v0}}{V_{H0}\tan\tau}\right)$
	$1/y_0 \equiv \kappa/(\kappa+1)$ where κ is approach parameter of Ref. 13
$\ddot{y}_n$	Nodal or c.g. acceleration, sprung systems
z, x_1	Displacement of m_L, m_3, B
z_s	Distance from keel to c.g. measured normal to keel, Fig. 6
β	Dead-rise angle
γ	Flight-path angle $= \tan^{-1}(V_v/V_H)$
κ	Approach parameter of Ref. 13 $= \dfrac{V_T \sin\tau}{V_{v0}}$
κ	Cyclic constant of circulation in impact
κ_p	Circulation constant when $V_v = 0$, *i.e.*, planing
Λ	Associated mass coefficient of Ref. 13 $= \mu^{1/3}/h$

λ		Wetted length
λ_p		Wetted length to peak-pressure location
μ		Associated mass coefficient; $(W/g)\mu$ is associated mass
π	=	3·1416
ρ		Water density, slugs/ft^3
σ, σ_R		Standard deviation. In expression, $E = AB^2/CD^2$ say, $\sigma_E^2 = \sigma_A^2 + + 4\sigma_B^2 + \sigma_C^2 + 4\sigma_D^2$, where A, B, C, and D are variables
σ		Generalized time of Ref. 13 $= tV_{v0}\Lambda$
τ		Attitude or trim angle. Suffix 0 denotes initial (touchdown) attitude or a reference value

It may be noted that, in order to adhere to the notation used by various writers, in a few cases the same symbol has more than one meaning.

REFERENCES

No.	*Author*	*Title, etc.*
1	Th. von Kármán	The impact on seaplane floats during landing. N.A.C.A. Tech. Note 321. October, 1929.
2	E. T. Jones and R. W. Blundell ..	Force and pressure measurements on V-shapes on impact with water compared with theory and seaplane alighting results. A.R.C. R. & M. 1932. January, 1938.
3	S. A. Batterson	The N.A.C.A. impact basin and water landing tests of a float model at various velocities and weights. N.A.C.A. Report 795. 1944.
4	Wilbur L. Mayo	Analysis and modification of theory for impact of seaplanes on water. N.A.C.A. Report 810. 1945.
5	L. Johnston	The impact load on flying boats when alighting. A.R.C. 9085. August, 1945.
6	A. G. Smith, I. W. McCaig and W. M. Inverarity.	Maximum impact pressures on seaplane hull bottoms. A.R.C. C.P. 4. March, 1946.
7	I. W. McCaig	Further note on the impact of an inclined wedge on water. A.R.C. 10,070. April, 1946.

REFERENCES—*continued*

No.	*Author*	*Title, etc.*
8	P. R. Crewe	A proposed theory to cover water impacts of seaplanes in which the craft has constant attitude and a tangential-to-keel velocity relative to the water. A.R.C. R. & M. 2513. December, 1946.
9	Anne Burns and A. J. Fairclough ..	Dynamic landing loads of flying boats with special reference to measurements made on *Sunderland* TX.293. A.R.C. R. & M. 2629. February, 1948.
10	J. A. Hamilton	A comparison between some full scale seaplane landing impact measurements and two impact theories. A.R.C. 11,345. February, 1948.
11	R. J. Monaghan	A review of the essentials of impact force theories for seaplanes and suggestions for approximate design formulae. A.R.C. R. & M. 2720. November, 1947.
12	R. J. Monaghan and P. R. Crewe ..	Formulae for estimating the forces in seaplane-water impacts without rotation or chine immersion. A.R.C. R. & M. 2804. January, 1949.
13	B. Milwitzky	Generalized theory for seaplane impact. N.A.C.A. Report 1103. 1952.
14	Philip M. Edge, Jr.	Hydrodynamic impact loads in smooth water for a prismatic float having an angle of dead rise of 10°. N.A.C.A. Tech. Note 3608. January, 1956.
15	S. A. Batterson	Variation of hydrodynamic impact loads with flight-path angle for a prismatic float at 0° and −3° trim and with a 22½° angle of dead rise. N.A.C.A. Tech. Note 1166, April, 1947.
16	S. A. Batterson and A. E. McArver	Water landing investigation of a model having a heavy beam loading and a 30° angle of dead rise. N.A.C.A. Tech. Note 2015. February, 1950.
17	E. Schnitzer	Theory and procedure for determining loads and motions in chine-immersed hydrodynamic impacts of prismatic bodies. N.A.C.A. Report 1152. 1953.
18	A. E. McArver	Water-landing investigation of a model having heavy beam loadings and 0° angle of dead rise. N.A.C.A. Tech. Note 2330. April, 1951.
19	S. A. Batterson	Water landing investigation of a hydro-ski model at beam loadings of 18·9 and 4·4. N.A.C.A. Research Memo. L51F27. TIB 2860. September, 1951.
20	R. W. Miller	Theoretical analysis of hydrodynamic impact of a prismatic float having freedom in trim. N.A.C.A. Tech. Note 2698. June, 1952.

REFERENCES—*continued*

No.	*Author*	*Title, etc.*
21	R. W. Miller and K. F. Merten ..	Comparison of theoretical and experimental response of a single-mode elastic system in hydrodynamic impact. N.A.C.A. Tech. Note 2343. April, 1951.
22	E. Schnitzer	Water-impact theory for aircraft equipped with nontrimming hydro-skis mounted on shock struts. N.A.C.A. Tech. Note 4256. September, 1958.
23	B. Milwitzky	A theoretical investigation of hydrodynamic impact loads on scalloped-bottom seaplanes and comparisons with experiment. N.A.C.A. Tech. Note 1363. July, 1947.
24	D. B. Chambliss and G. M. Boyd, Jr.	The planing characteristics of two V-shaped prismatic surfaces having angles of dead rise of 20° and 40°. N.A.C.A. Tech. Note 2876. January, 1953.
25	C. L. Shuford, Jr.	A review of planing theory and experiment with a theoretical study of pure-planing lift of rectangular flat plates. N.A.C.A. Tech. Note 3233. August, 1954.
26	J. D. Pierson, D. A. Dingee and J. W. Neidinger.	A hydrodynamic study of the chines-dry planing body. ETT Report No. 492. May, 1954.
27	J. M. Shoemaker	Tank tests of flat and V-bottom planing surfaces. N.A.C.A. Tech. Note 509. November, 1934.
28	R. F. Smiley	A study of water pressure distributions during landings with special reference to a prismatic model having a heavy beam loading and 30° angle of dead rise. N.A.C.A. Tech. Note 2111. July, 1950.
29	R. F. Smiley	An experimental study of water-pressure distributions during landings and planing of a heavily loaded rectangular flat-plate model. N.A.C.A. Tech. Note 2453. September, 1951.
30	R. W. Miller	Hydrodynamic impact loads in rough water for a prismatic float having an angle of dead rise of 30°. N.A.C.A. Tech. Note 1776. December, 1948.
31	J. W. McIvor	Full-scale measurements of impact loads on a large flying boat. Part I—Description of apparatus and instrument installation. A.R.C. C.P. 182. March, 1950.
32	J. Hamilton	Full-scale measurements of impact loads on a large flying boat (*Sunderland* Mk. 5). Part II—Results for impacts on main step. A.R.C. C.P. 205. February, 1951.
33	R. Parker	Preliminary pressure measurements during the landing of a *Sunderland* Mk. 5 flying boat in rough water conditions, including one in which the forebody was severely damaged. A.R.C. 15,201. September, 1952.

REFERENCES—*continued*

No.	*Author*	*Title, etc.*
34	R. Parker	Full-scale measurement of impact loads on a large flying boat (*Sunderland* Mk. 5). Part III—Data for impacts on main step. A.R.C. C.P. 340. August, 1954.
35	R. Parker	Full-scale measurements of impact loads on a large flying boat (*Sunderland* Mk. 5). Part IV—Data for impacts on the afterbody. A.R.C. C.P. 341. August, 1954.
36	R. Parker and J. K. Friswell	Full-scale measurements of impact loads on a large flying boat (*Sunderland* Mk. 5). Part V—Results of rough water tests. A.R.C. C.P. 342. March, 1955.
37	M. F. Steiner	Comparison of over-all impact loads obtained during seaplane landing tests with loads predicted by hydrodynamic theory. N.A.C.A. Tech. Note 1781. January, 1949.
38	—	Waterloads investigation—Martin Model 270. Glenn Martin Reports E.R. 7515–6. November, 1955.
39	Sir Horace Lamb	*Hydrodynamics.* 6th Edition, Cambridge University Press. 1932.
40	P. Ward Brown	Seaplane impact theory. Short Brothers & Harland Ltd. Hydrodynamics Note 46. A.R.C. 17,454. August, 1954.
41	P. Ward Brown	A critical review of full-scale seaplane impact tests with reference to the *Sunderland* V. A.R.C. 18,371. March, 1956.
42	P. Ward Brown	An empirical analysis of the planing characteristics of rectangular flat-plates and wedges. Short Brothers & Harland Ltd. Hydrodynamics Note 47. A.R.C. R. & M. 2998. September, 1954.
43	I. W. McCaig	Preliminary note on the impact of an inclined wedge on water A.R.C. 8747. April, 1945.
44	T. Arlotte	Some remarks on impact behaviour with reference to full-scale tests on the *Sunderland* Mk. 5. A.R.C. 18,566. June, 1956.
45	P. Ward Brown	The effect of variation in wing lift on seaplane impact. Short Brothers & Harland Ltd. Hydrodynamics Note 48. A.R.C. 17,453. February, 1955.
46	S. U. Benscoter	Effect of partial wing lift in seaplane landing impact. N.A.C.A. Tech. Note 1563. April, 1948.
47	J. D. Pierson and S. Leshnover	A study of the flow, pressures, and loads pertaining to prismatic vee-planing surfaces. Davidson Laboratory, Hoboken, N.J. Report 382. May, 1950.

REFERENCES—*continued*

No.	*Author*	*Title, etc.*
48	R. F. Smiley	A semiempirical procedure for computing the water-pressure distribution on flat and V-bottom prismatic surfaces during impact or planing. N.A.C.A. Tech. Note 2583. December, 1951.
49	P. R. Crewe and T. Arlotte.. ..	The prediction of planing normal force. Unpublished Saunders-Roe report. 1955.
50	T. Arlotte	Discussion of impact behaviour with reference to force build-up with time. Saunders Roe Ltd. Ref. TA/PEC/127. 20th May, 1954. And Addendum 'An investigation of wing flexibility effects in flying boat impacts'. 9th November, 1954. A.R.C. 17,165.
51	A. R. Collar	On the effect of wing bending on the acceleration due to landing impact. A.R.C. 16,960. June, 1954.
52	D. Williams	Effect of wing flexibility on landing impact of a flying-boat hull. A.R.C. 17,083. September, 1954.
53	W. L. Mayo	Hydrodynamic impact of a system with a single elastic mode. I. Theory and generalized solution with an application to an elastic airframe. N.A.C.A. Report 1074. 1952.
54	P. R. Crewe	A review of the seaplane hydrodynamic design problems of greatest present importance and possible solutions. Part II—Water skis and some associated devices. Saunders-Roe Report H/O/112/2. October, 1950.
55	E. Schnitzer	Estimation of water landing loads on hydro-ski equipped aircraft. N.A.C.A. Research Memo. L53D29. TIB 3821. July, 1953.
56	J. A. Hamilton	An investigation into the effect of forced and natural afterbody ventilation on the hydrodynamic characteristics of a small flying boat (*Saro* 37) with a 1:20 fairing over the main step. A.R.C. R. & M. 2714. November, 1947.
57	J. A. Hamilton	An interim report on the hydrodynamic performance of a large four-engined flying boat (*Sunderland* Mk. V) with a 1:16·75 main step fairing. A.R.C. 12,162. January, 1949.
58	M. A. Biot and R. L. Bisplinghoff ..	Dynamic loads on airplane structures during landing. N.A.C.A. ARR No. 4H10. Wartime Report W–92. A.R.C. 8748. October, 1944.

REFERENCES—*continued*

No.	*Author*	*Title, etc.*
59	J. D. Pierson	The penetration of a fluid surface by a wedge. Davidson Laboratory, Hoboken, N.J. Report 381. July, 1950.
60	K. F. Merten and E. B. Beck ..	Effects of wing flexibility and variable air lift upon wing bending moments during landing impacts on a small seaplane. N.A.C.A. Report 1013. 1951.
61	H. Wagner	Phenomena associated with impacts and sliding on liquid surfaces. *Z.A.M.M.*, Vol. 12. Part 4. pp. 193 to 215.
62	H. M. Garner	Recent full scale and model research on seaplanes. *Jahrbuch der deutschen Luftfahrtforschung.* Supplementary Volume. pp. 357 to 373. 1938.
63	W. Pabst	Theory of the landing impact of seaplanes. (1) D.V.L. Year Book, 1930. (2) Also published in *Zeitschrift für Flugtechnik und Motorluftschiffart.* Vol. 21. Part 9. pp. 217 to 226. 14th May, 1930. (3) Translated as N.A.C.A. Tech. Memo. 580. August, 1930.
64	W. Pabst	Landing shocks in seaplanes. (1) D.V.L. Year Book, 1931. (2) Also published in *Zeitschrift für Flugtechnik und Motorluftschiffart.* Vol. 22. Part I. pp. 13 to 27. 14th January, 1931. (3) Translated as N.A.C.A. Tech. Memo. 624. June, 1931.
65	U. J. Blanchard	The planing characteristics of a surface having a basic angle of dead rise of 40° and horizontal chine flare. N.A.C.A. Tech. Note 2842. December, 1952.
66	P. G. Barnett	Hydrodynamic problems associated with seaplane impact. A.R.C. 19,941. March, 1958.
67	H. B. Squire	The motion of a simple wedge along a water surface. *Proc. Roy. Soc.* A. Vol. 243. pp. 48 to 64. 1957.
68	R. J. Monaghan	A theoretical examination of the effect of deadrise on wetted area and associated mass in seaplane-water impacts. A.R.C. R. & M. 2681. March, 1949.
69	A. G. Smith	A generalized method of analysing the force characteristics of seaplanes when planing. A.R.C. 17,458. January, 1955.
70	A. G. Smith	Notes on water flow over a wedge. A.R.C. 15,934. March, 1953.

APPENDIX I

A Brief Summary of the Two-Dimensional Treatments of Water Impact

In 1929 von Kármán published his classical impact theory for the vertical impact of an infinitely long wedge at zero trim[1]. This was based on the concept that during impact the momentum lost by the impacting body can be considered to be transferred to a finite mass of water in contact with it and having the same downward velocity (the 'associated mass' concept). Since the complete initial momentum of the body is thus assumed to be distributed between the body and the associated mass, the motion subsequent to water contact is determined by the relation,

$$V_{n0} = (1+\mu)V_n$$

where subscript 0 denotes initial conditions and $(W/g)\mu$ is the associated mass.

Von Kármán assumed that the associated mass is one half of that obtained when a flat plate moves in an unbounded fluid, the width of the plate being the wetted width of the wedge. It is therefore the mass of half a circular cylinder of water on the wetted width of the wedge as diameter. The resultant force is then normal to the keel and is given by

$$F = \frac{d}{dt}\left(\frac{W}{g}\mu V_n\right) \text{ with } \frac{W}{g}\mu = \tfrac{1}{2}c^2\rho\pi$$

where c = half wetted width.

It may be noted that F is of the same form as the 'pure impact' term, F_i, in the Ref. 12 three-dimensional treatment (*see* Figs. 3 and 55).

It was shown in Ref. 1 that

$$F = \frac{V_n{}^2 \cot\beta}{(1+\mu)^3}\pi c\rho\,.$$

Wagner[61] elaborated the theory considerably by consideration of the flow past a flat plate, extending it to wedges with curved lateral cross-section of bottom and also to the determination of transverse pressure distributions. Wagner's expression for load is identical to the foregoing for a straight lateral cross-section bottom wedge, but with a multiplying factor of $\pi/2$ to allow for splash-up. A useful summary of the Wagner theory is given in the Appendix to Ref. 62.

The treatment of Wagner, particularly with respect to pressure distributions, was substantially confirmed by model experiment in Ref. 2, and empirical equations were developed therein for impacts with finite attitude and forward velocity. The experimental technique, however, gave mean pressures rather than peak values (*see* Ref. 6). The effect of forward velocity was interpreted in terms of the impact normal to the keel.

The theory of Pabst[63, 64] is similar to that of Wagner, but includes an experimentally derived equation for the determination of the associated mass in terms of the aspect ratio of the water plane,

$$\frac{w}{g}\mu = \frac{\pi}{2}\rho\frac{L^2c^2}{\sqrt{(L^2+4c^2)}} \qquad \left(1 = \frac{0{\cdot}85Lc}{L^2+4c^2}\right)$$

where L = wetted length.

These treatments, and other investigations published before 1940, share the important hypothesis that the assumed associated mass remains attached to the wedge throughout the impact.

They also assume that the value of the associated mass is completely determined by the value of the velocity component normal to the keel at the time considered and is independent of the previous history (Ref. 66).

This concept is valid for the vertical impact of a hull at zero trim and is also applicable to an impact with finite trim if the resultant velocity is normal to the keel, since in both cases the momentum lost by the hull is transmitted to the water which remains in contact with it throughout the impact apart from spillage from the ends of a finite wedge.

The concept is not valid, however, when a component of velocity tangential to the keel is present, as in seaplane landings, since the motion of the hull along its axis causes a loss of momentum in downwash behind the step. Thus, in seaplane practice, conservation of momentum exists between the hull and its associated mass (as in the two-dimensional case) and the wake. Treatments involving this effect have been advanced since the mid-1940's and are reviewed in detail in Section 3 of this report.

APPENDIX II

Effect of Structural Flexibility

A review of wing flexibility theories is contained in Ref. 50, but since considerable attention has been given to the possibility of this being the cause of discrepancies between impact theory and full-scale experiment, a brief summary is given below.

The general treatment of wing bending (which is the primary structural case for modern flying boats) during impact consists of reducing the fundamental mode to an equivalent two-mass system, *i.e.*,

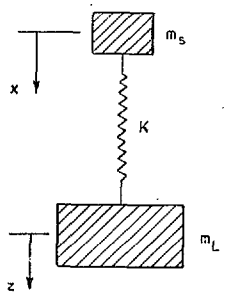

$$m_s + m_L = M \text{ (total mass)}$$

$$m_s/m_L = r \text{ (mass ratio)}$$

$$\text{If } \ddot{y}_n = \text{nodal or c.g. acceleration}$$

$$\text{then } M\ddot{y}_n = m_L\ddot{z} + m_s(\ddot{z}+\ddot{x})$$

$$\therefore \ddot{y}_n = \ddot{z} + \frac{m_s}{M}\ddot{x}$$

$$= \ddot{z}\left(\frac{t}{1+r}\right)\ddot{x}.$$

The spring constant in lb/ft deflection is

$$K = \frac{4\pi^2(m_L m_s)f_n^2}{m_L + m_s} = \frac{4\pi^2 f_n^2 W}{g}\frac{r}{(1+r)^2}$$

where f_n is the natural bending frequency in c/s. The applied hydrodynamic load and structural response are then assumed to be coupled throughout the impact.

In Ref. 51, Professor Collar assumes a three-mass system with two equal spring masses attached to a lower mass by two springs, *viz.*,

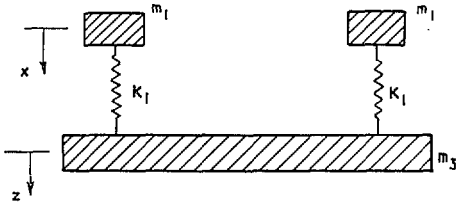

Writing down the kinetic (T) and potential (V) energies of the system he obtains

$$2T = m_3\dot{z}^2 + 2m_1(\dot{z}+\dot{x})^2$$

$$2V = 2K_1x^2.$$

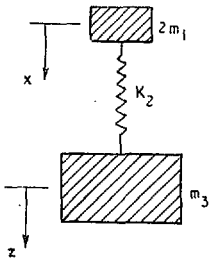

This can be transformed to a two-mass system:

$$2T = m_3\dot{z}^2 + 2m_1(\dot{z}+\dot{x})^2$$

$$2V = K_2x^2$$

$$i.e.,\ K_2 = 2K_1.$$

Putting r = mass ratio, the Lagrangian equations of motion for the system become:

$$\begin{cases} \dfrac{W}{g}\ddot{z} + \dfrac{W}{g}\left(\dfrac{r}{1+r}\right)\ddot{x} = 0 \\ \dfrac{W}{g}\left(\dfrac{r}{1+r}\right)(\ddot{z}+\ddot{x}) + K_x = 0. \end{cases}$$

When this system strikes the water the hull impact force must be added, and the final equations of motion assumed by Professor Collar are:

$$\begin{cases} \dfrac{W}{g}\ddot{z} + \dfrac{W}{g}\left(\dfrac{r}{1+r}\right)\ddot{x} + \dfrac{W}{g}(a\dot{z}+b\dot{z}) = 0 \\ \dfrac{W}{g}\left(\dfrac{r}{1+r}\right)(\ddot{z}+\ddot{x}) + Kx = 0 \end{cases}$$

where $K = 2K_1 = K$.

Dr. Williams has also applied a treatment for wing flexibility in Ref. 52. The diagram shows the spring system and notation used.

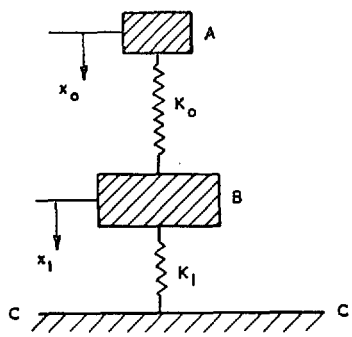

A = c.g. of hull-wing combination,

B = hull

x_0 is the c.g. movement, and the water force is represented by a spring k_1 attached to a rigid base CC.

He writes the equations of motion,

$$M\ddot{x}_0 + k_1 x_1 = 0$$

$$nM(\ddot{x}_1 - \ddot{x}_0) + k(x_1 - x_0) + k_1 x_1 = 0.$$

In the notation used in the foregoing we may write,

$$x_1 = z$$

$$x_0 = \left(\frac{1}{1+r}\right) z + \frac{r}{1+r}(z+x)$$

$$= z + \left(\frac{r}{1+r}\right) x$$

$$= z + x/(1+n), \text{ since } n = 1/r$$

$$k_0 = K/(r/1+r)^2.$$

The equations of motion may then be written

$$\begin{cases} \dfrac{W}{g}\ddot{z} + \dfrac{W}{g}\left(\dfrac{r}{r+1}\right)\ddot{x} + k_1\ddot{z} = 0 \\ \dfrac{W}{g}\left(\dfrac{r}{1+r}\right)(\ddot{z}+\ddot{x}) + Kx = 0. \end{cases}$$

Thus it is seen that the equations of motion used by Professor Collar and Dr. Williams are identical except that where the former has represented the water impact force by $(a\dot{z}+bz)$, the latter has assumed a simple spring. Professor Collar chooses his constants a and b to satisfy the Ref. 12 theoretical impact time to peak acceleration and then considers the impact as damped simple harmonic motion. Dr. Williams represents the water force by undamped simple harmonic motion of a period such that the first peak occurs at the theoretical time given by Ref. 12.

In the treatment of Ref. 50, a slightly simplified representation of the Ref. 12 rigid-body theoretical water impact force has been used in the form $(Az^2\dot{z}+Bz^2)$.

Thus, summarizing the above treatments for elastic two-mass systems in water impact, we have equations of motion:

$$\begin{cases} \dfrac{W}{g}\ddot{z} + \dfrac{W}{g}\left(\dfrac{r}{1+r}\right)\ddot{x} + F = 0 \\ \dfrac{W}{g}\left(\dfrac{r}{1+r}\right)(\ddot{z}+\ddot{x}) + Kx = 0 \end{cases}$$

where Ref. 51 uses $F = \dfrac{W}{g}(a\dot{z}+bz)$

Ref. 52 uses $F = k_1 z$

Ref. 50 uses $F = \dfrac{W}{g}(Az^2\dot{z}+Bz^2)$.

A similar treatment of the same problem was made by Mayo[53]. The equations used were obtained by inserting the theoretical rigid-body equation developed by Mayo[4] into a two-mass spring system. The equations of motion presented in Ref. 53 are very cumbersome.

In order to check the elastic system solution developed, tests were made on a model approximating a two-mass spring system, with a mass ratio $r = 0{\cdot}6$ and a natural frequency of $3{\cdot}0$ c/s. The tests[21] indicated that the Mayo treatment agreed very well with experimental results. Since direct comparison of the equations of motion developed by Mayo and those used in the Ref. 50 treatment appeared difficult, the latter method was used to obtain solutions in a case given in Ref. 21 for which experimental results and Mayo theoretical values were presented. The comparisons (*see* Fig. 8) indicate good agreement between the two theoretical treatments and both agree well with experiment. Thus, it is concluded that for a case where the system is a simple two-mass spring system of known mass ratio and natural frequency, the treatments of Ref. 50 or Ref. 53 will give good predictions of the motion.

In the systems discussed in the foregoing, the effect of damping in the structural response has been ignored. An American report[22] deals with the water impact of hydro-skis mounted on shock struts. In this treatment ski mass is neglected and the ski-fuselage connection is assumed to have velocity squared damping and a linear spring reaction. Consideration has been given to damping in the *Sunderland* case, and this is discussed in Section 6.2.

APPENDIX III

Selection of Symbols

In Ref. 44 a draught coefficient u and an acceleration coefficient u'' are employed because data are used from Ref. 13. Ref. 13 is very useful for general reference bearing in mind the following table of equivalent notations:

Quantity	*Ref. 13*	*Present report*
Flight-path angle	γ	$\gamma = \tan^{-1}(V_v/V_H)$
Approach parameter	κ	$\kappa = V_T \sin\tau/V_{v0}$
Initial value of V_v	$\dot{z}_{w0}$	V_{v0}
Associated mass coefficient	Λ	$\mu^{1/3}/h$
Generalised displacement	u	$\mu^{1/3}$
Generalised velocity	u'	V_v/V_{v0}
Generalised acceleration	u''	$\dfrac{dV_v}{dt}\Big/V_{v0}{}^2\Lambda$
Generalised time	σ	$tV_{v0}\Lambda$

It may be noted that

$$\kappa = \cos^2\tau\left(\frac{V_H\tan\tau}{V_{v0}}+1\right)-1$$

$$\frac{V_{v0}}{V_H\tan\tau} = \frac{1}{(\kappa+1)\sec^2\tau-1}$$

so that for τ small,

$$\frac{V_{v0}}{V_H\tan\tau} \doteqdot \frac{1}{\kappa}$$

κ tends to infinity for pure planing and to 0 for pure impact.

Since μ is assumed to be proportional to h^3, Λ is independent of h but depends on attitude and dead rise.

Ref. 13 assumes that V_T remains constant, but gives dV_v/dt, not dV_n/dt. When V_T is constant $dV_n/dt = \sec\tau(dV_v/dt)$ due to the relationship

$$V_n = V_v\sec\tau + V_T\tan\tau.$$

The relationship

$$F(1+\mu) = F_{p0}\{1 + V_v/(V_H\tan\tau)\}^2$$

is replaced in Ref. 13 by

$$-\mu'' = \{3(Ku)^2/(1+u^3)\}/\{1 + V_v/(V_T\sin\tau)\}^2.$$

Where $3(Ku)^2/(1+u^3)$ is formally equivalent to $F_{p0}(V_T/V_H)^2/\{(W/g)(1+\mu)V_{v0}{}^2\Lambda\cos\tau\}$. Thus if u'' is plotted against $u^2/(1+u^3)$ the 'planing scaffold' is a straight-line plot of the coefficient $F_{p0}(V_T/V_H)^2/\{(W/g)(1+\mu)V_{v0}{}^2\Lambda\cos\tau\}$ against $u^2/(1+u^3)$, and maximum draught still corresponds to the maximum value of the abscissa (unless the latter exceeds 0·53) (Fig. 10).

Furthermore if $(Ku)^2/(1+u^3)$ is used as abscissa all the scaffold lines have the same slope, irrespective of the value of the approach parameter κ. This is shown in Fig. 11 which also gives a line of maximum acceleration conditions. The intersections of the scaffold line with the loops gives the variation of maximum draught coefficient with K. This variation is isolated in Fig. 12, and is reasonably linear.

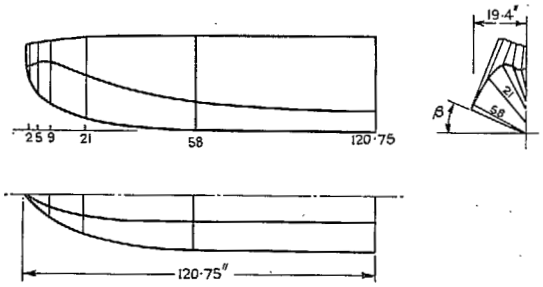

(a) Typical NACA float model

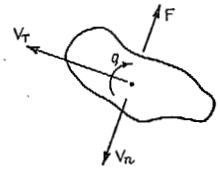

Kinetic energy of fluid in absence of circulation,
$2T = AV_n^2 + 2BV_n V_T + CV_T^2 + Qq^2 + 2(GV_n + HV_T)q$.
When e.g., $V_T = q = 0$, A is an associated mass in V_n direction

Deeply submerged cylinder (Ref. 39)

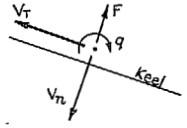

Impact analoque

(b) Hydrodynamic motions

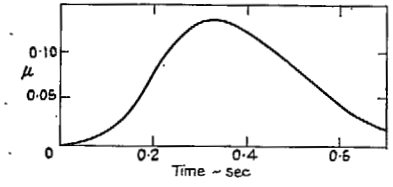

(c) Typical μ variation during impact (Ref.12 theory for Run 17 of Ref. 34)

FIGS. 1a, b and c.

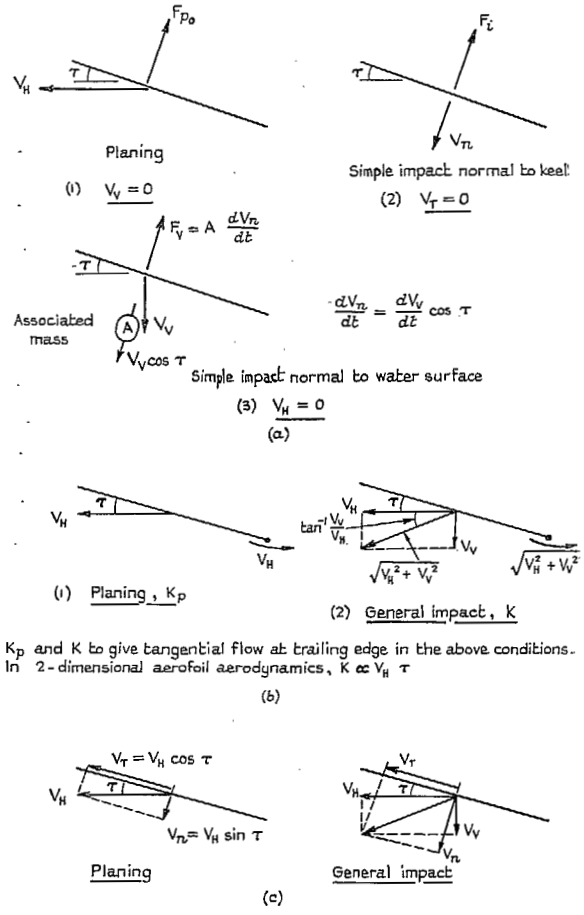

K_P and K to give tangential flow at trailing edge in the above conditions. In 2-dimensional aerofoil aerodynamics, $K \propto V_H\ \tau$

FIGS. 2a, b and c. Impact and planing definitions.

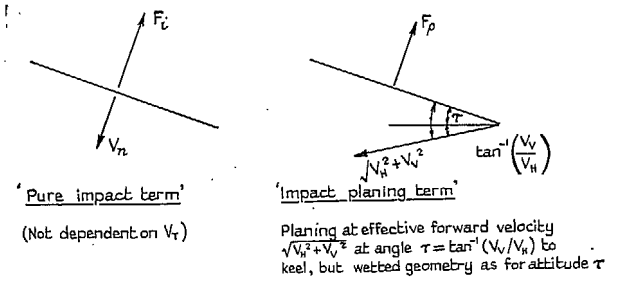

(a) Interpretation of component forces Ref. 12

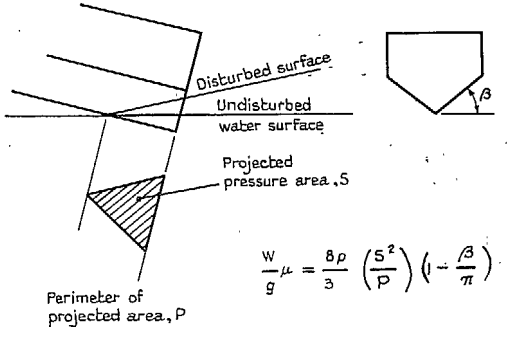

(b) Illustration of associated mass assumptions Ref. 12.

FIGS. 3a and b.

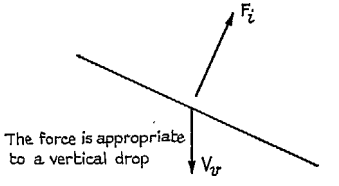

(a) Modified definition for F_i (Ref. 44)

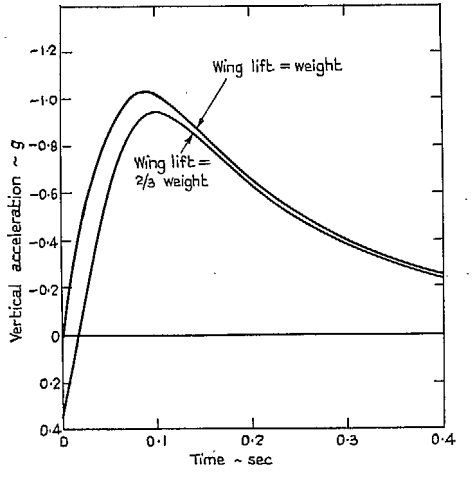

(b) Accelerations with full and partial wing lift calculated in Ref. 46

FIGS. 4a and b. The effect of wing lift in vertical drops.

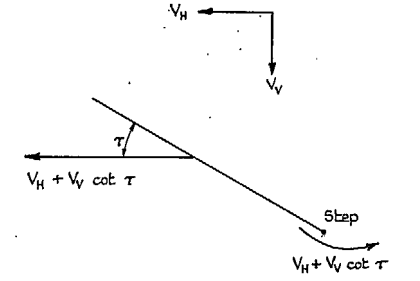

(a) Steady planing condition stated to be equivalent to impact

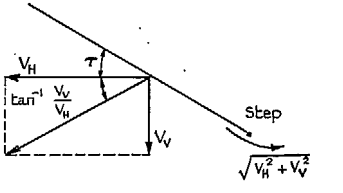

(b) More likely step flow velocity in actual impact

FIGS. 5a and b. The planing analogue of Ref. 48.

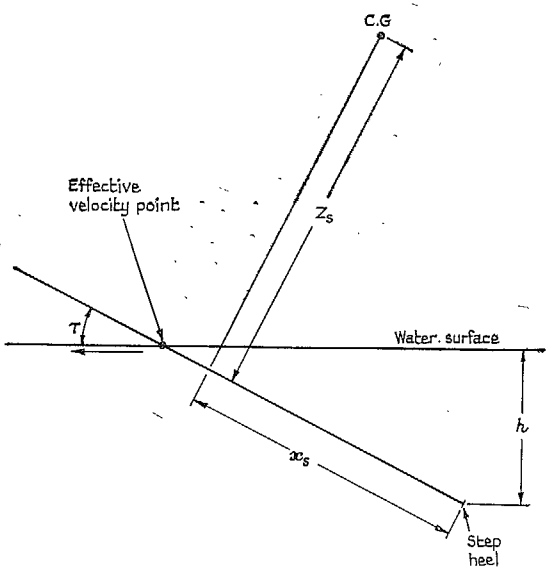

FIG. 6. Notation used in pitch notation analysis.

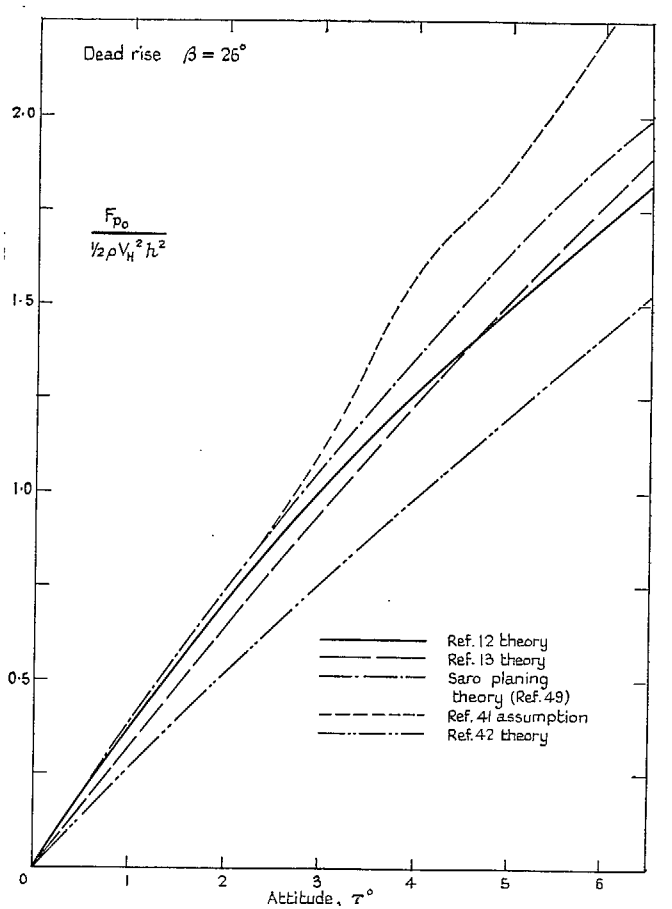

FIG. 7. Comparison of planing force estimates.

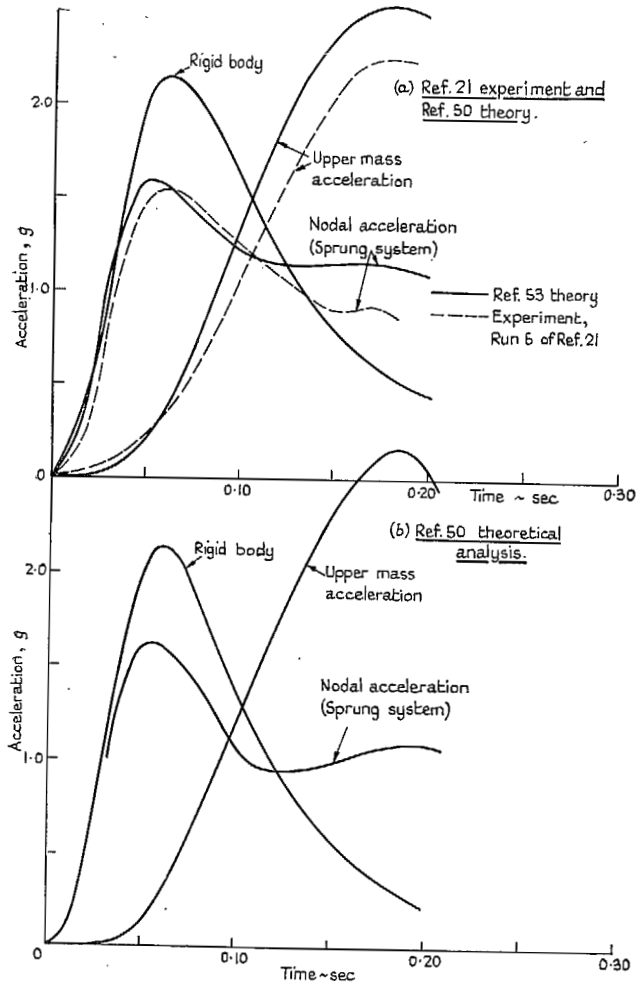

FIG. 8. Comparison of theoretical and experimental results for a simple sprung system ($r = 0{\cdot}6$, $f_n = 3$ c/s).

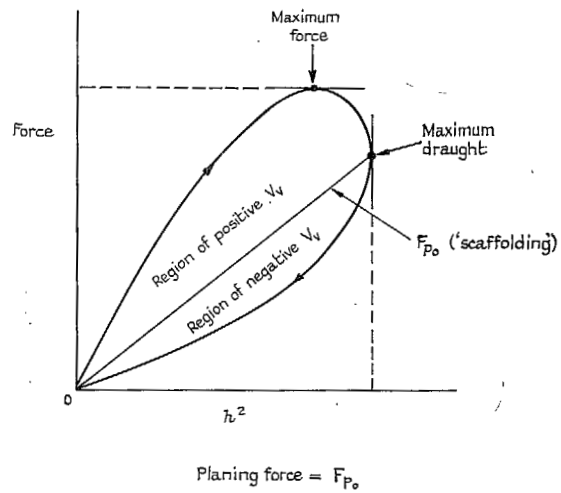

FIG. 9. Typical loop diagram of force against (draught)^2.

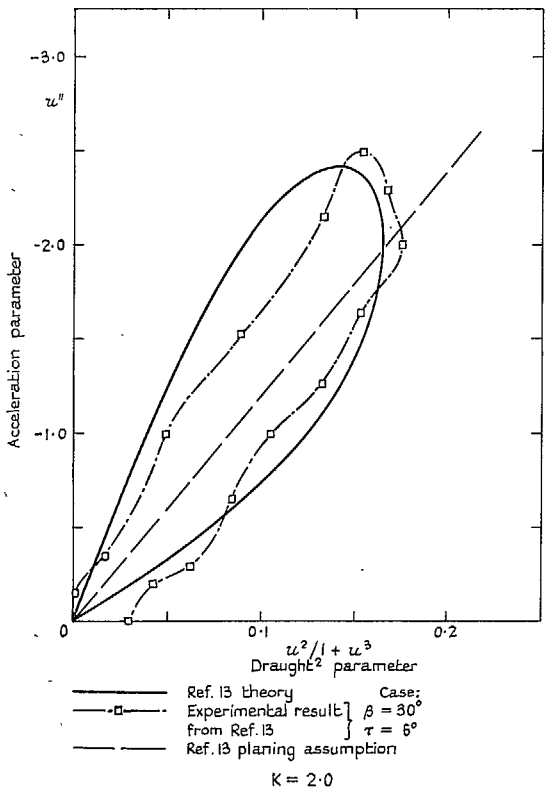

FIG. 10. Comparison of estimated with model results, Ref. 13.

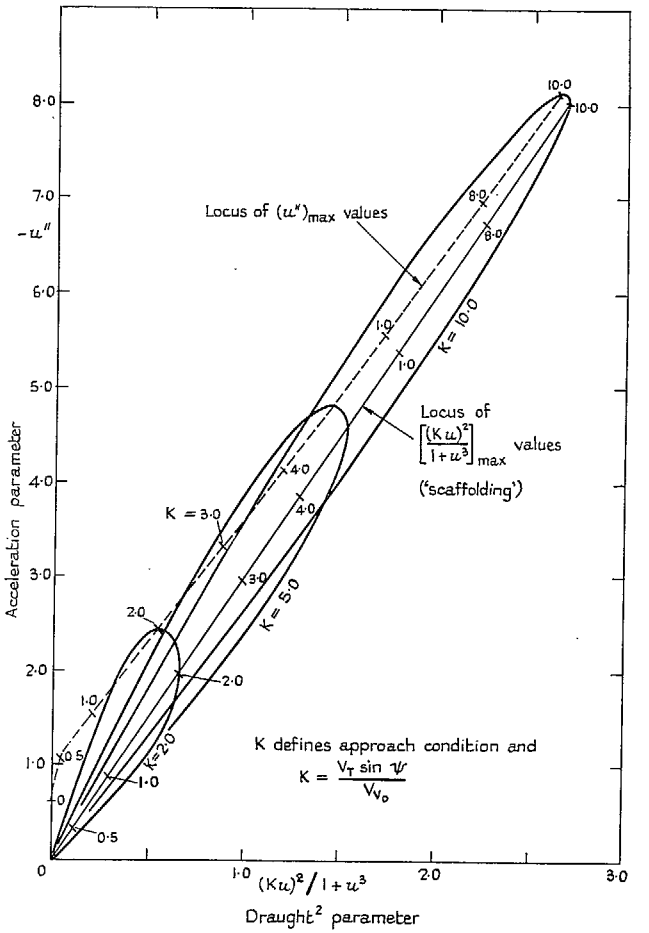

FIG. 11. Generalized acceleration results of Ref. 13 theory.

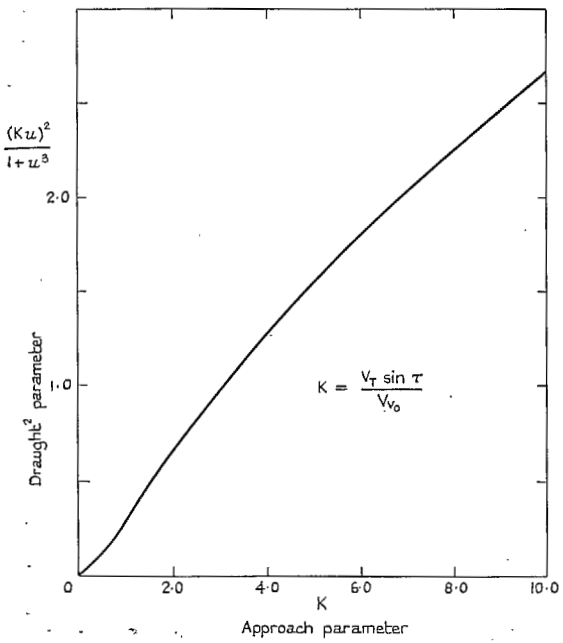

FIG. 12. Variation of maximum draught coefficient with approach parameter for Ref. 13 theory.

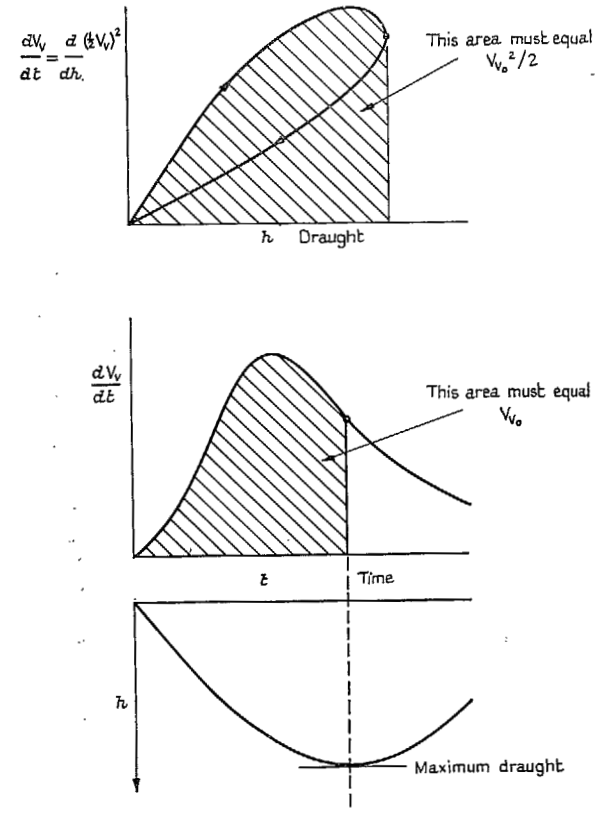

FIG. 13. Graphical checks of initial vertical velocity.

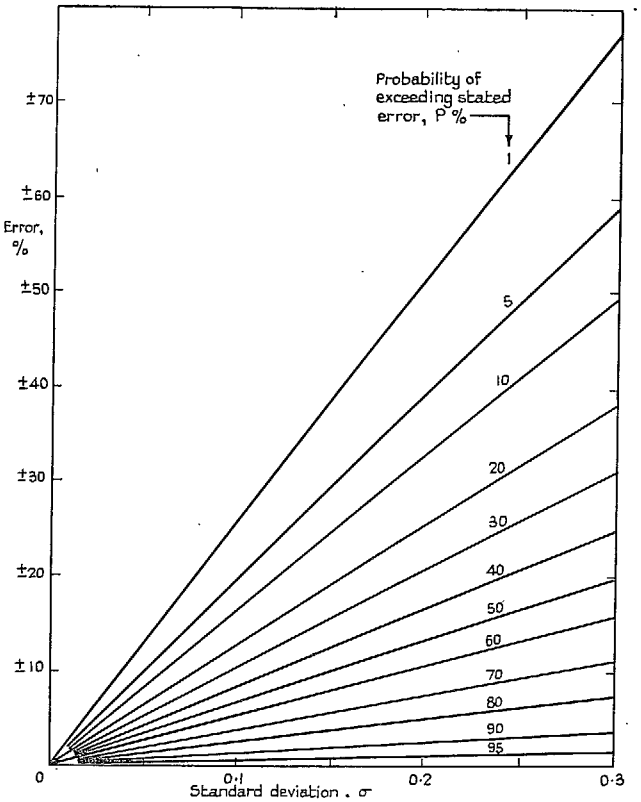

FIG. 14. Error probability curves for normal distributions of error.

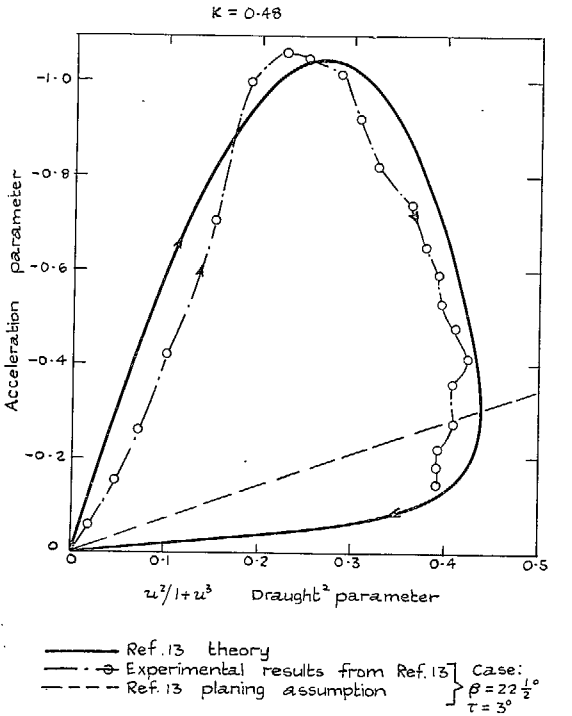

FIG. 15. Comparison of Ref. 13 estimates with model results Ref. 13.

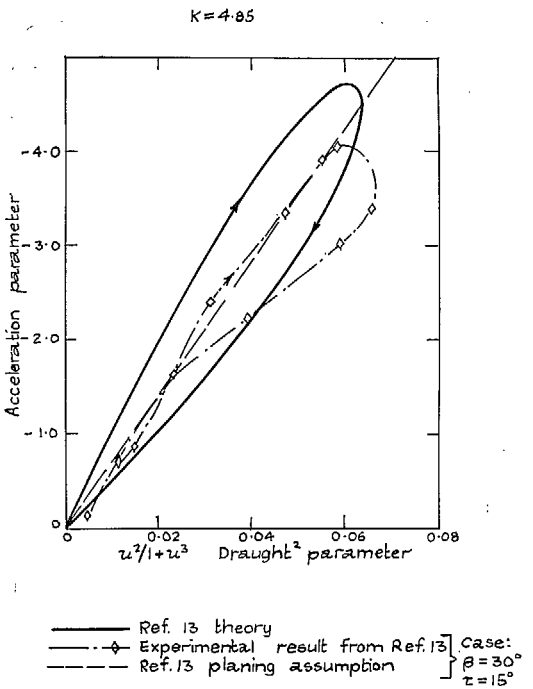

FIG. 16. Comparison of estimates with model results, Ref. 13.

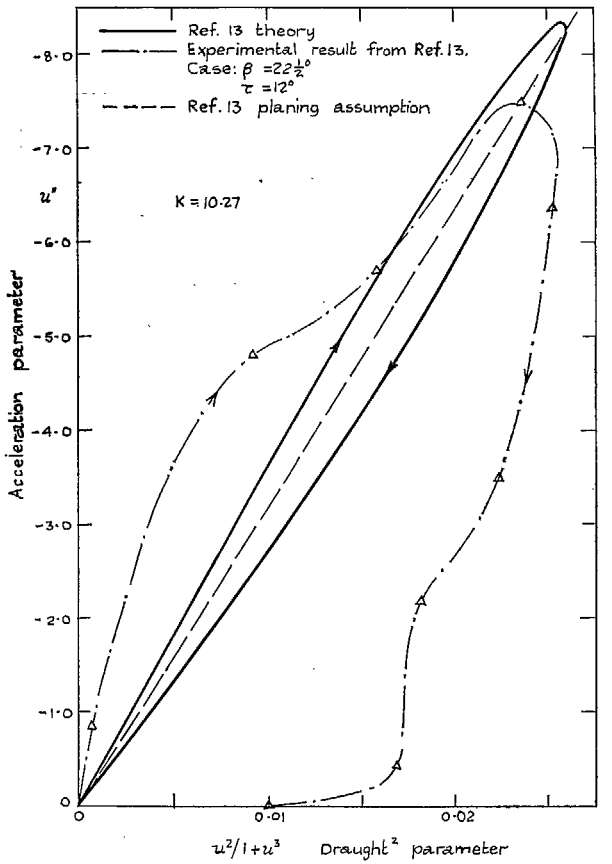

FIG. 17. Comparison of estimates with model results, Ref. 13.

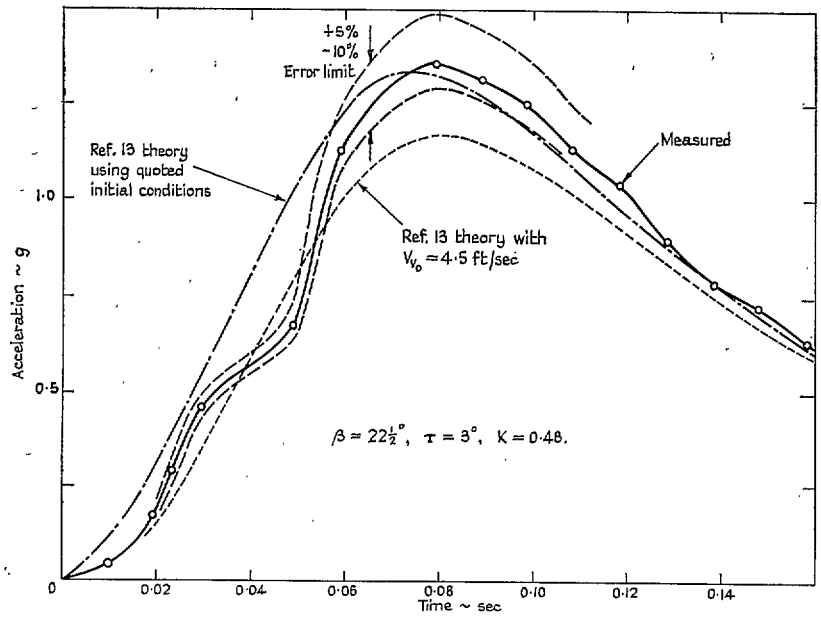

FIG. 18. Analysis of model impact results, Ref. 13.

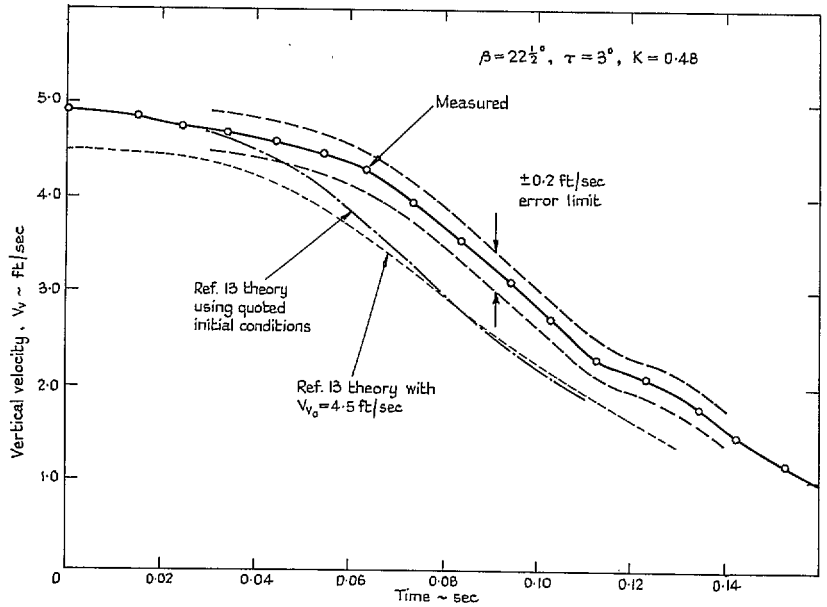

FIG. 19. Analysis of model impact results, Ref. 13.

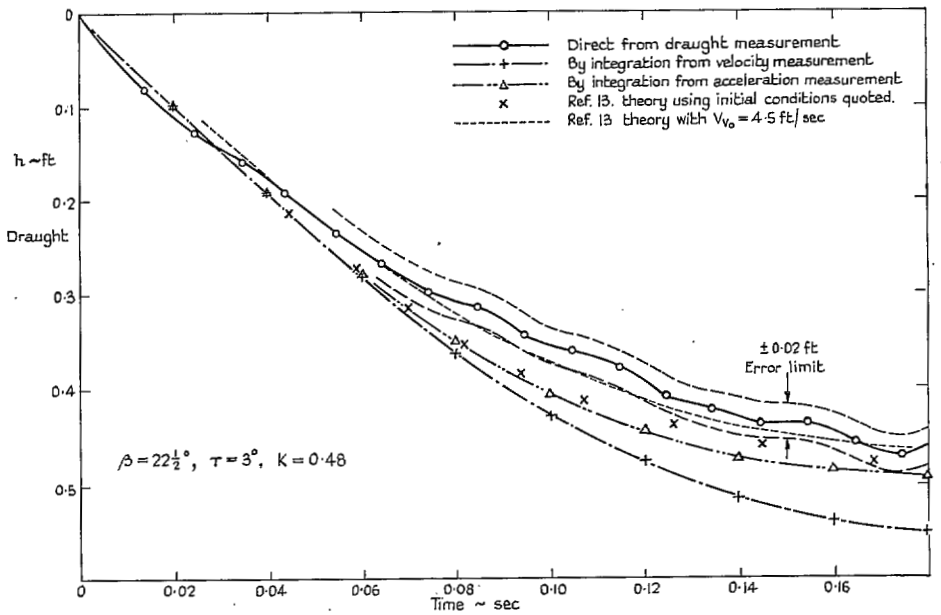

FIG. 20. Analysis of model impact results, Ref. 13.

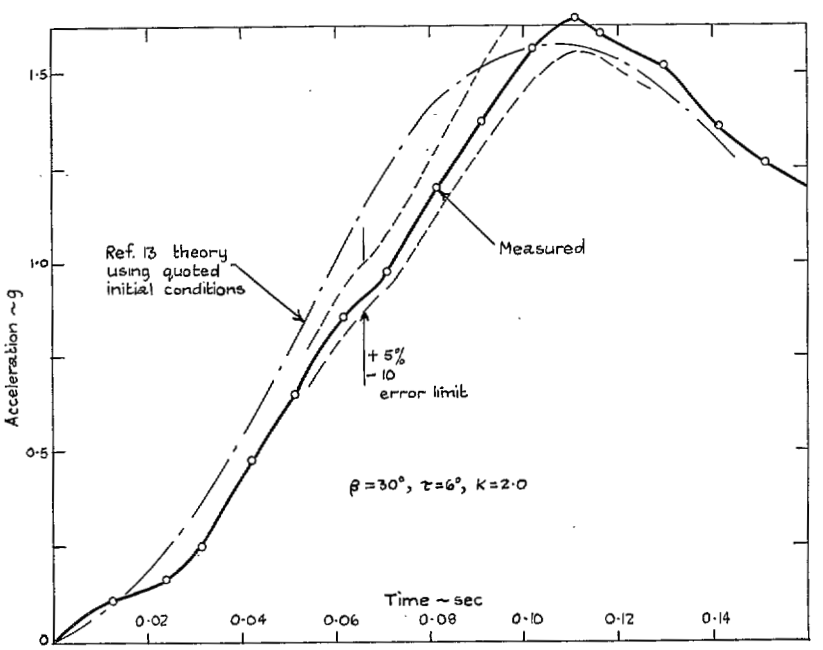

FIG. 21. Analysis of model impact results, Ref. 13.

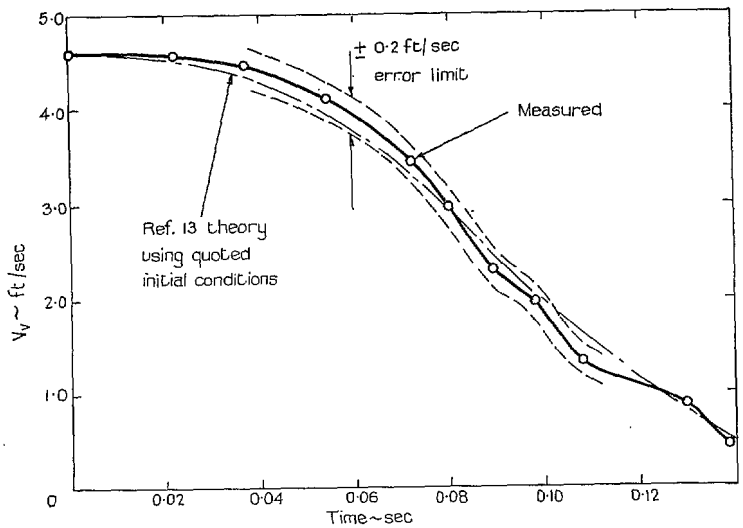

FIG. 22. Analysis of model impact results, Ref. 13.

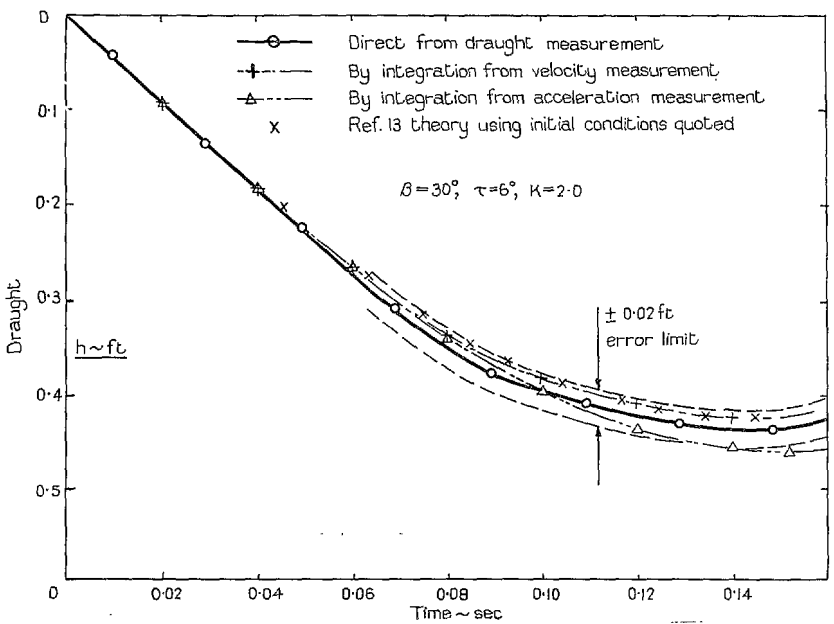

FIG. 23. Analysis of model impact results, Ref. 13.

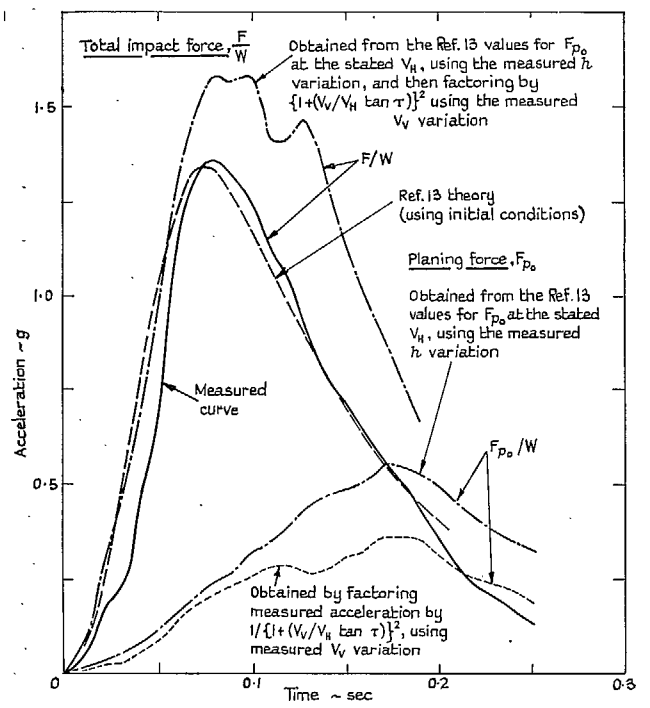

$\beta = 22\frac{1}{2}°$, $\tau = 3°$, $\kappa = 0{\cdot}48$

FIG. 24. Analysis of model impact results, Ref. 13.

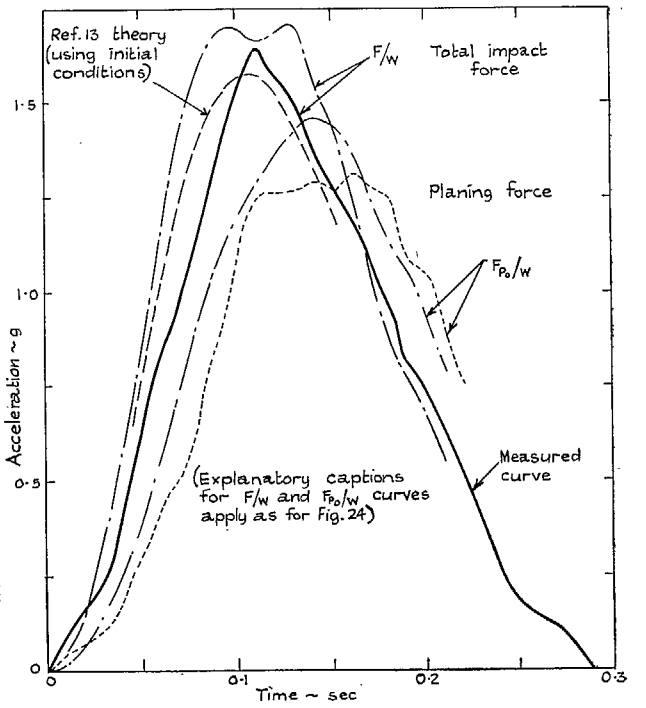

$\beta = 30°$, $\tau = 6°$, $K = 2{\cdot}0$

FIG. 25. Analysis of model impact results, Ref. 13.

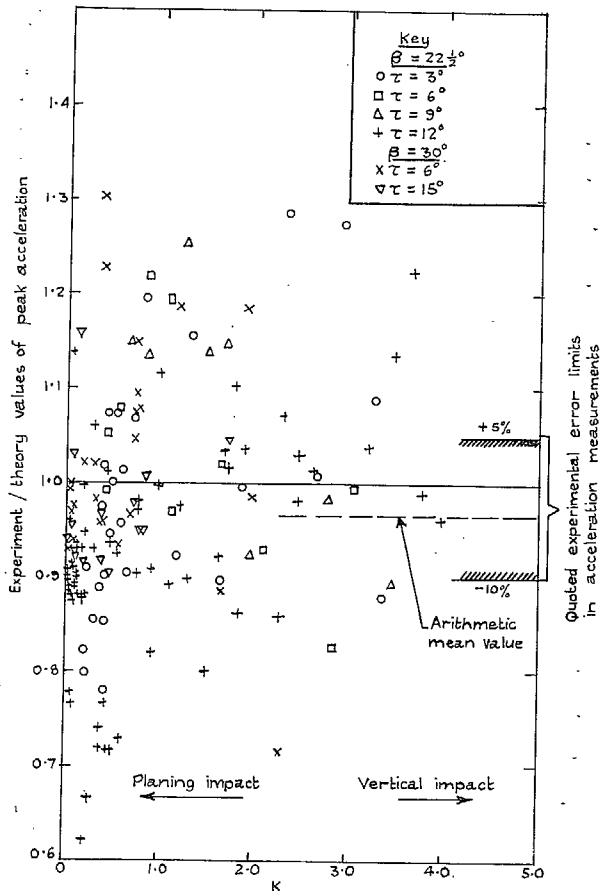

FIG. 26. Comparison of estimated with model results for maximum acceleration, Ref. 13.

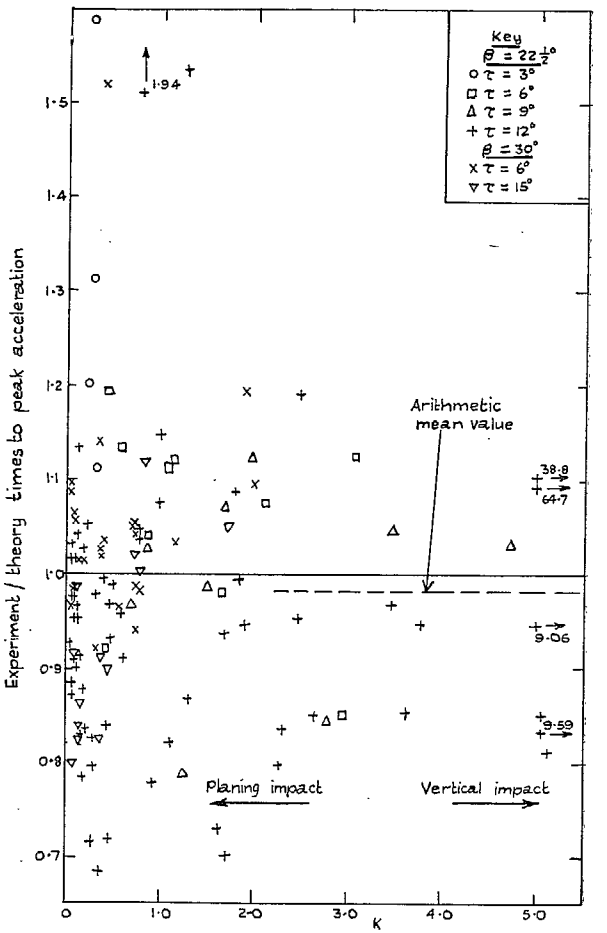

FIG. 27. Comparison of estimated, Ref. 12, with model results Ref. 13, for time to maximum acceleration.

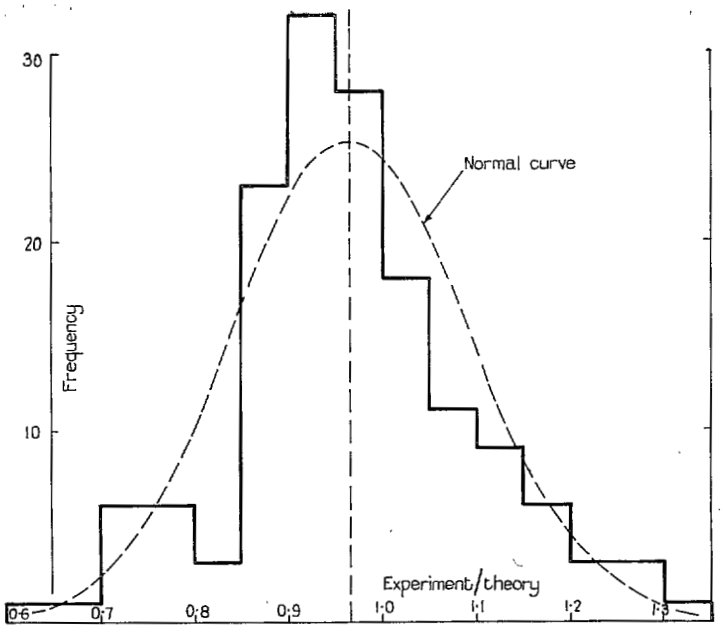

FIG. 28. Histogram for comparison of experiment with theory for maximum acceleration given in Fig. 26.

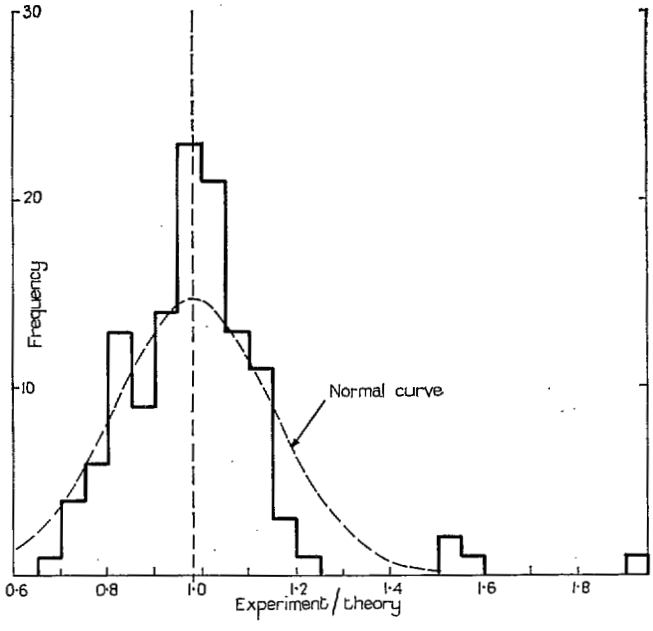

FIG. 29. Histogram for comparison of experiment with theory for time to maximum acceleration given in Fig. 27.

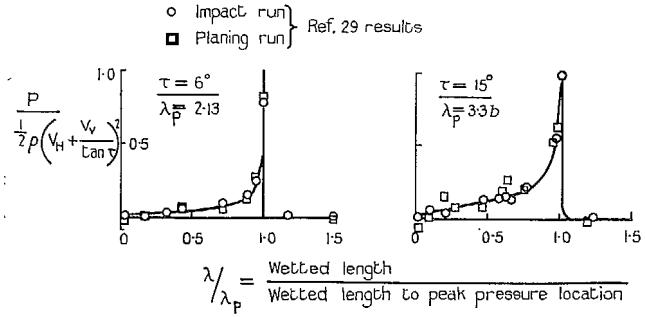

(a) Comparisons of impact and planing pressure coefficients along the centre line of a flat plate.

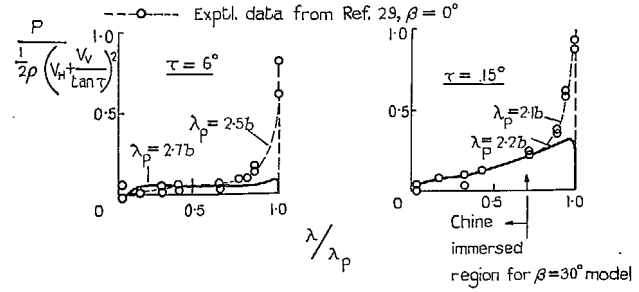

(b) Comparisons of pressure distribution coefficients along the keel for similar models with $\beta = 0°$ & $30°$

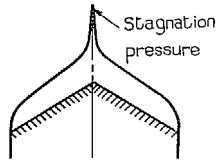

(c) Typical pressure distribution along peak pressure line for a vee-wedge

FIGS. 30a, b and c. Pressure-distribution measurements.

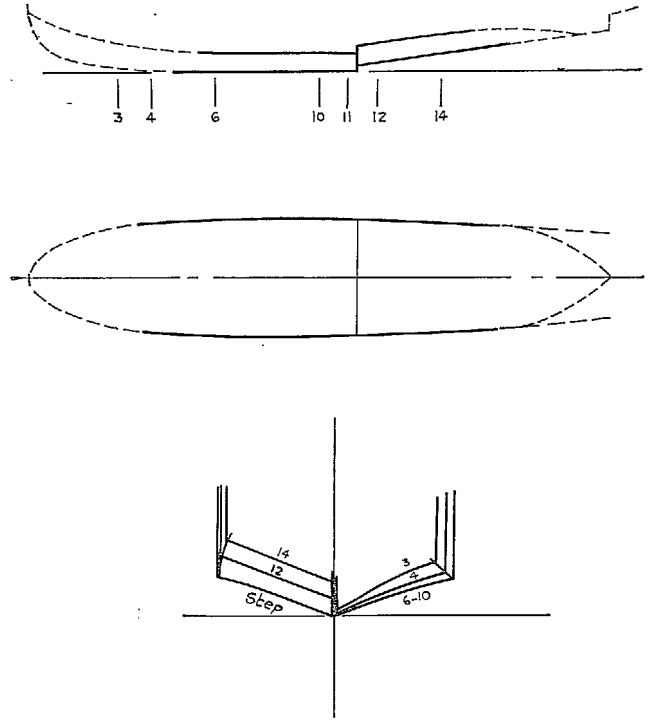

FIG. 31. *Vought Sikorsky* S–43 hull geometry near main step.

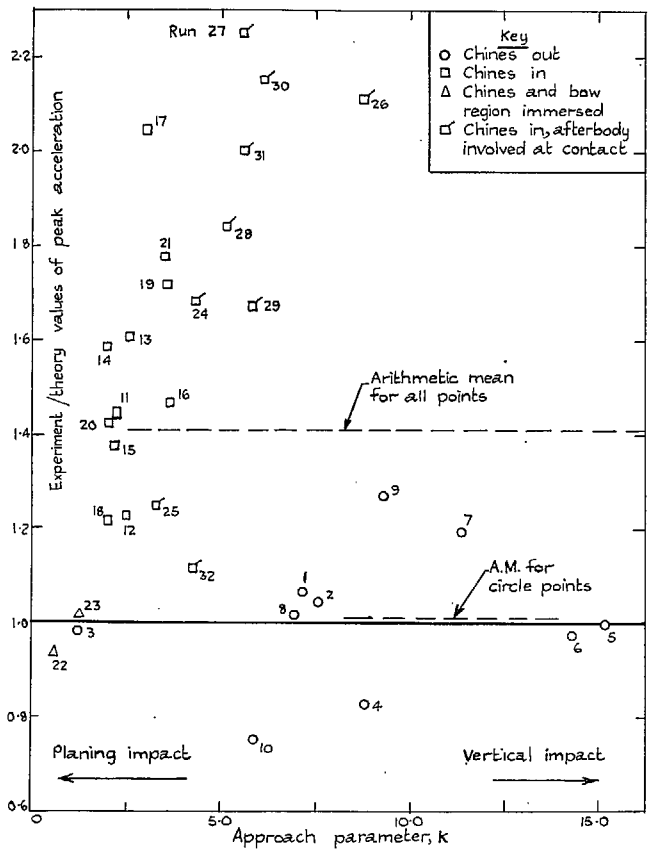

FIG. 32. Comparison of Ref. 12 theory with Ref. 37 full-scale results for maximum acceleration.

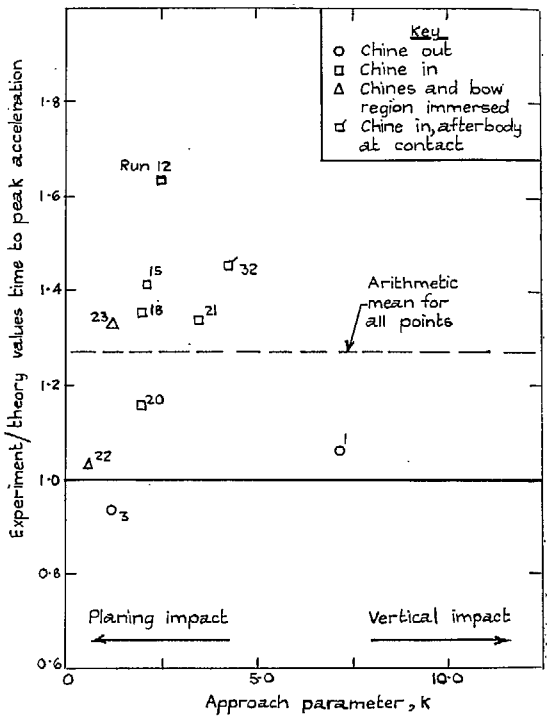

FIG. 33. Comparison of Ref. 12 theory with Ref. 37 full-scale results for time to maximum acceleration.

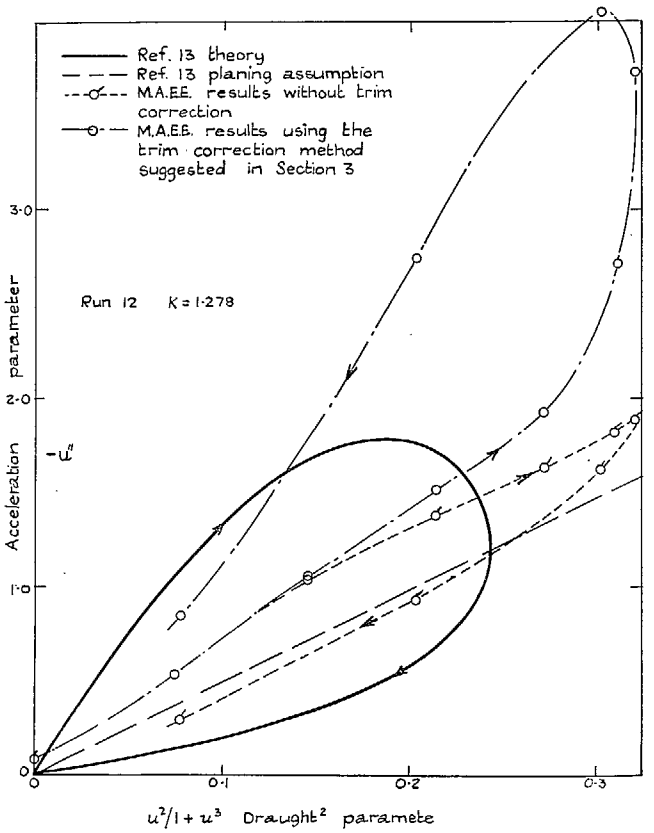

FIG. 34. Comparison of Ref. 13 theory with M.A.E.E. full-scale results of Ref. 34.

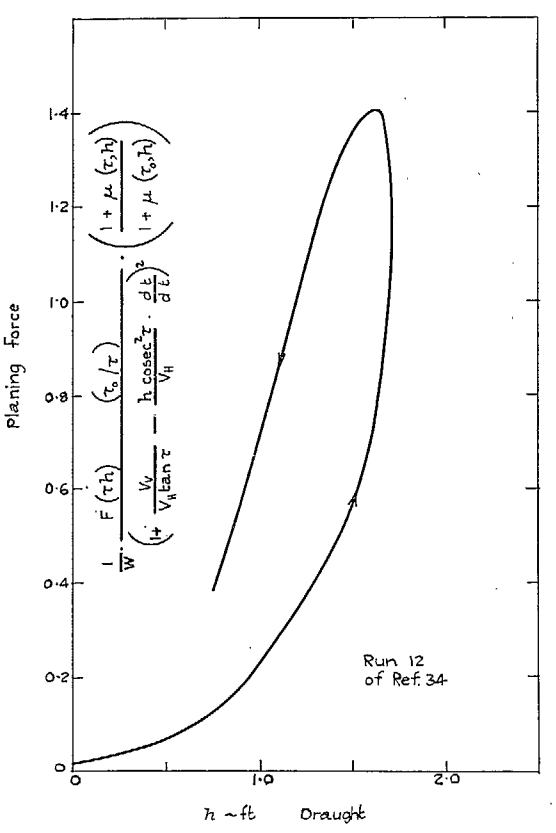

FIG. 35. Effective planing force corrected to initial attitude.

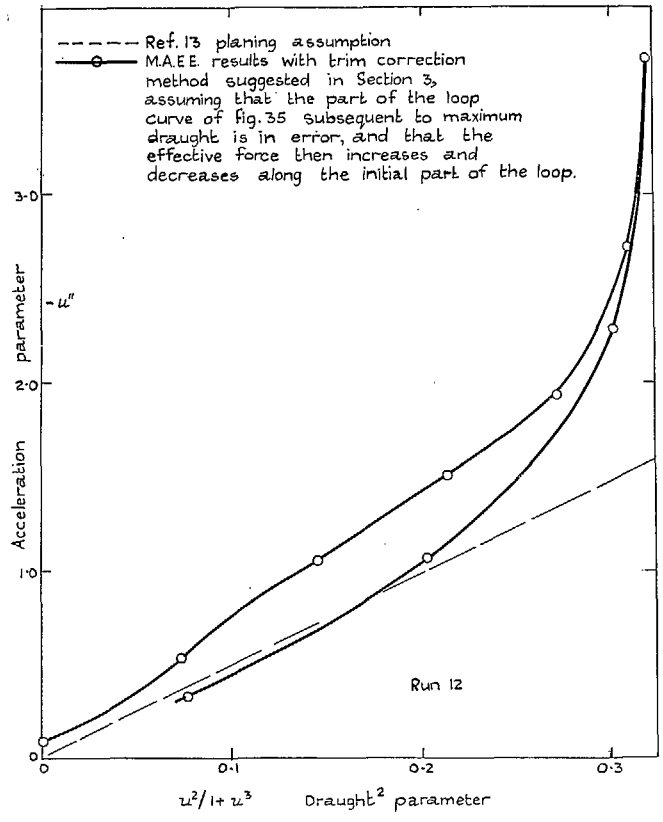

FIG. 36. Analysis of M.A.E.E. results of Ref. 34 assuming erroneous measurements subsequent to maximum draught when applying a trim correction.

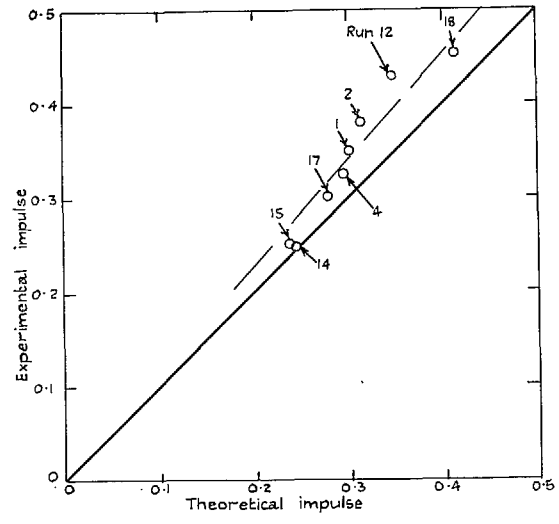

FIG. 37. Comparison of theoretical and experimental values of total impulse.

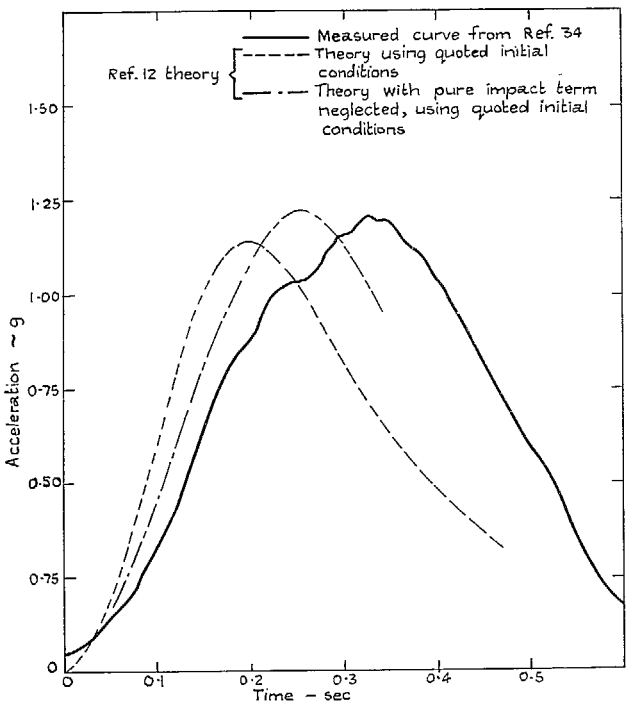

FIG. 38. Comparison of experiment with theory for run 12 of Ref. 34.

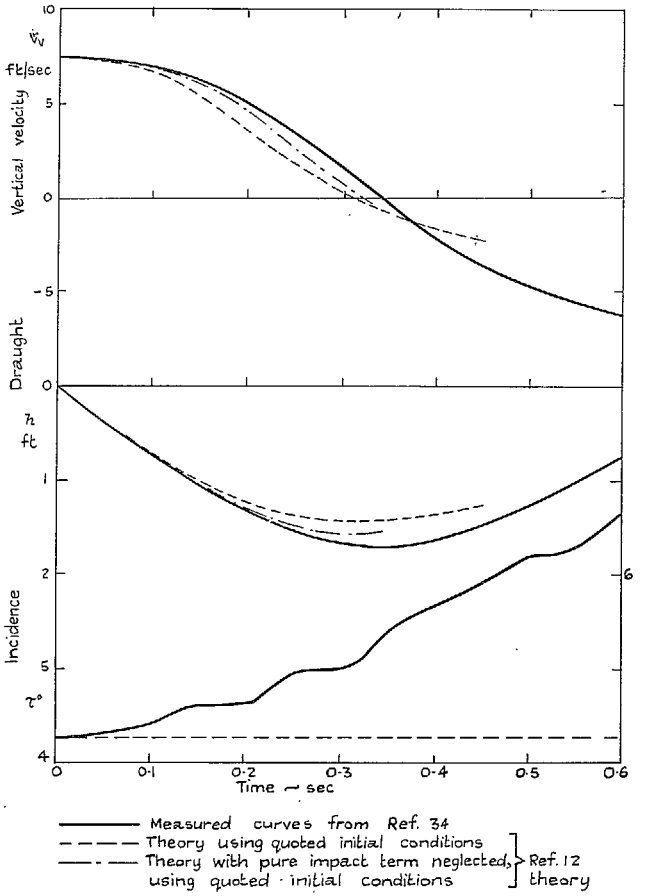

FIG. 39. Comparison of experiment with theory for run 12 of Ref. 34.

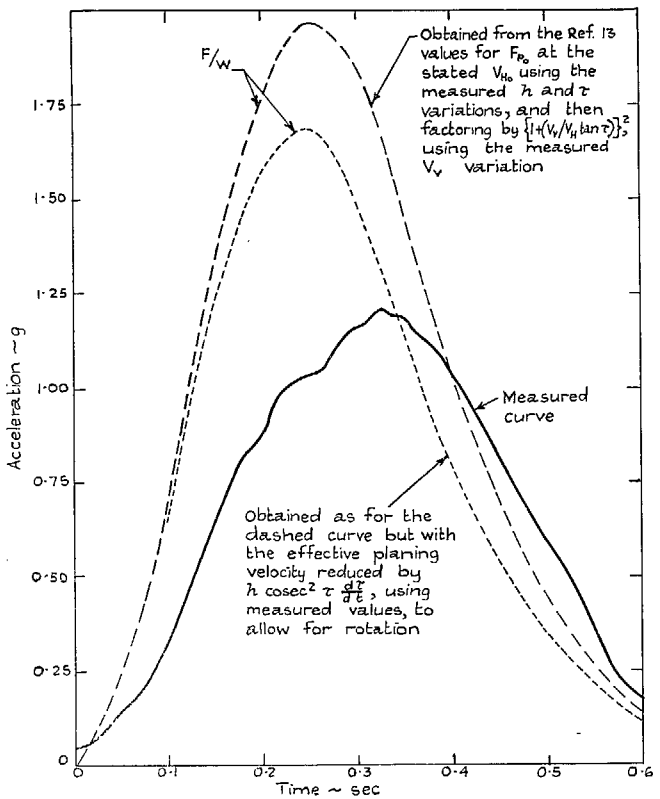

FIG. 40. Comparison of experiment with theory for run 12 of Ref. 34.

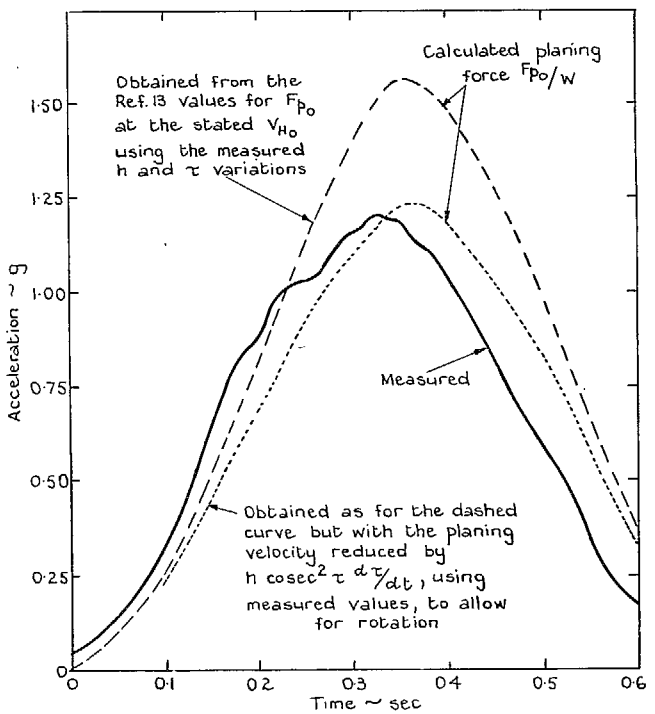

FIG. 41. Comparison of experiment with theory for run 12 of Ref. 34.

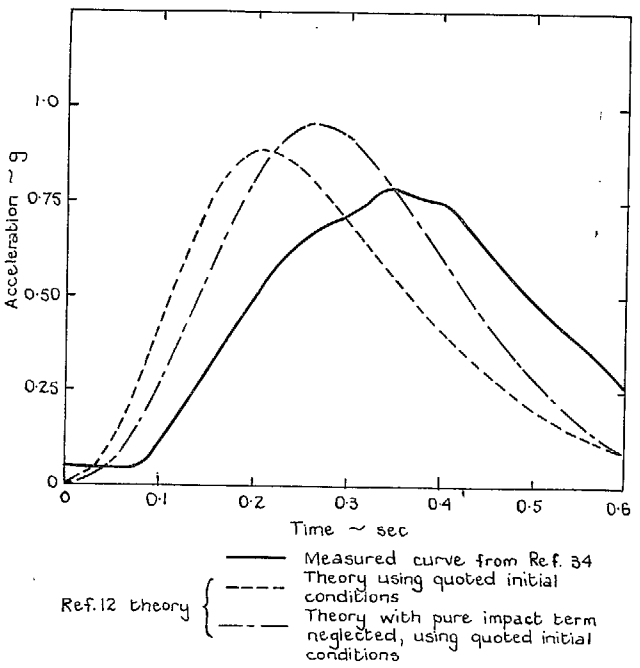

FIG. 42. Comparison of experiment with theory for run 17 of Ref. 34.

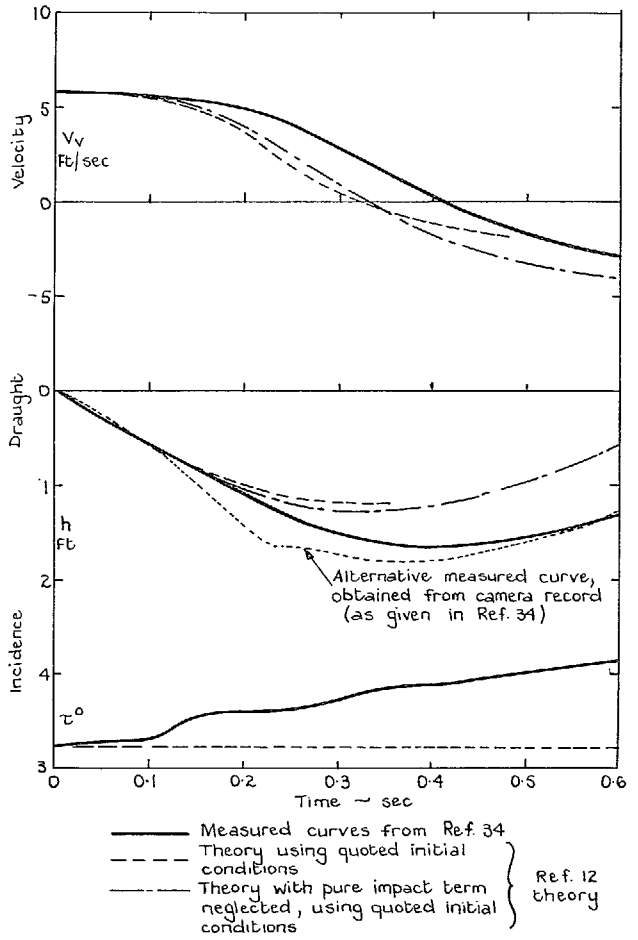

FIG. 43. Comparison of experiment with theory for run 17 of Ref. 34.

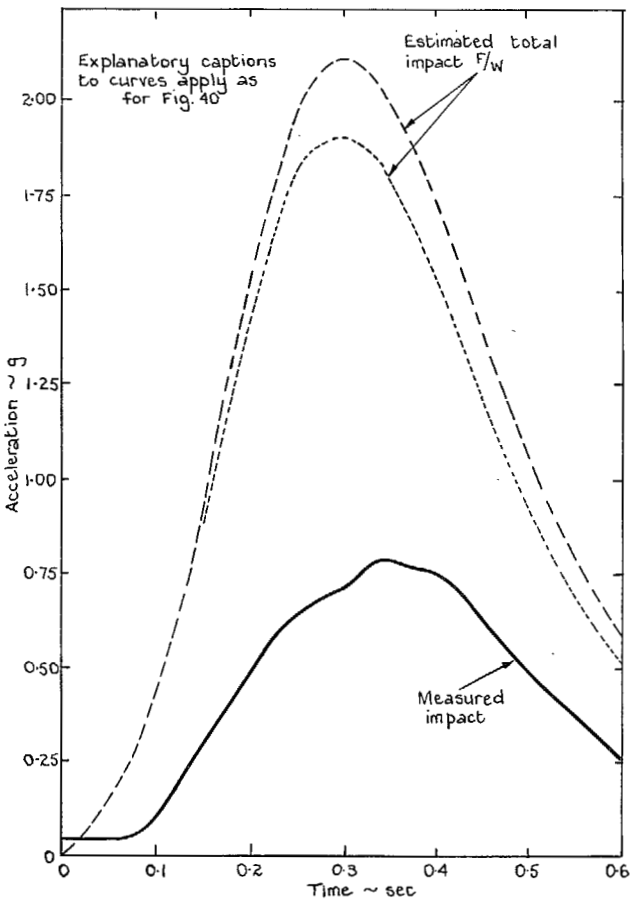

FIG. 44. Comparison of experiment with theory for run 17 of Ref. 34.

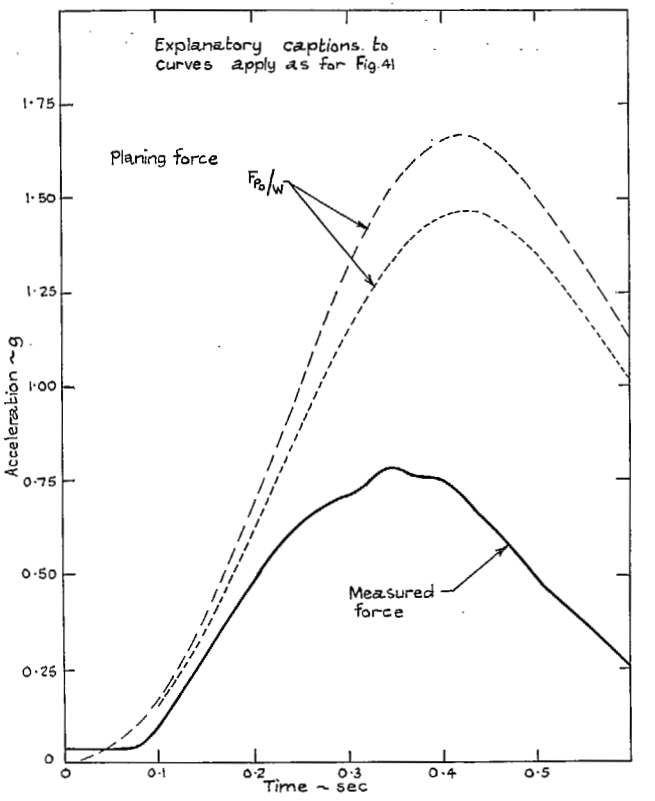

FIG. 45. Comparison of experiment with theory for run 17 of Ref. 34.

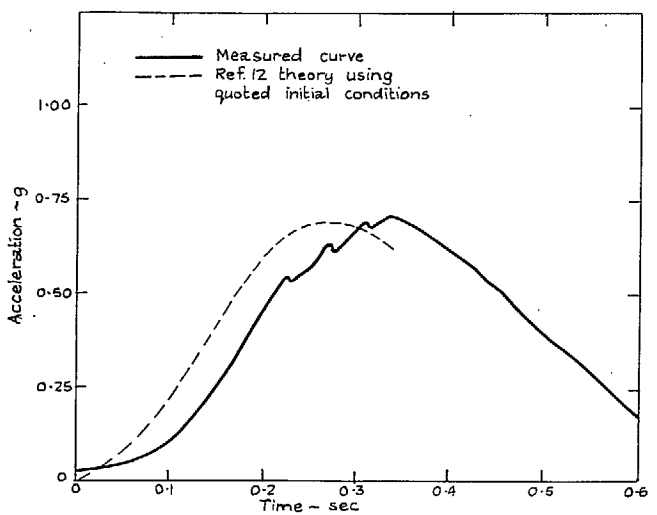

FIG. 46. Comparison of experiment with theory for run 14 of Ref. 34.

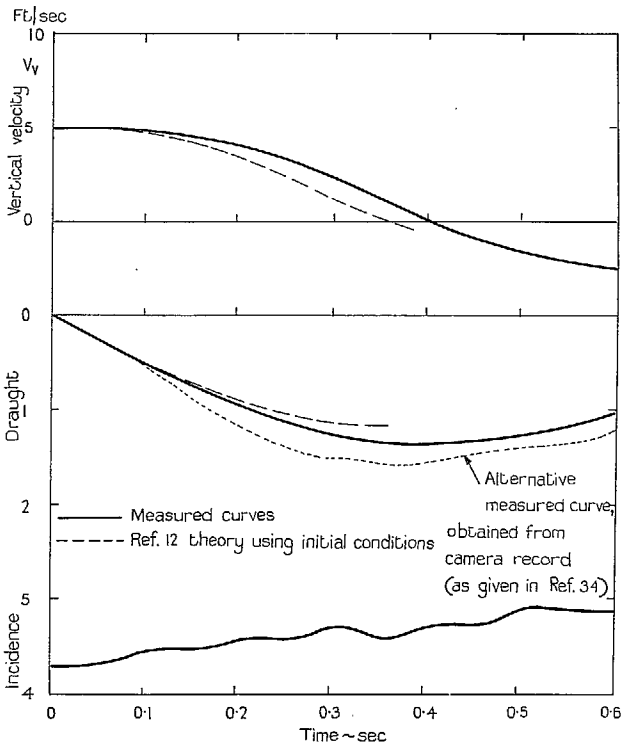

FIG. 47. Comparison of experiment with theory for run 14 of Ref. 34.

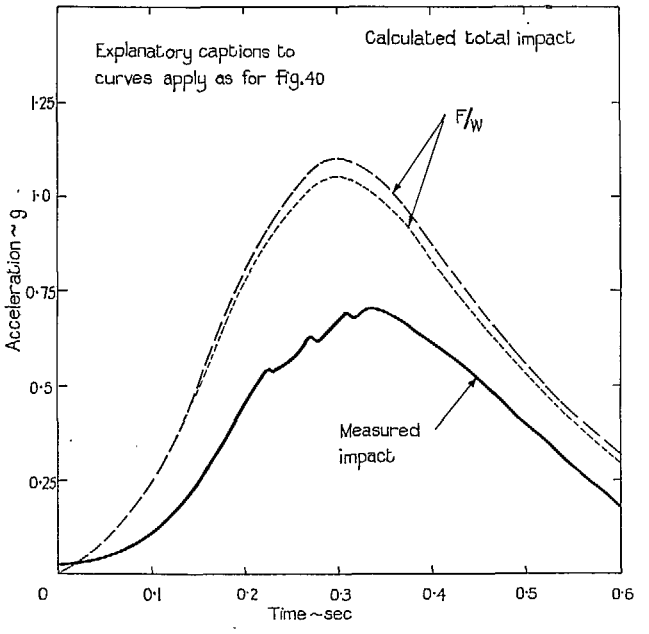

FIG. 48. Comparison of experiment with theory for run 14 of Ref. 34.

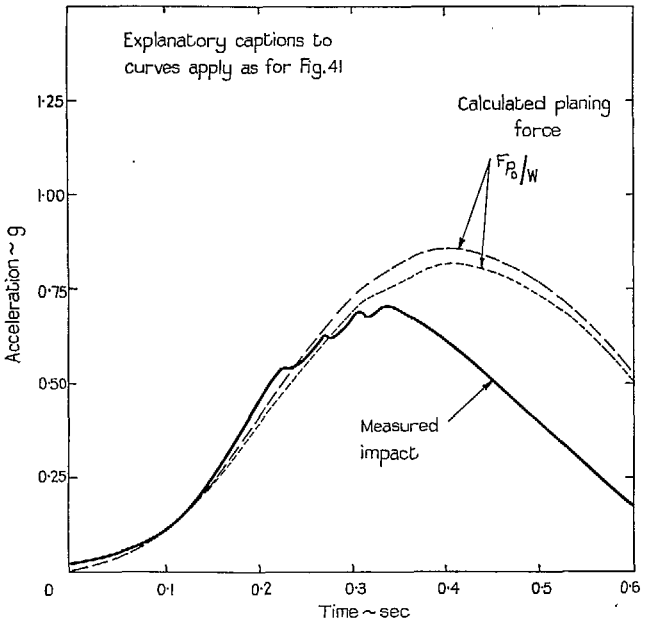

FIG. 49. Comparison of experiment with theory for run 14 of Ref. 34.

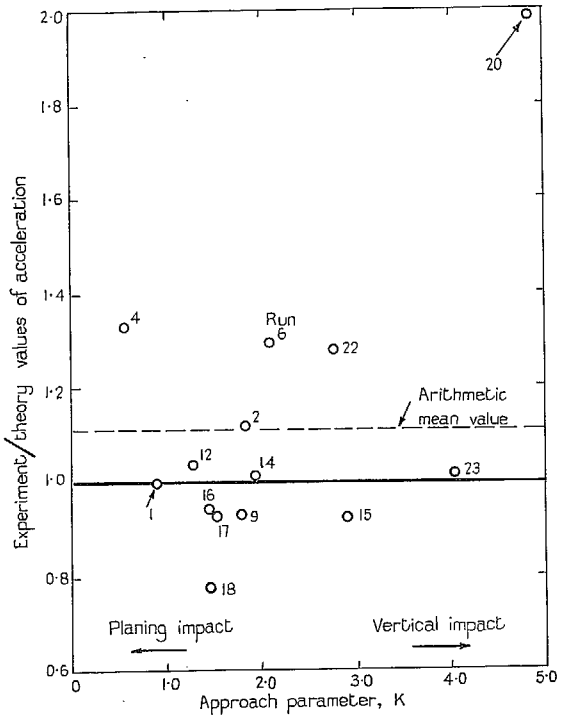

FIG. 50. Comparison of Ref. 13 theory with M.A.E.E. results from Refs. 32 and 34 for maximum acceleration.

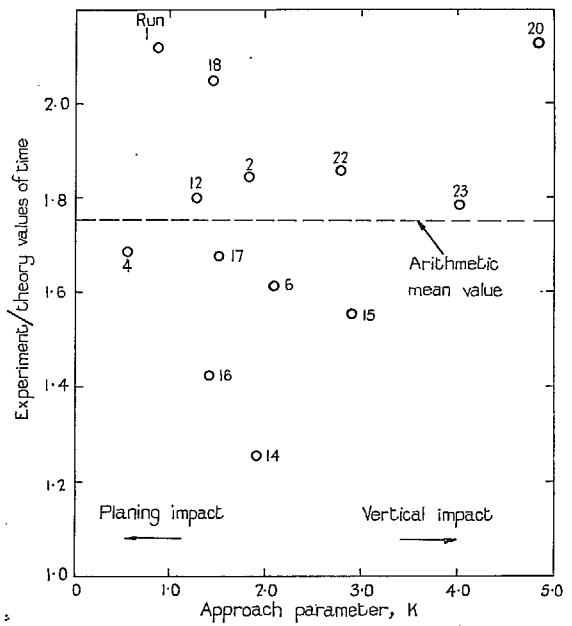

FIG. 51. Comparison of Ref. 12 theory with M.A.E.E. results from Refs. 32 and 34 for time to maximum acceleration.

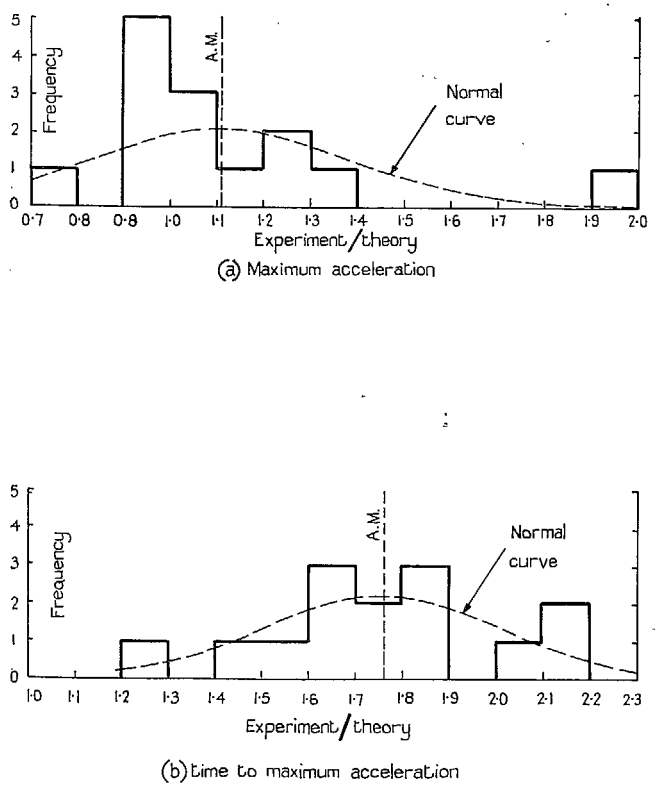

FIG. 52. Histograms for comparisons between *Sunderland* results and theory given in Figs. 50 and 51.

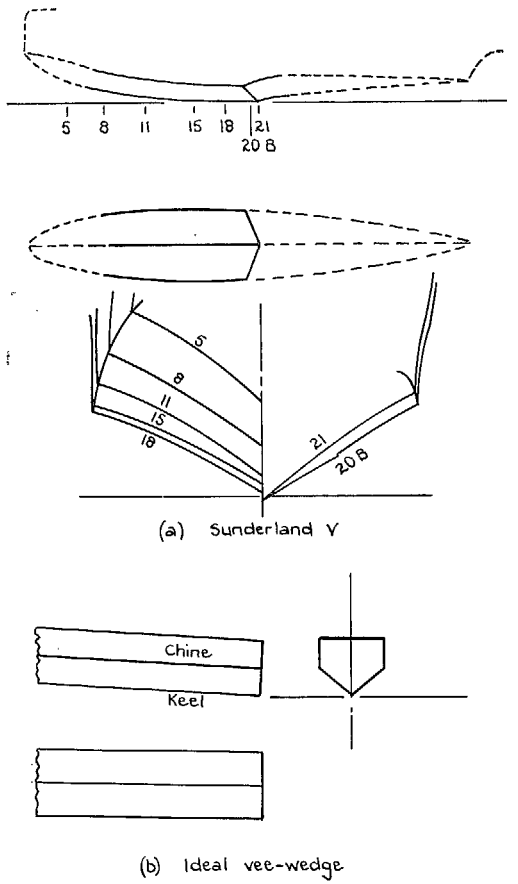

FIG. 53. Comparison of *Sunderland* planing bottom near main step with ideal V-wedge used in theory.

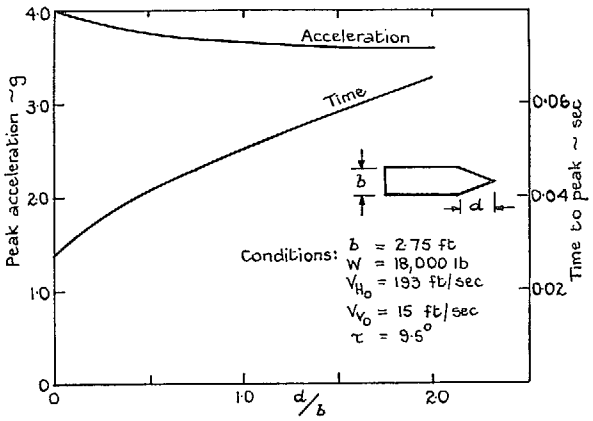

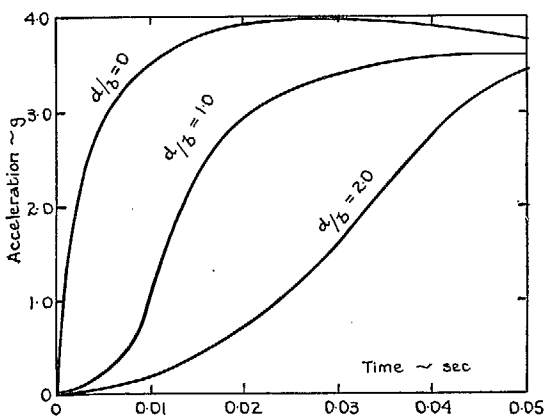

FIG. 54. Estimated effect of pointed aft planform on impact behaviour of flat-plate hydro-skis.

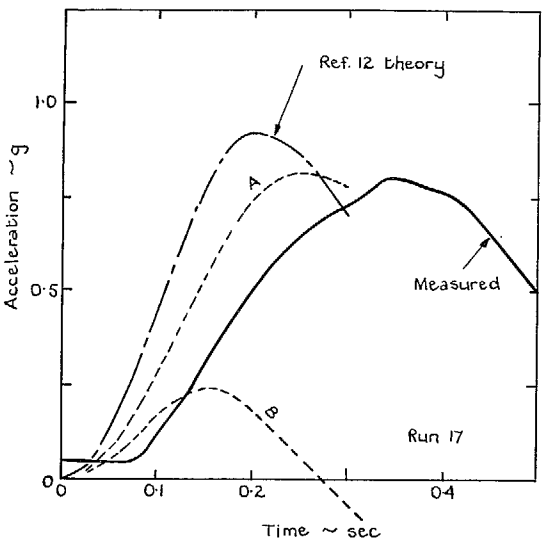

Ref. 12 theory: $\frac{dV_n}{dt} = \frac{3\mu}{l} V_n V_T + \frac{d}{dt}(\mu V_n)$

$= A + B$

where A = 'Impact planing' term

B = 'Pure impact' term

FIG. 55. Comparison of estimates of Ref. 12 theory with *Sunderland* results of Ref. 34.

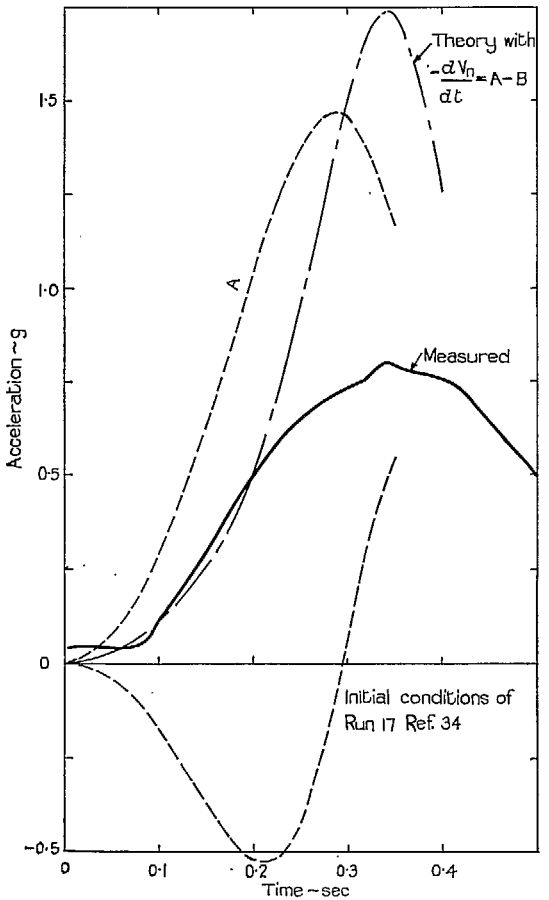

FIG. 56. Examination of modifications to theory of Fig. 55 to represent suctions.

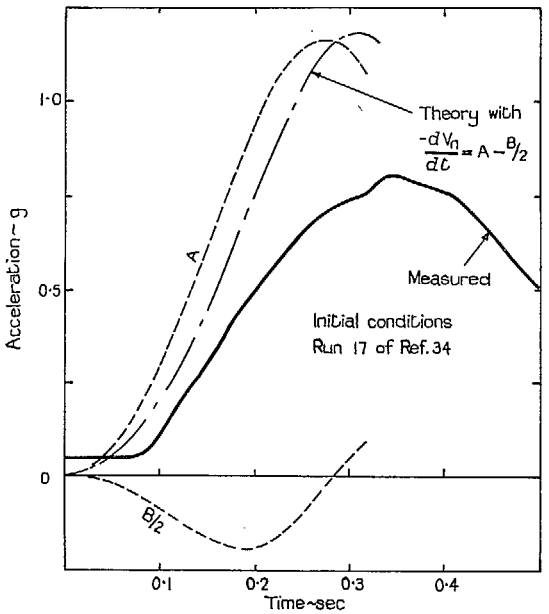

FIG. 57. Examination of modifications to theory of Fig. 55 to represent suctions.

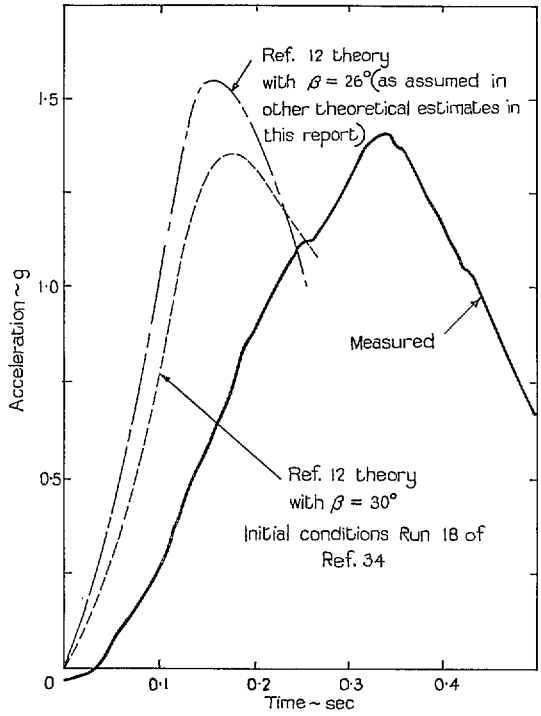

FIG. 58. Effect of change in dead-rise assumption on theoretical predictions.

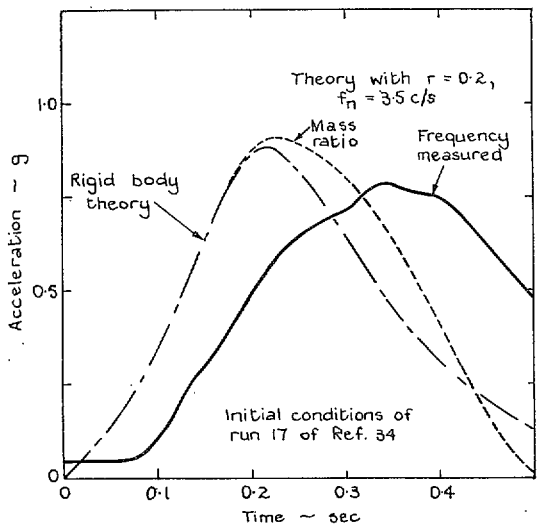

FIG. 59. Effect of wing flexibility.

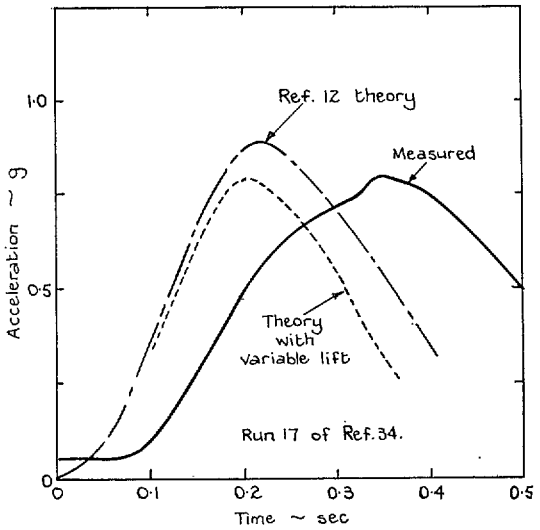

FIG. 60. Estimated effect of wing lift variation.

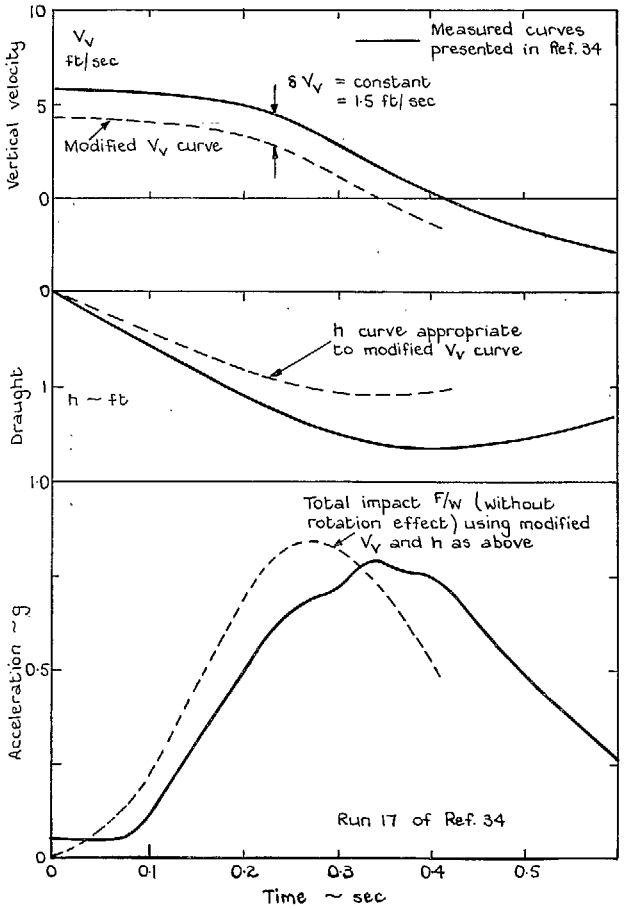

FIG. 61. Estimated effect of change of vertical velocity.

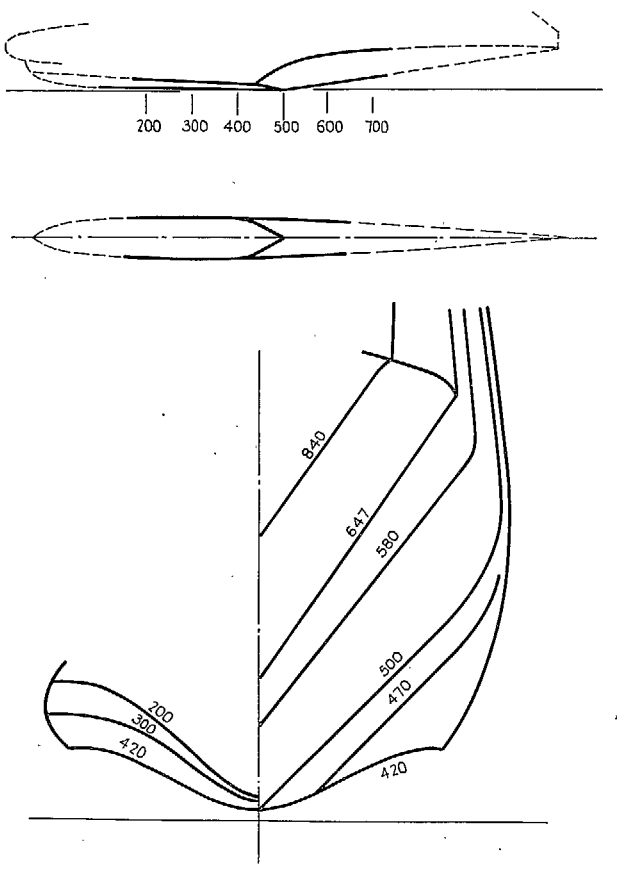

FIG. 62. Martin Model 270 hull geometry near step.

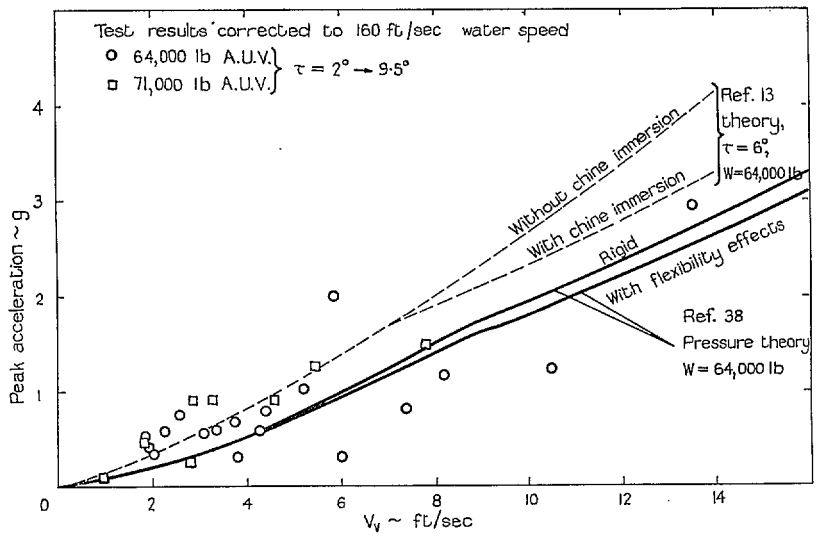

FIG. 63. Comparison of full-scale results on Martin Model 270 with theories.

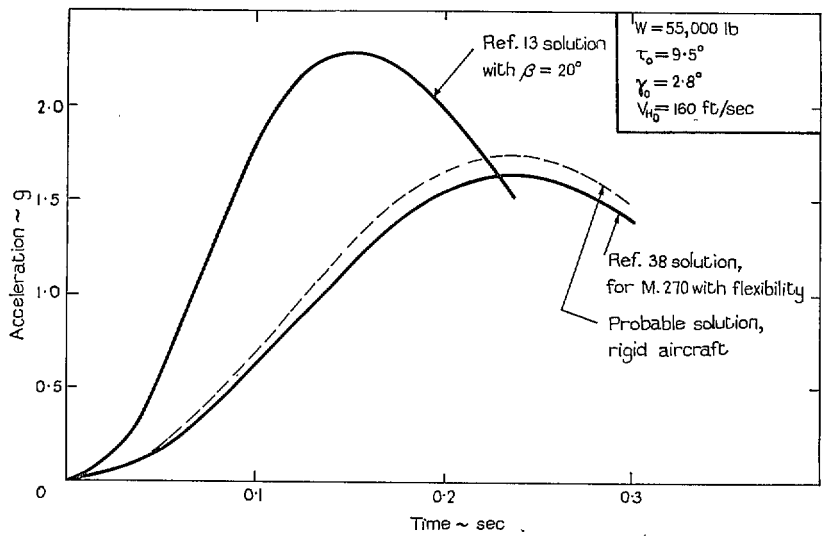

FIG. 64. Comparison of estimated total impact forces for M. 270 with Ref. 13 estimation for simple V-wedge of same basic dead rise.

(85424) Wt. 64/1857 K.5 11/62 Hw.

Publications of the Aeronautical Research Council

ANNUAL TECHNICAL REPORTS OF THE AERONAUTICAL RESEARCH COUNCIL (BOUND VOLUMES)

1942 Vol. I. Aero and Hydrodynamics, Aerofoils, Airscrews, Engines. 75*s.* (post 2*s.* 9*d.*)
Vol. II. Noise, Parachutes, Stability and Control, Structures, Vibration, Wind Tunnels. 47*s.* 6*d.* (post 2*s.* 3*d.*)

1943 Vol. I. Aerodynamics, Aerofoils, Airscrews. 80*s.* (post 2*s.* 6*d.*)
Vol. II. Engines, Flutter, Materials, Parachutes, Performance, Stability and Control, Structures. 90*s.* (post 2*s.* 9*d.*)

1944 Vol. I. Aero and Hydrodynamics, Aerofoils, Aircraft, Airscrews, Controls. 84*s.* (post 3*s.*)
Vol. II. Flutter and Vibration, Materials, Miscellaneous, Navigation, Parachutes, Performance, Plates and Panels, Stability, Structures, Test Equipment, Wind Tunnels. 84*s.* (post 3*s.*)

1945 Vol. I. Aero and Hydrodynamics, Aerofoils. 130*s.* (post 3*s.* 6*d.*)
Vol. II. Aircraft, Airscrews, Controls. 130*s.* (post 3*s.* 6*d.*)
Vol. III. Flutter and Vibration, Instruments, Miscellaneous, Parachutes, Plates and Panels, Propulsion. 130*s.* (post 3*s.* 3*d.*)
Vol. IV. Stability, Structures, Wind Tunnels, Wind Tunnel Technique. 130*s.* (post 3*s.* 3*d.*)

1946 Vol. I. Accidents, Aerodynamics, Aerofoils and Hydrofoils. 168*s.* (post 3*s.* 9*d.*)
Vol. II. Airscrews, Cabin Cooling, Chemical Hazards, Controls, Flames, Flutter, Helicopters, Instruments and Instrumentation, Interference, Jets, Miscellaneous, Parachutes. 168*s.* (post 3*s.* 3*d.*)
Vol. III. Performance, Propulsion, Seaplanes, Stability, Structures, Wind Tunnels. 168*s.* (post 3*s.* 6*d.*)

1947 Vol. I. Aerodynamics, Aerofoils, Aircraft. 168*s.* (post 3*s.* 9*d.*)
Vol. II. Airscrews and Rotors, Controls, Flutter, Materials, Miscellaneous, Parachutes, Propulsion, Seaplanes, Stability, Structures, Take-off and Landing. 168*s.* (post 3*s.* 9*d.*)

1948 Vol. I. Aerodynamics, Aerofoils, Aircraft, Airscrews, Controls, Flutter and Vibration, Helicopters, Instruments, Propulsion, Seaplane, Stability, Structures, Wind Tunnels. 130*s.* (post 3*s.* 3*d.*)
Vol. II. Aerodynamics, Aerofoils, Aircraft, Airscrews, Controls, Flutter and Vibration, Helicopters, Instruments, Propulsion, Seaplane, Stability, Structures, Wind Tunnels. 110*s.* (post 3*s.* 3*d.*)

Special Volumes

Vol. I. Aero and Hydrodynamics, Aerofoils, Controls, Flutter, Kites, Parachutes, Performance, Propulsion, Stability. 126*s.* (post 3*s.*)
Vol. II. Aero and Hydrodynamics, Aerofoils, Airscrews, Controls, Flutter, Materials, Miscellaneous, Parachutes, Propulsion, Stability, Structures. 147*s.* (post 3*s.*)
Vol. III. Aero and Hydrodynamics, Aerofoils, Airscrews, Controls, Flutter, Kites, Miscellaneous, Parachutes, Propulsion, Seaplanes, Stability, Structures, Test Equipment. 189*s.* (post 3*s.* 9*d.*)

Reviews of the Aeronautical Research Council

1939–48 3*s.* (post 6*d.*) 1949–54 5*s.* (post 5*d.*)

Index to all Reports and Memoranda published in the Annual Technical Reports

1909–1947 R. & M. 2600 (out of print)

Indexes to the Reports and Memoranda of the Aeronautical Research Council

Between Nos. 2351–2449	R. & M. No. 2450	2*s.* (post 3*d.*)
Between Nos. 2451–2549	R. & M. No. 2550	2*s.* 6*d.* (post 3*d.*)
Between Nos. 2551–2649	R. & M. No. 2650	2*s.* 6*d.* (post 3*d.*)
Between Nos. 2651–2749	R. & M. No. 2750	2*s.* 6*d.* (post 3*d.*)
Between Nos. 2751–2849	R. & M. No. 2850	2*s.* 6*d.* (post 3*d.*)
Between Nos. 2851–2949	R. & M. No. 2950	3*s.* (post 3*d.*)
Between Nos. 2951–3049	R. & M. No. 3050	3*s.* 6*d.* (post 3*d.*)
Between Nos. 3051–3149	R. & M. No. 3150	3*s.* 6*d.* (post 3*d.*)

HER MAJESTY'S STATIONERY OFFICE

from the addresses overleaf

Printed and published by
HER MAJESTY'S STATIONERY OFFICE

To be purchased from
York House, Kingsway, London W.C.2
423 Oxford Street, London W.1
13A Castle Street, Edinburgh 2
109 St. Mary Street, Cardiff
39 King Street, Manchester 2
50 Fairfax Street, Bristol 1
35 Smallbrook, Ringway, Birmingham 5
80 Chichester Street, Belfast 1
or through any bookseller

Printed in England

S.O. Code No. 23-3285